

**SMALL MOLECULE ASSOCIATIVE CO₂ THICKENERS FOR IMPROVED
MOBILITY CONTROL**

by

Jason Jiwoo Lee

BS Chemical Engineering, University of Rochester, 2010

MS Chemical Engineering, University of Rochester, 2011

Submitted to the Graduate Faculty of
Swanson School of Engineering in partial fulfillment
of the requirements for the degree of
Doctor of Philosophy

University of Pittsburgh

2016

UNIVERSITY OF PITTSBURGH
SWANSON SCHOOL OF ENGINEERING

This dissertation was presented

by

Jason Lee

It was defended on

May 3, 2016

and approved by

Eric J. Beckman, PhD, Professor, Department of Chemical and Petroleum Engineering

Sachin Velankar, PhD, Associate Professor, Department of Chemical and Petroleum Engineering

Geoffrey Hutchison, PhD, Assistant Professor, Departmental of Chemistry

Dissertation Director: Robert M. Enick, PhD, Department of Chemical and Petroleum Engineering

Copyright © by Jason Jiwoo Lee

2016

SMALL MOLECULE ASSOCIATIVE CO₂ THICKENERS FOR IMPROVED MOBILITY CONTROL

Jason Jiwoo Lee, PhD

University of Pittsburgh, 2016

Mobility control is one of the largest problems in carbon dioxide (CO₂) miscible enhanced oil recovery. This can be traced back to the very low viscosity of high pressure carbon dioxide, 10-100 times lower than the original oil in place, which gives it an unfavorably high mobility ratio that results in viscous fingering, early CO₂ breakthrough, decreased sweep efficiency, and high CO₂ injected:oil recovered utilization ratios. CO₂'s viscosity can also cause conformance control issues in stratified formations because it promotes CO₂ flow into higher permeability, watered-out zones leaving a much smaller fraction of CO₂ available to flow the lower permeability, oil-bearing zones of interest.

An economical, direct CO₂ thickener that is effective at dilute concentrations would be disruptive technology because it would not only mitigate all of the problems associated with an unfavorable mobility ratio, but it would also eliminate the need for the water-alternating-gas process for the reduction of CO₂ relative permeability. These effects would be especially pronounced in horizontal, relatively homogeneous porous media. However, CO₂ has never been thickened using an affordable or small molecule. To circumvent these obstacles, we have designed novel small molecules that self-assemble into viscosity enhancing supramolecular structures. Generally, our designs utilize both CO₂-philes to enhance dissolution and steric effects that promote linear supramolecular structures. CO₂-phobic groups are also included to promote self-assembly. This work primarily focuses on molecular designs based on highly CO₂-

philic silicones and CO₂-phobic hydrogen bonding groups such as aromatic amides and ureas. Initial phase behavior studies on un-functionalized oligomeric silicones of varying molecular weight in CO₂ served as solubility limits in that the inclusion of a CO₂-phobic associating group(s) will result in a decrease in solubility (i.e. an increase in cloud point pressure). Along with exploration of various functional groups, we also demonstrate the effect of molecular geometry on final solution properties. Specifically, terminally functionalized branched silicones required a much higher mass concentration than silicone tailed core-associative molecules to achieve similar solution viscosities. The most promising thickening results are obtained with trisureas functionalized with three relatively short, branched CO₂-philic silicone-based functionalities, most notably benzene tris((tri(trimethylsiloxy)silyl)propyl) urea. Replacement of one or two of these branched (tri(trimethylsiloxy)silyl) functional groups with linear oligomers of dimethyl siloxane renders compounds more CO₂-soluble but less effective at thickening. In most cases, however, an organic co-solvent is required to attain solubility levels great enough for viscosity enhancement to occur.

TABLE OF CONTENTS

PREFACE.....	XII
1.0 INTRODUCTION.....	1
1.1 CO₂ MISCIBLE ENHANCED OIL RECOVERY	3
1.2 MOBILITY CONTROL	4
1.3 CO₂ SOLVENT CHARACTER	7
1.4 RESEARCH OBJECTIVES.....	9
2.0 PREVIOUS ATTEMPTS AT THICKENING CO₂.....	18
2.1 POLYMERIC THICKENERS.....	19
2.2 SMALL MOLECULE THICKENERS	23
2.2.1 Trialkyltin fluorides and semi-fluorinated trialkyltin fluorides	24
2.2.2 Hydroxyaluminum disoaps and fluorinated hydroxyaluminum disoaps	25
2.2.3 Bis-Ureas.....	26
2.2.4 Fluorinated, dual, twin-tailed surfactants with divalent metal cations	27
2.2.5 Other compounds	28
3.0 EXPERIMENTAL METHODS.....	29
3.1 PHASE BEHAVIOR	29
3.2 CLOSE CLEARANCE FALLING BALL VISCOMETRY	31
3.3 SYNTHETIC METHODS AND CHARACTERIZATION.....	34

4.0	PHASE BEHAVIOR OF LINEAR PDMS WITH AROMATIC ENDGROUPS	35
4.1	MATERIALS	39
4.1.1	General hydrosilylation procedure for vinyl compounds	41
4.2	RESULTS AND DISCUSSION	42
4.2.1	Trimethylsilyl-terminated Linear Silicones	44
4.2.2	PDMS-NAP Phase Behavior in CO₂	47
4.2.3	CO₂-solubility of Other End-functionalized PDMS Compounds.....	49
4.3	VISCOSITY ENHANCING POTENTIAL	53
4.4	CONCLUSIONS	54
5.0	AROMATIC AMIDE END-FUNCTIONAL SILICONES	56
5.1	LINEAR AROMATIC AMIDE ENDFUNCTIONAL PDMS.....	56
5.2	MULTIFUNCTIONAL AQCA PDMS THICKENERS	62
5.3	CONCLUSIONS	70
6.0	CYCLIC AMIDES AND UREAS.....	72
6.1	SYNTHESIS.....	74
6.1.1	Thickening ability in organic solvents	84
6.2	HIGH PRESSURE PHASE BEHAVIOR	86
6.3	HIGH PRESSURE VISCOMETRY	89
6.4	CONCLUSIONS	93
7.0	SUMMARY OF RESULTS.....	95
8.0	FUTURE WORK	98
	APPENDIX A	101
	BIBLIOGRAPHY	124

LIST OF TABLES

Table 4.1 Novel CO ₂ -soluble compounds composed of a CO ₂ -philic PDMS segment and CO ₂ -phobic functional groups.....	38
Table 4.2 Polydimethylsiloxane (PDMS) and α,ω -bis(2-ethylnaphthyl)polydimethylsiloxane (PDMS-NAP) samples.....	40
Table 4.3 End-functionalized Polydimethylsiloxane (PDMS) samples.	50
Table 4.4 Bubble Point Pressures of CO ₂ -(Phenyl-R-functionalized PDMS) mixtures.	51
Table 5.1 Low MW, Linear PDMS Bisamides.....	57
Table 5.2 Cloud Point Pressures at 60°C.....	58
Table 5.3 Cloud Point Pressures (psi) at various temperatures for 1wt% linear PDMS 4-Nitrobenzamides in CO ₂ solutions with x=40 and 50.....	60
Table 5.4 Viscosity Increase for Silicone Anthraquinone Amides.....	66
Table 6.1 Organic liquid thickening and CO ₂ solubility data for compounds 1-11 and 18-34. ...	85
Table 6.2 Cloud point pressures and relative viscosities of compounds in dense CO ₂	90

LIST OF FIGURES

Figure 1.1 Natural reservoir forces driving production in primary recovery	1
Figure 1.2 A simplified illustration of waterflooding	2
Figure 1.3 Dependence of residual oil saturation on capillary number	3
Figure 1.4 Realistic ($M=17.3$) and ideal ($M=0.151$) sweep miscible displacement experiments for a quarter 5-spot pattern with homogeneous porous media [4]. Lines show position of leading edge of solvent at various times up to breakthrough.....	4
Figure 1.5 Simplified illustration of WAG injection process [6]	6
Figure 1.6 Schematic representation of the LA-LB interaction between the carbonyl oxygen atom and the carbon atom of CO_2 and the cooperative C-H---O hydrogen bonding between the CO_2 oxygen and the C_αH bond [13].....	8
Figure 1.7 Qualitative P-x diagram illustrating the V-L region for sub-critical ($T < 31^\circ\text{C}$) mixtures of CO_2 with lower molecular weight PDMS. The dashed ellipse indicates region where V-L bubble points were measured. V.P. = vapor pressure	11
Figure 1.8 Qualitative P-x diagram illustrating the two-phase region for supercritical ($T > 31^\circ\text{C}$) mixtures of CO_2 with low molecular weight PDMS (237) dotted ellipse F-L bubble points; PDMS dashed ellipse F-L cloud/dew points. V.P. = vapor pressure	12
Figure 1.9 Qualitative P-x diagram illustrating the three two-phase regions and three-phase line for sub-critical ($T < 31^\circ\text{C}$) mixtures of CO_2 with higher molecular weight PDMS. The dashed ellipse indicates region where L2-L1 cloud/dew points were measured. V.P. = vapor pressure	13
Figure 1.10 Qualitative P-x diagram illustrating the three two-phase regions and three-phase line for supercritical ($T > 31^\circ\text{C}$) mixtures of CO_2 with higher molecular weight PDMS. The dashed ellipse indicates region where F-L cloud/dew points were measured. V.P. = vapor pressure	14

Figure 1.11 Qualitative P-x diagram illustrating the three two-phase regions and three-phase line for sub-critical ($T < 31^{\circ}\text{C}$) mixtures of CO_2 with PDMS-NAP. The dashed ellipse indicates region where L2-L1 cloud/dew points were measured for PDMS-NAP of intermediate molecular weight. V.P. = vapor pressure.....	15
Figure 1.12 Qualitative P-x diagram illustrating the three two-phase regions and three-phase line for sub-critical ($T < 31^{\circ}\text{C}$) mixtures of CO_2 with CO_2 -philic solid [24].	16
Figure 1.13 Qualitative P-x diagram of subcritical CO_2 - CO_2 -philic solid mixture exhibiting two three-phase lines [24]......	16
Figure 2.1 Schematic representation of thickener self-assembly into fibrous networks [20].....	18
Figure 2.2: Polymeric CO_2 thickeners. PDMS requires co-solvent, PFOA and polyFAST are effective without co-solvent, polyBOVA is modest thickener that requires extremely high pressure for dissolution	23
Figure 2.3: Fluorinated twin-tailed surfactants, the divalent version (right) provided modest CO_2 thickening.....	28
Figure 3.1 Falling ball in Pyrex tube prior to assembly.....	33
Figure 4.1 General hydrosilylation reaction scheme for vinyl compounds	41
Figure 4.2 A comparison of the solubility of CO_2 -phobic naphthalene (Mw 128.17) (triangles, reference [91]) and CO_2 -philic PDMS (Mw 237) (stars, this work) in CO_2 at 35°C . Naphthalene cloud point pressures indicate a limiting solubility of 6.5wt% at extreme pressure. The PDMS- CO_2 mixture bubble point data are indicative of a high degree of miscibility between PDMS 237 and CO_2	43
Figure 4.3 Structures of PDMS (top) and ethylnaphthalene-terminated PDMS (PDMS-NAP) (bottom). The two possible end groups shown on the ethylnaphthalene-terminated PDMS illustrate that this compound is a mixture of isomers.	43
Figure 4.4 Two-phase boundaries of trimethylsilyl-terminated PDMS in CO_2 at 23°C . Mixtures containing PDMS 410 or 1250 exhibited bubble points; mixtures containing PDMS 2000, 3780, 5970 or 9430 exhibited cloud points. The curves are guides to the eye; they are not model results.	46
Figure 4.5 Solubility of trimethylsilyl-terminated PDMS in CO_2 at 40°C . All data represent cloud point data. The curves are guides to the eye; they are not model results.....	46
Figure 4.6 Solubility of the PDMS-NAP compounds in CO_2 at 40°C , as represented by cloud point data. PDMS-NAP 1181 is soluble at 1wt%, but is insoluble at 2wt%. The curves are guides to the eye; they are not model results. PDMS-454 and PDMS-NAP 5986 are not shown because they are insoluble to 10,000 psi.	48

Figure 5.1 Preparation of Low MW Linear PDMS Bisamides.....	57
Figure 5.2 DSC Melting Peak Temperature vs PDMS chainlength for Bis 4-Nitrobenzamides..	59
Figure 5.3 Compounds 7a (x= 25), 7b (x=40)	60
Figure 5.4 Compound 8	61
Figure 5.5 Solid D40+ Bisamides: 4-Nitrobenzamide (left), Anthraquinone-2-carboxamide (center) and Biphenyl-4-carboxamide (right).	62
Figure 5.6 Synthesis of Branched Aminosilicones	63
Figure 5.7 Preparation of Branched Anthraquinone Amides.....	63
Figure 5.8 Viscosity increase at 25°C for a Hexane Solution of Compound 13 in a CO ₂ rich solution; The curves are guides to the eye; they are not model results.....	65
Figure 5.9 Allyl Anthraquinone-2-Carboxamide 15.....	67
Figure 5.10 Synthesis of Compounds 21 and 22	68
Figure 5.11 Preparation of Compound 24.....	69
Figure 6.1 Structural components of small molecule CO ₂ thickeners	73
Figure 6.2 Synthesis of cis-1,3,5-cyclohexanetrisamides.....	76
Figure 6.3 Synthesis of trans-1,2-cyclohexanebisamides.....	77
Figure 6.4 Synthesis of branched aminopropyl siloxanes 15 – 17.	78
Figure 6.5 Synthesis of benzene trisamides 18-21.....	80
Figure 6.6 Synthesis of benzene bisamides 22-23.....	81
Figure 6.7 Synthesis of benzene triester 25.	82
Figure 6.8 Synthesis of benzene trisureas 26-36.	83
Figure 6.9 Synthesis of benzene bisurea 37.....	84
Figure 6.10 Comparison of benzene trisurea solution viscosities with varying tail composition; TMS represents the branched tail while D11 represents the linear tail	92

PREFACE

A very scientific thank you Bob Perry, Mark Doherty, Mike O'Brien and to my committee for being there to exchange ideas and keep me in line.

A somewhat blurry thank you to Alex Grelli at Wigle Whiskey for taking on this wacky guy and surrendering some creative freedom to me. Your mentorship continues to be invaluable to my career.

A huge and warm thank you to my family and friends for loving me unconditionally. Without your support, I'd be nothing but a sack of organs.

An eternally grateful thank you to the man, the myth, the legend; Bob Enick. Thank you for steering my ship after it had gone astray. My time working with you was a genuine once in a lifetime experience that I wouldn't trade for anything. Exposure to your insane work ethic, overall positive outlook and love of what you do was truly infectious and a prime example of leading by behavior that I will do my best to pass onto others.

1.0 INTRODUCTION

Upon discovery, crude oil is initially produced via primary recovery methods which rely on the oil-bearing formation's natural sources of energy to drive reservoir fluids until production slows to an uneconomical oil rate. Fluid drive into wellbores is initially dependent on reservoir liquid expansion and rock compaction mechanisms under decreasing pressure. As the pressure drops below the oil's bubble point, gas caps expand above the oil-gas line and may also help drive reservoir fluids. If the formation is also connected to an aquifer, water encroachment will displace oil from reservoir pore space and help moderate declining pressure that results from reservoir fluid withdrawal. These mechanisms are illustrated in Figure 1.1.

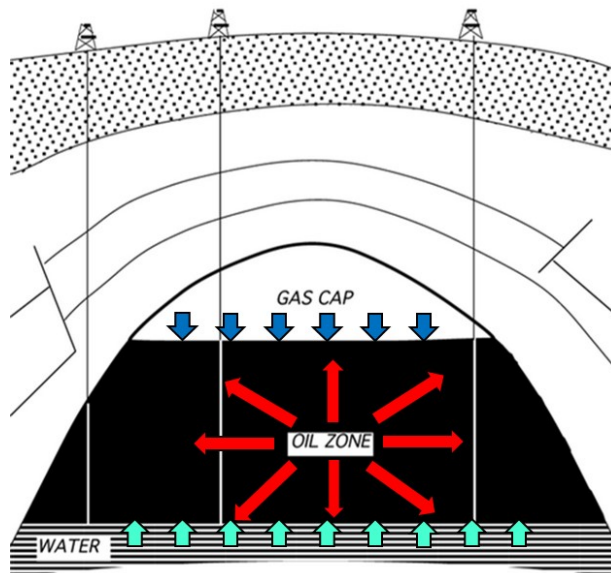


Figure 1.1 Natural reservoir forces driving production in primary recovery

Secondary recovery methods involve fluid injection, typically water, into the reservoir over long periods of time as illustrated in Figure 1.2. Water injection, referred to as waterflooding, helps moderate declining reservoir pressure associated with primary recovery to maintain production rates for longer than if only primary methods were used. Along with pressure maintenance, waterflooding helps displace and drive oil to producing wells resulting in increased ultimate recovery. However, immiscibility of the oil and water and high interfacial tension between these phases cause high residual oil saturations in the swept reservoir rock. Ultimate oil recovery resulting from both primary and secondary recovery methods are generally in the range of 20-40% of the original oil in place [1].

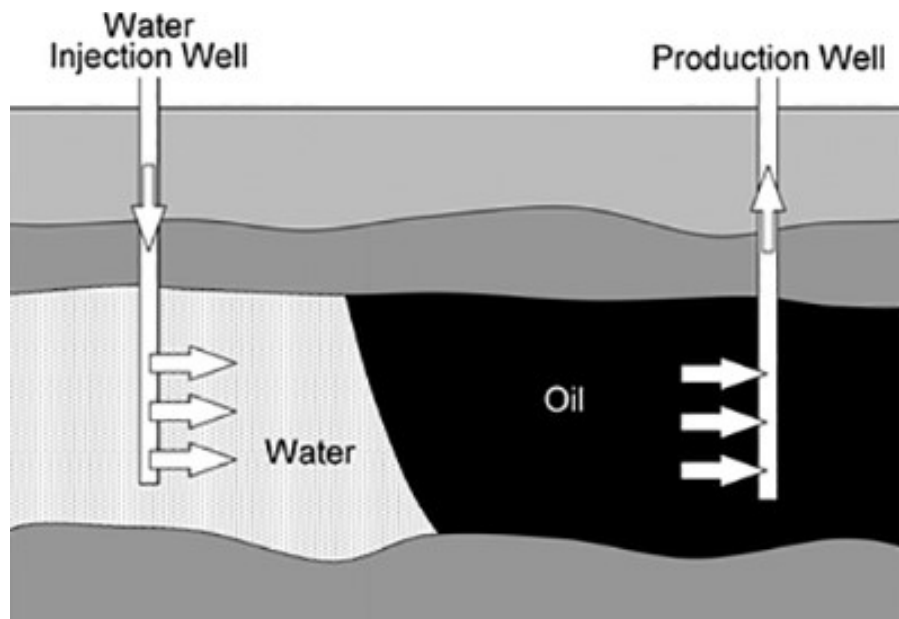


Figure 1.2 A simplified illustration of waterflooding

1.1 CO₂ MISCIBLE ENHANCED OIL RECOVERY

Enhanced oil recovery (EOR) encompasses a range of techniques that can be utilized to further increase oil production after primary and secondary methods. One method recognized as a viable technology that was invented in the 1950's and practiced since the 1960's is miscible flooding which relies on the injection of oil-miscible fluids like dense CO₂ (multiple contact miscibility developed via condensation of CO₂ into oil and extraction of light hydrocarbons into CO₂) and light hydrocarbon solvents (typically complete miscibility) to help mitigate the problematic high residual oil saturations typical of waterflooding. Figure 1.3 shows the dependence of residual oil saturation on capillary number; reduction in interfacial tension increases the capillary number leaving behind less residual oil after a sweep. Generally, hydrocarbons are less commonly used than CO₂ due to their unfavorably high cost. Additionally, natural gas requires a much higher minimum miscibility pressure (MMP), the pressure required to develop miscibility with the oil in place, than CO₂ [2]. Domestic oil production via CO₂ miscible EOR in 2014 was about 292,000 barrels per day (bbl/d) whereas hydrocarbon miscible flooding accounted for 71,500 bbl/d [3].

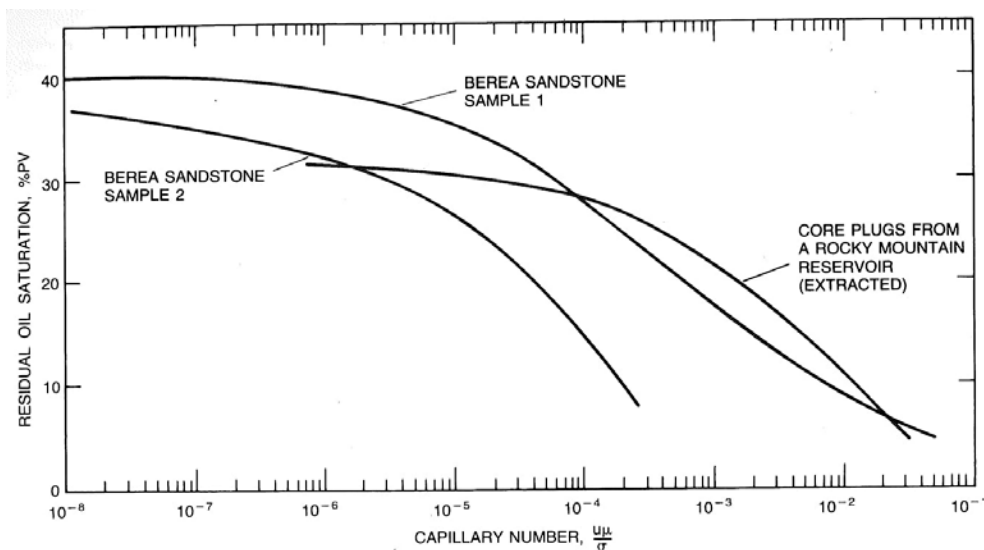


Figure 1.3 Dependence of residual oil saturation on capillary number

1.2 MOBILITY CONTROL

The very low viscosity of dense CO₂ (1200-4000 psi) is problematic for EOR projects because it exacerbates gravity override of the CO₂ and it induces an unfavorable mobility ratio that results in viscous fingering, early breakthrough, poor sweep efficiency, and high CO₂ injected:oil recovered utilization ratios [4,5]. These effects are visually shown by experimental results of two dimensional sweeps (no gravity effects) [4] shown in figure 1.4 where the bottom left corners of the diagrams are injectors and the top right corners producers. The mobility ratio, M , is defined as the ratio of CO₂ to oil mobilities which are functions of relative permeability, k_r , and viscosity, μ . The relationship is shown in the equation below.

$$M_{CO_2:oil} = \frac{k_{r,CO_2}/\mu_{CO_2}}{k_{r,oil}/\mu_{oil}}$$

Viscous fingering and early solvent breakthrough, B.T., are present in the high M scenario while in the low M scenario, breakthrough occurs after much of the area has been swept due to an absence of fingering.

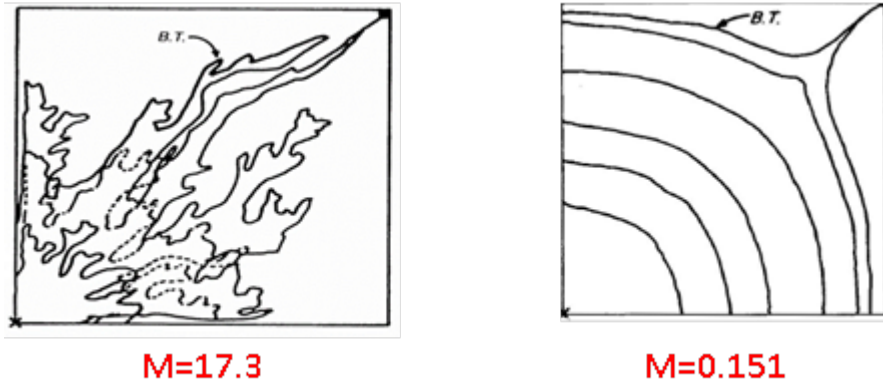


Figure 1.4 Realistic ($M=17.3$) and ideal ($M=0.151$) sweep miscible displacement experiments for a quarter 5-spot pattern with homogeneous porous media [4]. Lines show position of leading edge of solvent at various times up to breakthrough

Further, in stratified formations where layers of rock have inconsistent properties, the low CO₂ viscosity causes conformance control issues because it promotes the flow of a significant portion of the CO₂ into the higher permeability, watered-out zones while a much smaller fraction of the CO₂ enters the lower permeability, oil-bearing zones of interest.

In a recent, extensive DOE-sponsored literature review of strategies for improved mobility and conformance control during CO₂ floods [5], it was shown that the state-of-the-art technique for mitigating the unfavorable mobility ratio remains the water-alternating-gas (WAG) process shown in Figure 1.5. In an attempt to provide a more effective means of mobility and conformance, more than a dozen field tests of CO₂-in-brine foams tests were conducted during the 1980s and 1990s using brine-soluble surfactants. About half of these fields tests were technical successes, and most proved to be economically viable as well. Interest in CO₂ foams may be re-kindled by recent developments in CO₂ soluble surfactants that are also capable of stabilizing foams in the pores of the rock.

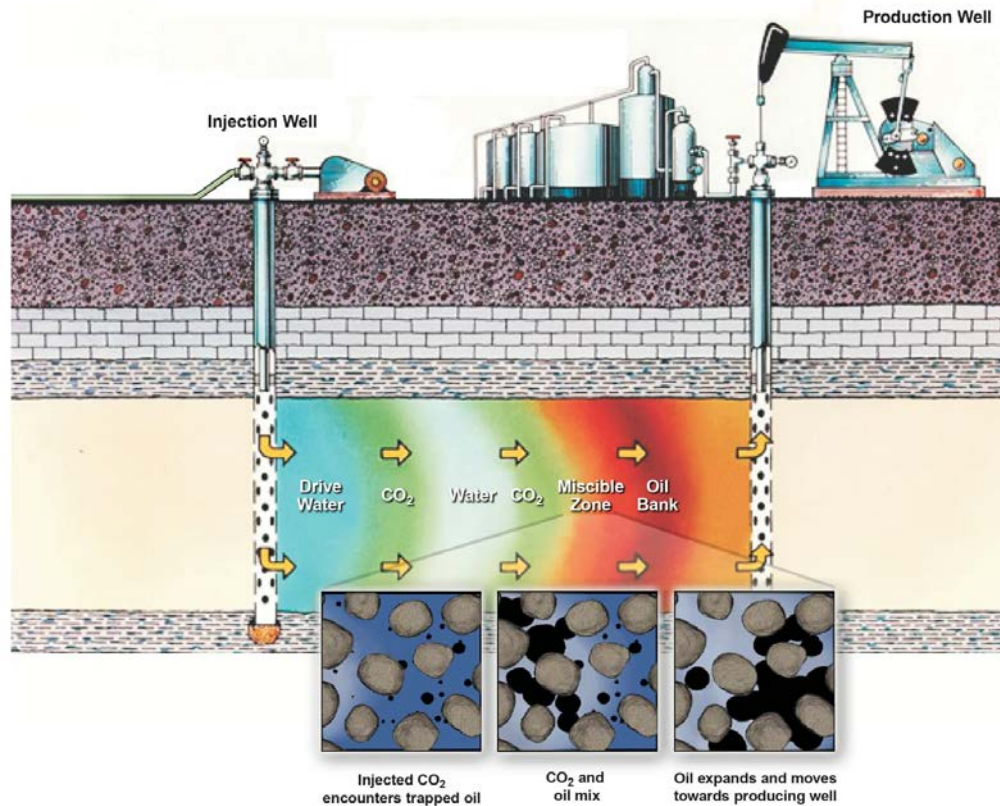


Figure 1.5 Simplified illustration of WAG injection process [6]

Rather than continuing to implement WAG processes that require substantial amounts of water in an attempt to lower gas permeability, or generate CO₂-in-brine foams to reduce the CO₂ mobility, CO₂ could be thickened by dissolving a dilute (<1wt%) amount of a “thickener” or “viscosifier” in the CO₂, thereby yielding a transparent, thermodynamically stable, high pressure CO₂-rich phase with a viscosity that is comparable to that of the oil being displaced. The thickener must be both CO₂-soluble and capable of dramatically increasing the viscosity of CO₂. The viscosity of CO₂ is ~0.05 cP at typical EOR conditions, and it must be thickened by a factor of ~20 to attain a viscosity comparable to that of water (1 cP), or by a factor of ~30 to attain the viscosity of a typical light oil (1.5 cP); the lightest oils have a viscosity of 0.5 cp. It would be ideal if the viscosity of the CO₂ could be made comparable to that of the oil, which can be as high

as 10 cP (a 200-fold increase) simply by changing its concentration in the CO₂. If an economic CO₂ thickener could be identified, favorable mobility ratios could be achieved during CO₂ floods without the need for water injection. Therefore the emphasis of this project is increasing the viscosity of the CO₂ by a factor of roughly 10-30 (~1000 – 3000% increase) via the dissolution of a dilute concentration of a thickener for the specific purpose of improving mobility control during EOR. Ultimately, the thickener would either adsorb onto the rock, partition into the oil or brine, or precipitate in the pores as the pressure of the CO₂ is reduced near the production well.

The notion of thickening CO₂ is not a new one; a substantial amount of work has been done on this topic since the early 1980s, and this body of work is thoroughly detailed in two DOE-sponsored literature reviews [5,7]

1.3 CO₂ SOLVENT CHARACTER

Dense CO₂ can act as a solvent as demonstrated by its use in EOR and supercritical fluid technology [1,8]. Although it is a rather weak solvent for most polar, ionic and high molecular weight compounds, it can dissolve low molecular weight volatiles [9–11]. It is a symmetric, linear molecule comprised of a central carbon atom bonded to two oxygen atoms resulting in a low dielectric constant and no dipole moment. However, the charge separation in the bonds themselves results in low polarizability and a significant quadrupole giving it the tendency to form site specific interactions [12,13].

CO₂ is hard to characterize with a single solvent parameter. The cohesive energy density of CO₂ is temperature and pressure dependent and at certain conditions, 400 bar 40°C, the simple Hildebrand solubility parameters of CO₂ and hexane are similar ($\delta=7.3 \text{ cal}^{1/2} \text{ cm}^{-3/2}$) leading us to

follow conventional wisdom of “like dissolves like” and the two are certainly miscible. The limitations of this method, which does not account for polar or hydrogen bonding interactions, quickly become apparent as CO₂ is miscible with high δ value methanol, dimethyl formamide, dimethyl sulfoxide, and N-methyl pyrrolidone [8].

Studies have shown that CO₂ has some polar attributes based on the notion of quadrupole-dipole interactions. As seen with sugar acetates and some fluorocarbons, the schematic in Figure 1.6 the electron deficient carbon is able to participate as an electron acceptor in Lewis acid-base pairings while the oxygen can simultaneously act as an electron donor or hydrogen bond acceptor [12–16]. These subtle modes of interaction are not captured by current solvent and solubility parameters. Consequently, CO₂ is incorrectly compared to various solvents even when using multicomponent solubility parameters [12].

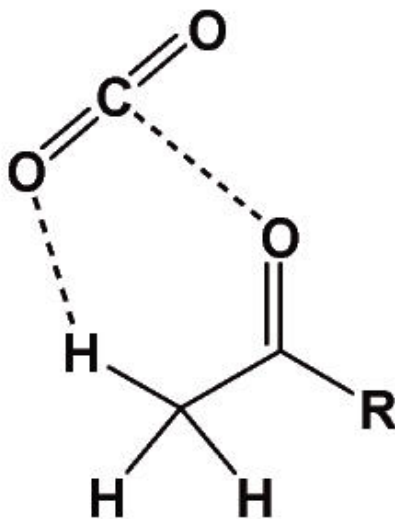


Figure 1.6 Schematic representation of the LA-LB interaction between the carbonyl oxygen atom and the carbon atom of CO₂ and the cooperative C-H...O hydrogen bonding between the CO₂ oxygen and the C_αH bond [13].

1.4 RESEARCH OBJECTIVES

Designing a CO₂ thickener candidate is not a trivial task due to CO₂'s limited solvent power. Past attempts dissolving non-fluorous high molecular weight (MW) polymers in CO₂ with the intention of thickening it have been largely unsuccessful, hence the new foray into using smaller molecules. Since smaller molecules with only slightly solvent-phobic associating groups may be easier to dissolve than a high MW polymer, our design strategies involve functionalization of CO₂-philic molecules/oligomers with moieties (proton donor/acceptors, aromatic groups) responsible for inducing intermolecular associations (hydrogen bonding, π - π stacking) between adjacent thickener molecules in solution. This is not unlike the general strategy used to thicken water or various organic solvents where a small molecule has a solvent-philic portion to impart solubility and a solvent-phobic portion that associates with itself resulting in a viscosity enhancing supramolecular structure [17–23]. As a starting point, guidelines for determining a CO₂-phile chain length are established by phase behavior of unfunctionalized oligomers which represent a “maximum solubility” of the molecule in question, in that the incorporation of associating groups will make the compound less soluble.

Determining the solubility of the designed molecule in CO₂ is crucial as a specific formation's physical state dictates the actual EOR pressure and temperature at which EOR will be conducted. The solubility experiments are conducted in a high pressure variable volume view cell in a controllable air bath. The pressures at which the one phase solution becomes a two-phase mixture, are determined visually and may be a cloud or bubble point depending on the system. The two phases are combinations of vapors, liquids, solids and fluids (supercritical). Ideally, the cloud point of the thickener candidate at the desired concentration in CO₂ would be at or below the minimum miscibility pressure (MMP) of the formation to ensure the solubility of

the compound in CO₂ at field conditions. Qualitative pressure-composition (P-x) diagrams of CO₂-solute mixtures are shown in Figures 1.7-1.13 where the solutes are either liquids or solids at room temperature and pressure.

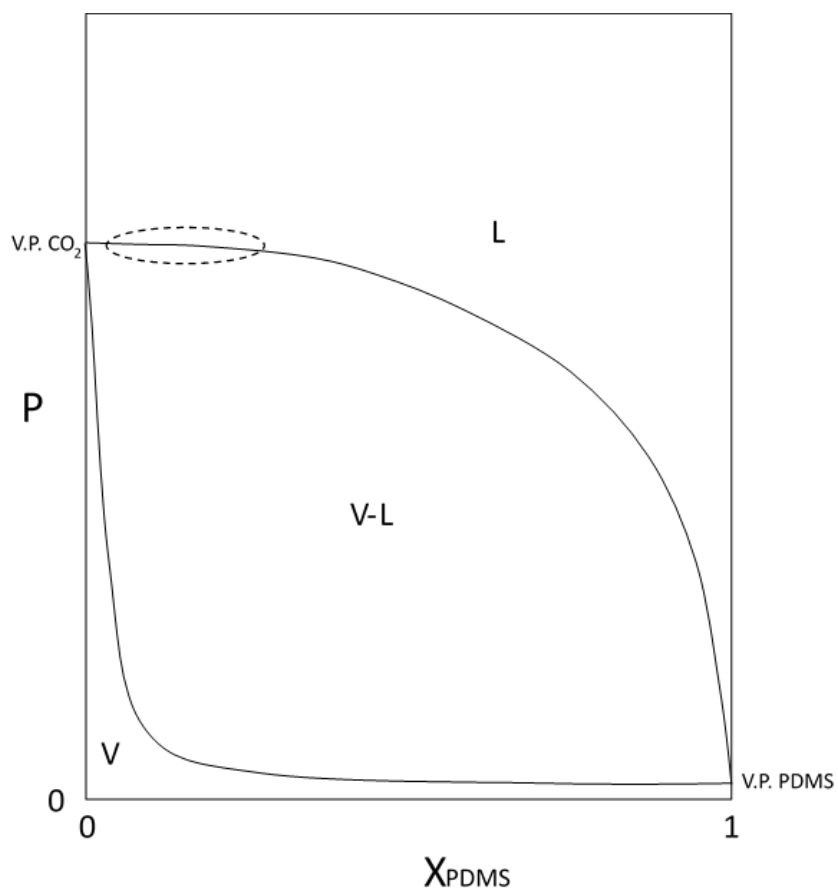


Figure 1.7 Qualitative P - x diagram illustrating the V-L region for sub-critical ($T < 31^\circ\text{C}$) mixtures of CO_2 with lower molecular weight PDMS. The dashed ellipse indicates region where V-L bubble points were measured. V.P. = vapor pressure

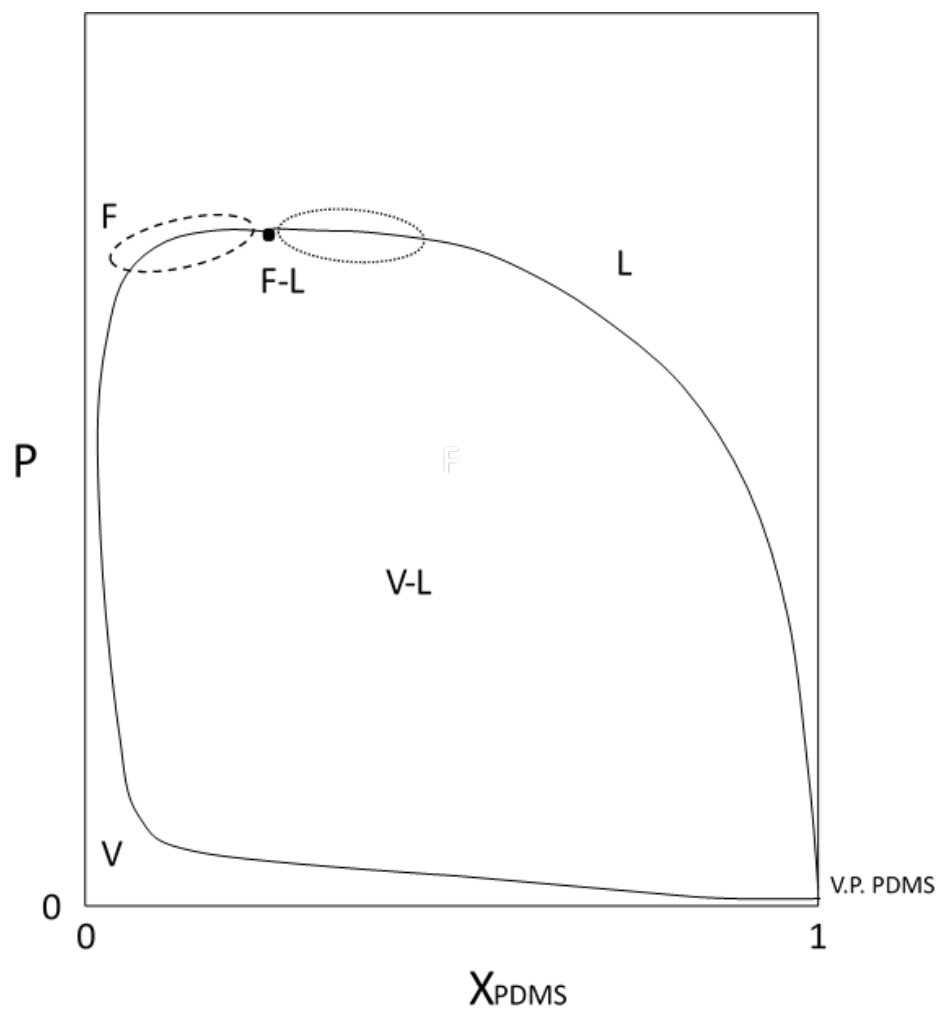


Figure 1.8 Qualitative P-x diagram illustrating the two-phase region for supercritical ($T > 31^{\circ}\text{C}$) mixtures of CO_2 with low molecular weight PDMS (237) dotted ellipse F-L bubble points; PDMS dashed ellipse F-L cloud/dew points. V.P. = vapor pressure

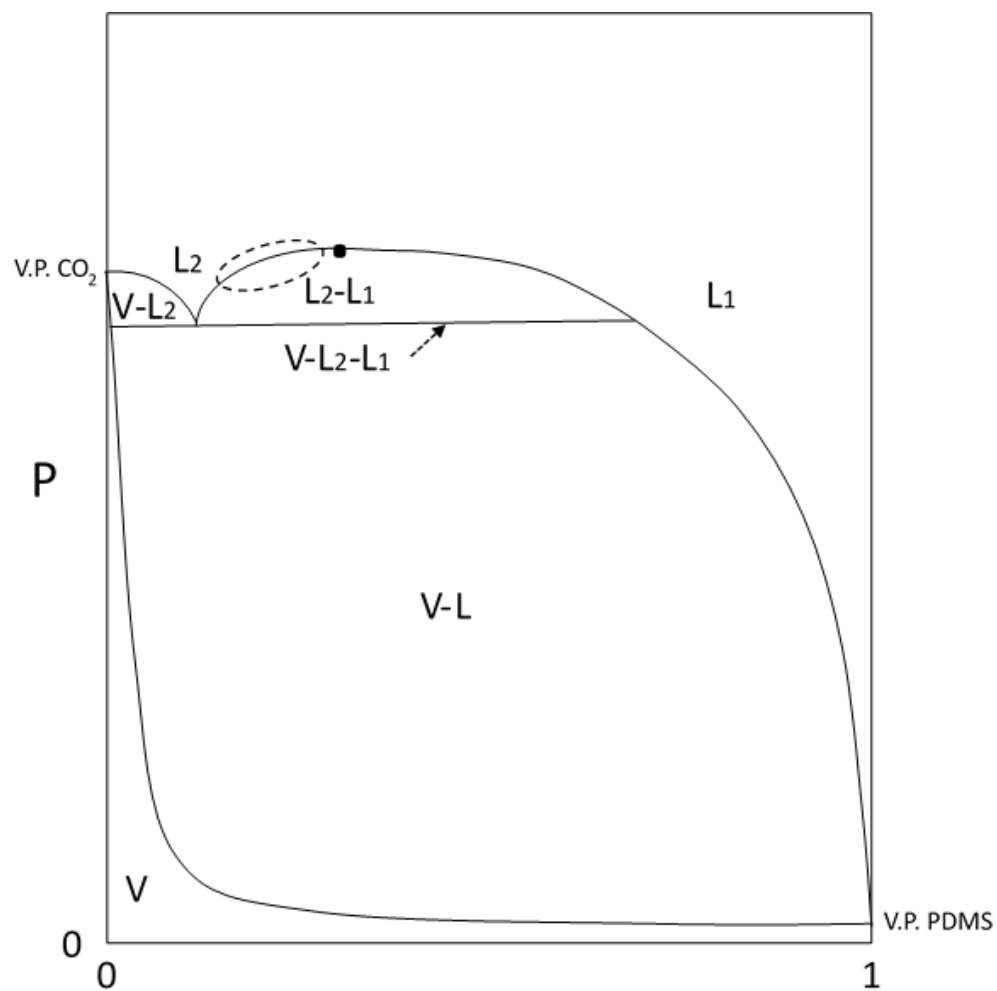


Figure 1.9 Qualitative P-x diagram illustrating the three two-phase regions and three-phase line for sub-critical ($T < 31^{\circ}\text{C}$) mixtures of CO_2 with higher molecular weight PDMS. The dashed ellipse indicates region where L2-L1 cloud/dew points were measured. V.P. = vapor pressure

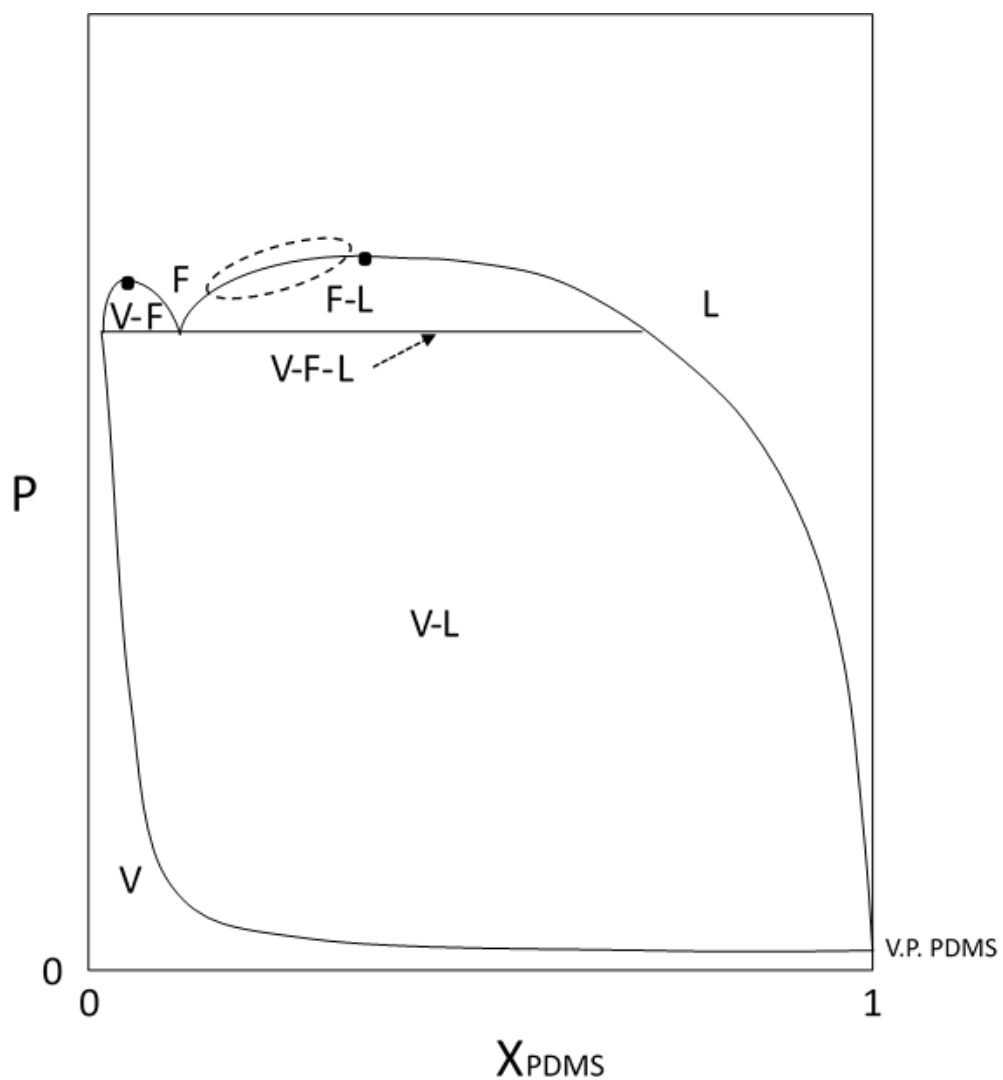


Figure 1.10 Qualitative P - x diagram illustrating the three two-phase regions and three-phase line for supercritical ($T > 31^\circ\text{C}$) mixtures of CO_2 with higher molecular weight PDMS. The dashed ellipse indicates region where F-L cloud/dew points were measured. V.P. = vapor pressure

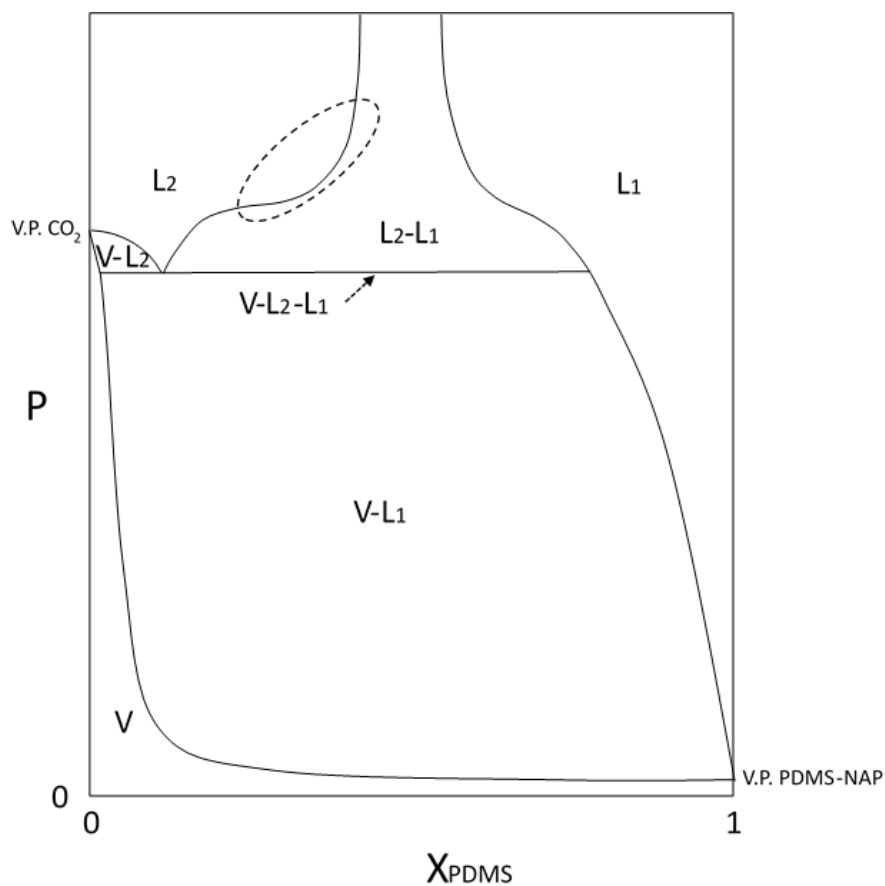


Figure 1.11 Qualitative P - x diagram illustrating the three two-phase regions and three-phase line for sub-critical ($T < 31^\circ\text{C}$) mixtures of CO_2 with PDMS-NAP. The dashed ellipse indicates region where L2-L1 cloud/dew points were measured for PDMS-NAP of intermediate molecular weight. V.P. = vapor pressure

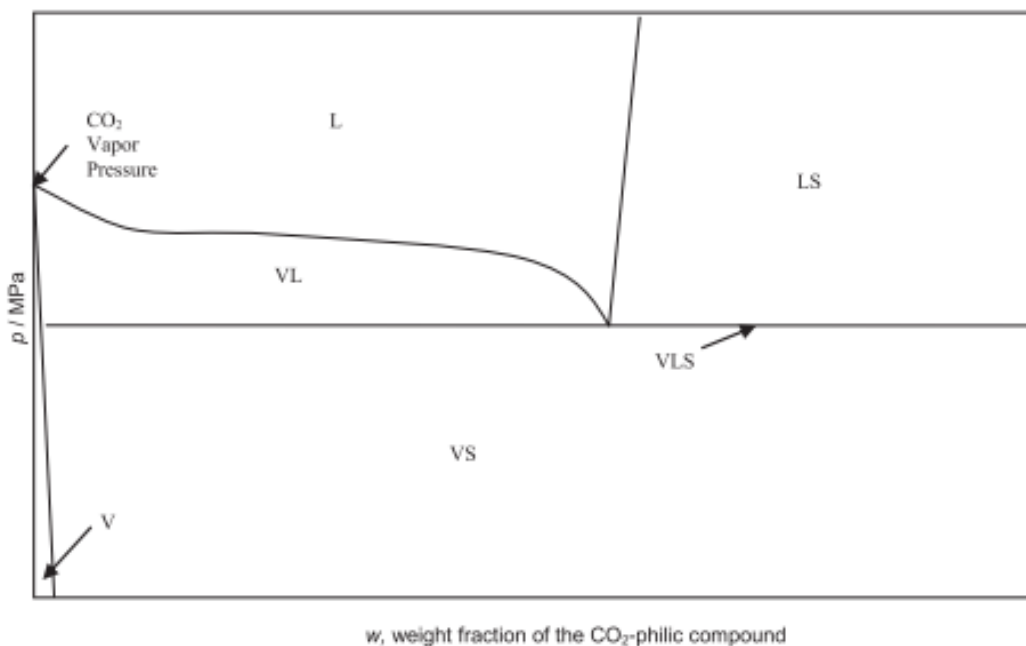


Figure 1.12 Qualitative P - x diagram illustrating the three two-phase regions and three-phase line for sub-critical ($T < 31^\circ\text{C}$) mixtures of CO_2 with CO_2 -philic solid [24].

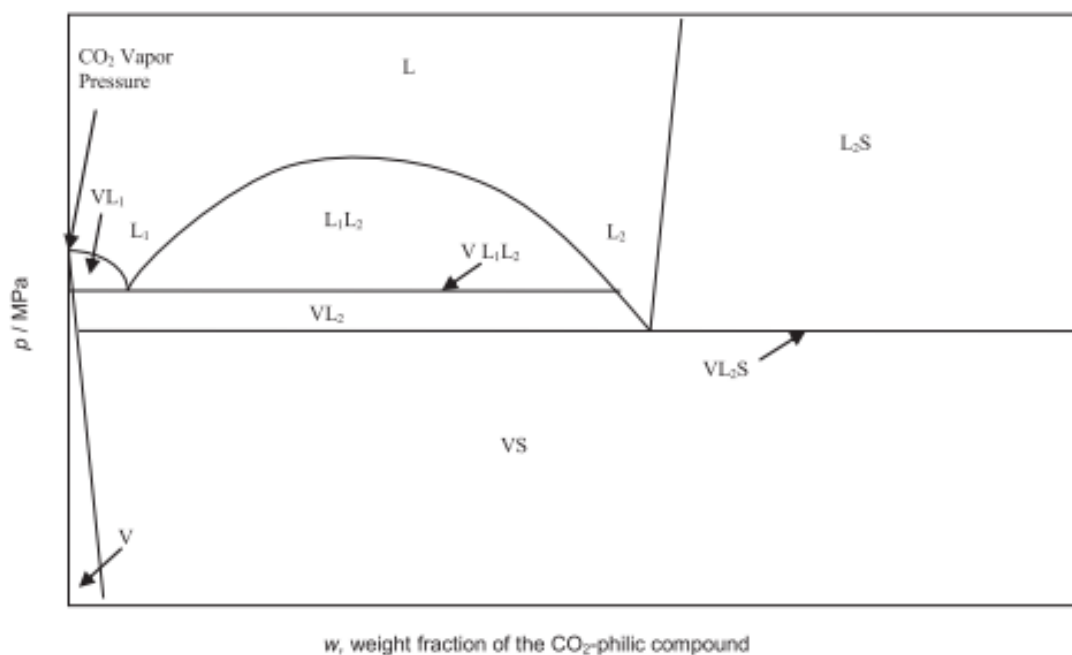


Figure 1.13 Qualitative P - x diagram of subcritical CO_2 - CO_2 -philic solid mixture exhibiting two three-phase lines [24].

Any CO₂-thickening candidate that demonstrates solubility in CO₂ will be assessed as a viscosity-enhancing agent. The viscosity will only be determined at single-phase conditions above the cloud point. To ensure that the CO₂-thickener solution will be a single, transparent, thermodynamically stable single phase at the test conditions, the solution viscosity can be tested with a windowed high pressure viscometer. A windowed falling object (cylinder or sphere) viscometer is available in our lab (rated to 10,000 psi at 180°C). The viscometer is windowed such that it is easy to verify that all of the thickener has been completely dissolved and remains completely dissolved during the test. Although non-windowed high pressure rolling ball viscometers are more common, one cannot tell if the long time required for the ball to roll down the inclined apparatus is due to the high viscosity of the solution or small un-dissolved thickener particles impeding the movement of the ball. Similarly, extreme caution must be employed with capillary viscometers because a small particle of un-dissolved thickener stuck in the capillary can restrict fluid flow and increase pressure drop, giving the illusion of high viscosity.

2.0 PREVIOUS ATTEMPTS AT THICKENING CO₂

Gels based on small molecule thickeners are generally an ensnarement of solvent molecules within a stable, self-assembled, fibrous three dimensional network of thickener molecules that span the entire liquid volume at dilute conditions of less than 5 wt% [17–23,25]. Figure 2.1 illustrates the formation of one dimensional aggregates via an anisotropic growth process followed by intertwining of these aggregates to form a 3D network. Polymeric thickeners have a degree of “pre-assembly” as they are initially held together in at least one dimension by covalent bonds [26]. The need for a heating and cooling cycle is dependent on the temperature dependence of thickener-thickener and thickener-solvent interactions. The prevention of crystallization or precipitation of the self-assembled aggregate is achieved through a delicate balance between order and disorder making the design of a thickener a tedious and difficult task. For CO₂ thickening, a transparent viscous fluid formed with a very dilute amount of the gelling agent is required for EOR rather than a rigid gel.

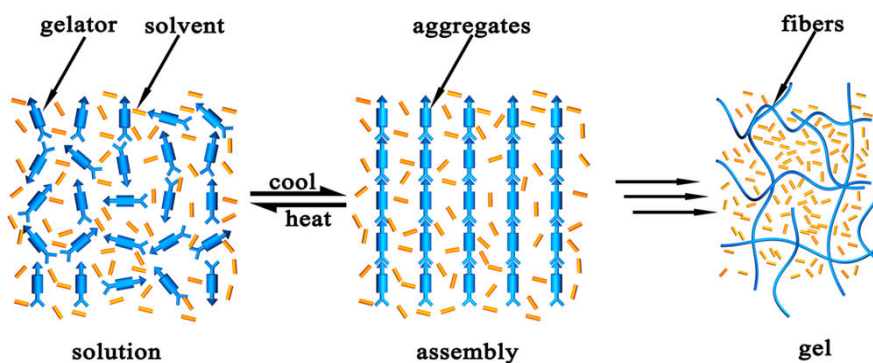


Figure 2.1 Schematic representation of thickener self-assembly into fibrous networks [20]

Over the past 30 years, there have been many attempts at thickening CO₂ but an effective and affordable thickener has not yet been identified. Past research efforts based on polymeric and small molecule candidates are outlined in the following sections.

2.1 POLYMERIC THICKENERS

The polymeric thickeners that are effective at dilute concentrations are those with the highest molecular weight. For example, water can be readily thickened with dilute concentrations (<1wt%) of high molecular weight ($\sim 10^7$) polyacrylamide. It has proven to be extraordinarily difficult to thicken CO₂ using polymers, primarily because CO₂ is a feeble solvent for high molecular weight polymers ($M_w > 10^5$). The initial attempts to thicken CO₂ were primarily associated with assessments of compounds used to thicken oils (rather than water) because CO₂ is miscible with many light oil components but only slightly soluble in water. Therefore, it was anticipated that non-polar organic polymers that were oil-soluble would be more likely to dissolve in CO₂ than water-soluble polymers. Heller and co-workers investigated numerous hydrocarbon polymers [9,27] and identified 18 polymers that exhibited solubility values of 0.22 to 10 g/liter (0.24 to 1.1wt%) at pressures of 1700 to 3100 psia, yet none of the polymers were capable of inducing significant viscosity increases in their falling cylinder experiments (viscosity increases were <25%). In general, in order to realize even a small measure of CO₂ solubility, the molecular weight of the polymers had to be $\sim 1,000$ or less, a value far below the high- and ultra-high molecular weights that characterize thickeners. Therefore we view with skepticism a recent claim [28] that some of the very same low molecular weight polymers identified by Heller can thicken CO₂ by a factor of ~ 15 in capillary viscometer tests at a concentration of 0.5wt%. In our

labs we recently found that at 0.5wt% these polymers cannot induce a 5% increase in liquid CO₂ viscosity in high-pressure falling cylinder and rolling ball viscometry tests.

In a patent related to CO₂ fracturing [29], the inventors claimed that CO₂ can be thickened with the addition of a small amount of a polycarbonate copolymer (Mw of 20000 – 150000) that is formed via the ~16 hour long, low-temperature reaction of the CO₂ with an alkene oxide, preferably propylene oxide, catalyzed by a homogeneous catalyst (e.g. diethylzinc and/or acetic acid anhydride) dissolved in a CO₂-miscible organic solvent. A (propylene oxide/acetic acid anhydride/zinc acetate/1,4-dioxane) mixture was reacted and then added at 1.75wt% of a CO₂ stream to successfully fracture a well with good results, but the patent presented no details of the viscometer nor analysis of the viscosity results.

Chevron researchers [30] selected candidates that exhibited solubility parameters less than $\sim 7 \text{ (cal/cc)}^{0.5}$ in an attempt to match the temperature- and pressure-dependent solubility parameter of CO₂ [31] at typically encountered pressures, which is roughly $6 \text{ (cal/cc)}^{0.5}$. It was determined that very high molecular weight silicone oil (polydimethylsiloxane, PDMS, Mw = 197,000) could effectively thicken (by a factor up to ~ 100) CO₂ flowing through either a capillary tube viscometer or a sandstone or carbonate core, but only if a significant amount (20%) of a co-solvent such as toluene was added. Oil recovery results from core floods clearly demonstrated that relative to WAG, the thickened CO₂ significantly delayed breakthrough, increased the rate of oil recovery, and increased the ultimate amount of oil recovery from the core.

The first breakthrough concerning the design of high molecular weight polymers capable of dissolving in CO₂ at moderate pressures without the need for a co-solvent was reported by DeSimone and co-workers [32]. These researchers found that poly(1-,1-, dihydroperfluorooctyl

acrylate) (a.k.a. PFOA, PFA or polyfluoroacrylate), $M_w = 1,400,000$, could dissolve in CO_2 and induce a significant increase in viscosity by a factor of 2.5 using 3.7 wt/vol % (0.037g/ml) at 4500 psia and 50 °C as measured with a falling object viscometer.

Enick, Beckman, and co-workers developed a functionalized version of PFA in hopes of attaining greater increases in viscosity at lower concentrations. Therefore they synthesized a co-polymer based on fluoroacrylate (to enhance CO_2 solubility) and an associative group (to promote intermolecular interactions that enhance viscosity) [33,34]. The most effective thickener was a random co-polymer composed of ~79 mol% of a CO_2 -philic fluoroacrylate monomer (1-,1,2-,2-tetrahydro heptadecafluorodecylacrylate) and 21 mol% of a mildly CO_2 - phobic monomer with a pendant associating group, in this case styrene. The styrene monomers and fluoroacrylate monomers reacted in such a manner that there was a random alternation of these two monomers in the polymer. Although not as common as other types of polar or ionic associating groups, aromatic rings are known to associate with one another via a mechanism referred to as π - π stacking, which results from a different electron density along the periphery of the aromatic ring than in the core of the ring. This fluoroacrylate-styrene copolymeric thickener, referred to as polyFAST, was capable of thickening CO_2 in both falling cylinder viscometry (by factor of ~50 at 3 wt %) and mobility measurements using Berea sandstone cores (by a factor of ~20 at a superficial velocity of 1'/day at 1.5wt%). To date, this is still the only compound that has been demonstrated to thicken CO_2 under CO_2 EOR conditions without the need for a co-solvent. However, the high cost of the fluoroacrylate monomer makes it impractical for EOR unless the polymer is effective at extremely low concentrations. Key lessons from the design of polyFAST that can be transferred to other thickeners include the use of CO_2 -philic groups to enhance solubility and the use of weakly associating phenyl groups to enhance viscosity because

the phenyl-phenyl associations are sufficient to create physical networks in solution, yet not so strong as to impede dissolution of the thickener in CO₂.

Enick and co-workers then examined the design of a non-fluorinated version of polyFAST in the hope of identifying a cost-effective thickener. Because polyvinyl acetate (PVAc) has been shown to be the most CO₂-philic oxygenated hydrocarbon polymer [15], an attempt was made to copolymerize vinyl acetate with a monomer containing a pendant aromatic ring, thereby making a non-fluorous analog of polyFAST. This resulted in the successful synthesis of polyBOVA, a benzoyl-vinyl acetate copolymer. Although modest increases in CO₂ viscosity of ~40% and ~80% were realized at 1 and 2wt% concentrations of polyBOVA, the pressure required to dissolve this vinyl acetate-styrene random polymer (Mw = 12,000) in CO₂ was more than ~64 MPa (~ 9,300 psia) at 25°C [35].

In summary, despite over 30 years of work, an affordable, non-fluorous, polymeric or copolymeric CO₂ thickener capable of dissolving in CO₂ in dilute concentrations under typical field pressures and increasing the CO₂ viscosity by a factor of ~20-30 has yet to be identified. Further, the likelihood of such an affordable polymeric thickener for EOR conditions being discovered is very low because an incredibly wide array of polymers has been considered, including new polymers designed specifically for CO₂ solubility. Only the expensive and environmentally suspect fluoroacrylate-based high molecular weight polymers could dissolve in CO₂ and thicken it at reservoir conditions; significant amounts of organic co-solvents would be required for silicone or hydrocarbon-based polymers to dissolve in CO₂ at pressures similar to the MMP. Therefore in the proposed work we will not consider new high molecular weight polymers.

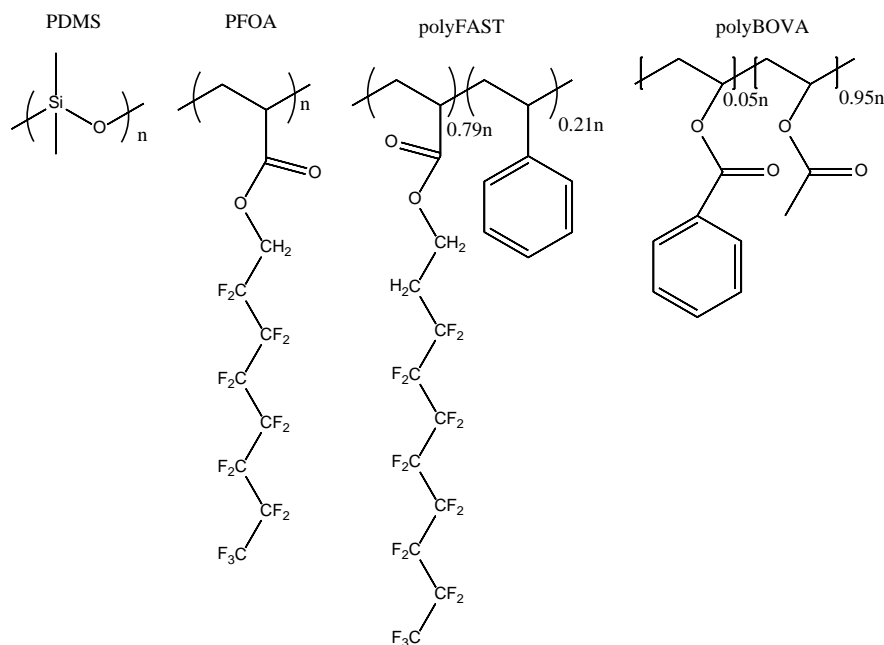


Figure 2.2: Polymeric CO₂ thickeners. PDMS requires co-solvent, PFOA and polyFAST are effective without co-solvent, polyBOVA is modest thickener that requires extremely high pressure for dissolution

2.2 SMALL MOLECULE THICKENERS

The second strategy that has been explored for CO₂ thickeners has been the design of small molecules that have the capability to associate and form viscosity-enhancing supramolecular structures. In each case, the molecule contains a segment that is sufficiently CO₂-philic to promote dissolution of the compound in CO₂ plus one or more CO₂-phobic moieties that are intended to be attracted to/associate with the CO₂-phobic moieties of neighboring molecules, thereby establishing a viscosity-enhancing, associating, non-covalently bound, macromolecular network. While self-assembly of these thickeners can certainly be inferred by dramatic changes in viscosity, more quantitative proof of self-assembly can be obtained via small angle neutron scattering (SANS), circular dichroism, FT-IR, x-ray diffraction, differential scanning

calorimetry, and electron microscopy [20,21,23,36–41]. There has been little success in using small, associating molecules to thicken CO₂, primarily because CO₂ is an extremely poor solvent for the polar and ionic associating groups that are commonly incorporated into small molecule thickeners. High pressure SANS has been used in the past to determine aggregate geometries in CO₂ [32,37,38,42–44]

2.2.1 Trialkyltin fluorides and semi-fluorinated trialkyltin fluorides

Heller and co-workers recognized the remarkable ability of tributyltin fluoride to induce incredibly large viscosity increases in light alkanes at dilute concentration (e.g., ~ three orders of magnitude at 1wt%, with no heating required to attain dissolution in some solvents). The tin atom is slightly electropositive and the fluorine atom is electronegative, while the three butyl arms extending from the tin atom enhance the solubility of the molecule in alkanes. These molecules apparently form linear, transient, associating polymers in solution as the tin atom of one molecule is attracted to the fluorine atom of the neighboring molecule. The butyl arms do not interfere with these associations and help to stabilize the linear macromolecule. Unfortunately, neither tributyltin fluoride nor any other trialkyltin fluoride synthesized by Heller was CO₂-soluble enough to serve as a CO₂ thickener, although some success was realized in thickening propane and butane [45,46]. After it had been established that fluorination of alkyl groups could enhance CO₂ solubility, Enick and co-workers synthesized tri(2-perfluorobutyl ethyl)tin fluoride [47]; although this compound was soluble in CO₂ without the need for a co-solvent the viscosity increase was far less than expected (factor of 3 at 3 wt%). Apparently, the fluorine atoms at the ends of the C₆ arms of the compounds competed with the fluorine atom bound to the tin, thereby disrupting the formation of extraordinarily long associating polymers.

2.2.2 Hydroxyaluminum disoaps and fluorinated hydroxyaluminum disoaps

Perhaps one of the most famous hydrocarbon thickeners was developed for the purpose of weaponizing gasoline [48]. Dilute concentrations of a hydroxyaluminum disoap transformed low-viscosity gasoline into a sticky, extremely high viscosity fluid referred to by the trade name Napalm. This aluminum disoap dissolves in light alkanes via heating, and self-assembles into long, cylindrical, viscosity-enhancing, dry micelles during cooling. The core of this macromolecular structure is composed of the hydroxyaluminum head groups (electropositive aluminum, electronegative oxygen atoms in the hydroxyl group). Rather than using the mixture of disoaps found in Napalm, it has been established that the most dramatic thickening can be attained with 2-ethyl hexanoate chains that provide the precise stiffness and steric hindrance required for the micelles to form cylindrical (rather than spherical) micelles. A modest change in the structure, such as the use of linear, rather than branched C8 chains, causes the surfactant to lose its ability to thicken the oil. Enick and co-workers synthesized a series of hydroxyaluminum disoaps in the hope of identifying a CO₂ soluble version capable of thickening CO₂. Although some of these disoaps can thicken propane, none of the hydroxyaluminum disoaps were CO₂ soluble [49]. Recent unpublished results from Enick's lab have shown that even when the alkyl arms of the disoap are fluorinated, or when they are replaced with highly branched alkyl chains that have been shown to enhance CO₂ solubility of some small compounds [50], the resultant hydroxyaluminum disoaps remained CO₂ insoluble. Attempts to thicken CO₂ by heating a mixture of CO₂ and metallic stearate powders were also unsuccessful. When this mixture is heated in hydrocarbon oils, the attractive forces between these compounds are weakened,

enabling the compound to dissolve in the oil and form viscosity enhancing metallic stearates as the solution cools. Even at high temperature and pressure conditions, however, the metallic stearates could not dissolve in CO₂ [51].

2.2.3 Bis-Ureas

Researchers at the University of Pittsburgh and Yale University designed small compounds with either one or two urea groups. Urea groups can interact via hydrogen bonding with urea groups in neighboring molecules and “stack” in solution, thereby providing a mechanism for the formation of long, viscosity enhancing, associating macromolecules in CO₂-rich solutions [52]. In four of the twelve compounds studied, the bis-urea was capable of dissolving in CO₂ without being heated and increasing the viscosity of CO₂ by factors of about 3–5 at concentrations of ~5wt% at 25 °C and 4,500 psia. In an attempt to design a non-fluorous analog of these expensive bis-ureas, CO₂-philic hydrocarbon groups and CO₂-philic carbonyl and ether groups were incorporated into the structure [53]. It was hoped that these compounds might also dissolve in CO₂, self-assemble into long rods, remain in solution, and thicken CO₂. Several non-fluorinated, hydrocarbon-based compounds were CO₂ soluble at 25 °C to ~1wt% at elevated pressures of 9000 psi and 9400 psi, respectively. This single-phase, transparent solution slowly turned into a dispersion of interlocking white fibers at a constant temperature and pressure, however. Apparently, as the molecules began to self-assemble, they came out of solution and formed fibers rather than remaining in solution and thickening CO₂.

2.2.4 Fluorinated, dual, twin-tailed surfactants with divalent metal cations

Researchers at Bristol University and the University of Pittsburgh designed surfactants that were not only CO₂-soluble, but also capable of forming viscosity-enhancing rodlike micelles with the addition of small amounts of water [37]. The design of the surfactant was based on previous observations for normal AOT-stabilized microemulsions in organic solvents, such as cyclohexane. In such systems, the exchange of Na⁺ with Co²⁺ or Ni²⁺ is known to drive a sphere-to-rod transition, promoting viscosity enhancements up to 40-fold at 10 wt % surfactant [38,42,54]. Modeling of small-angle neutron scattering (SANS) data is consistent with occurrence of rigid, rather than flexible, micellar rods. Eastoe and co-workers at Bristol University synthesized the semi-fluorinated, CO₂-soluble surfactants shown in Figure 2.3 [37], which were assessed at our facilities at the University of Pittsburgh. These compounds are the first CO₂-soluble surfactants that do not require a co-solvent for dissolution and are capable of thickening CO₂. However, the pressure required for dissolution is very high, the required concentration to generate viscosity-enhancing rodlike micelles is high (5-7 wt%), and the viscosity increase was modest (50-80%).

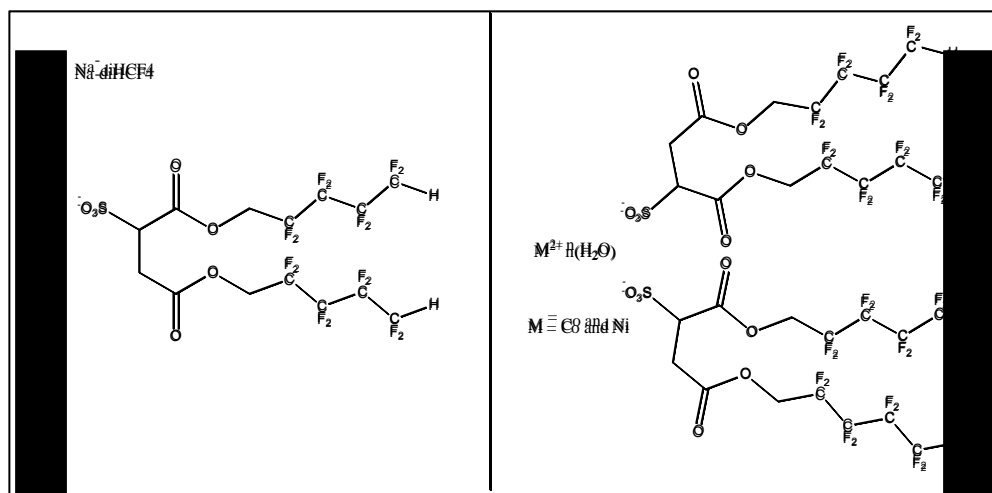


Figure 2.3: Fluorinated twin-tailed surfactants, the divalent version (right) provided modest CO_2 thickening

2.2.5 Other compounds

A number of other low molecular weight compounds that have been shown to form gels in organic solvents were also evaluated as thickeners for CO_2 (metallic stearates, 12-hydroxystearic acid, hydrocarbon and/or aromatic co-solvents, diesel fuel thickeners, alkyl amines, semi-fluorinated alkanes, fluorinated ureas, fluorinated ionic surfactants), however none of these were able to thicken CO_2 , owing to either poor solubility in CO_2 or the formation of dispersed microfibers in CO_2 (rather than transparent, viscous, stable solutions that could flow through porous media) once dissolved [5,7]. We consider suspect a patent containing capillary viscometry results indicating that the addition of 2.3wt% of ethylene glycol to supercritical CO_2 can roughly triple or quadruple its viscosity [28]; we recently prepared such solutions in our labs and displaced them through sandstone cores at superficial velocities of 1-10 ft/day and observed decreases in mobility no greater than 5% (i.e. 5% increase in apparent viscosity) relative to pure CO_2 .

3.0 EXPERIMENTAL METHODS

3.1 PHASE BEHAVIOR

The solubility of the silicone solutes in CO₂ were determined via a standard, non-sampling technique using a high pressure, windowed, agitated, variable-volume view cell [DB Robinson – Schlumberger] rated to 10,000 psig and at 180°C with a constant temperature air bath (-20 °C to 180°C, ±1°C) [55]. A stainless steel phase behavior cell with two thick borosilicate opposing windows retains a thick-walled Pyrex tube (3.175 cm I.D.). This tube contains a sliding (i.e. floating) piston with an O-ring around its perimeter that separates the (CO₂ + solute) sample volume above the seal from the transparent overburden liquid below. Because a pressure drop of ~ 4 psi is required to move the piston, the pressure in the sample volume is about the same as the pressure of the overburden fluid. The overburden fluid also surrounds the Pyrex tube and a short length of tubing ensures that the pressure of the overburden fluid below the sample volume and the pressure around the Pyrex tube are equivalent; therefore there is no pressure drop across the Pyrex tube wall.

Initially, a specified amount of solute is weighed out on the piston before insertion into the Pyrex tube. Overburden fluid is pumped around and then into the bottom of the tube (below the floating piston) to displace the floating piston upward, thereby minimizing the sample volume. The small vapor space in the sample volume is purged of air with CO₂. A known

amount of CO₂ is then added to the sample from a positive displacement pump to obtain the desired composition. Typically, this is accomplished by injecting compressed liquid CO₂ into the sample volume at the same volumetric flow rate (± 0.01 cm³/hour) as the overburden fluid is withdrawn, which results in a well-controlled, isothermal, isobaric addition of CO₂ into the sample volume. The volume of CO₂ (± 0.01 cm³) that is introduced is determined by the software settings and confirmed by tracking the graduations on the positive displacement pump. The mass of CO₂ is determined as the product of the added CO₂ volume and the CO₂ density as estimated with the NIST web book correlation [56]. The valve at the top of the sample volume is closed after the desired amount of CO₂ has been introduced, which isolates the mixture.

The mixture of invariant overall composition is then compressed and stirred using a magnetically driven slotted fin impeller spinning at 2500 rpm at elevated pressure as high as 10,000 psig at the temperature of interest until a transparent, single-phase solution was attained. A light source behind the cell allows the observer to look through the flat glass windows of the high pressure vessel, the overburden fluid, and the wall of the Pyrex tube to view the single phase residing within the entire sample volume.

The mixture is then expanded very slowly via the withdrawal of the overburden fluid situated below the floating piston until a second phase appears in the sample volume. Typically, a solute-rich cloud point is observed in the form of a fine mist of droplets precipitating throughout the sample volume. In order to provide a reproducible and conservative measure of solubility (i.e. so as to not overestimate the solubility), the cloud point pressure is reported as the pressure at which the extremely fine suspended droplets prevent one from seeing clearly through the solution (i.e. the outlines of objects behind the sample volume could not be discerned). This cloud pressure value is typically 70-100 psi greater than the lower cloud point pressure at which

a greater proportion of the solute comes out of solution and the sample volume becomes opaque. The measurement was repeated at least three times with a reproducibility of ± 100 psi.

3.2 CLOSE CLEARANCE FALLING BALL VISCOMETRY

Solution viscosities were assessed using the previously mentioned pressure cell as a close clearance, high pressure falling ball viscometer [57]. A Pyrex ball (2.23 gr/cm³, 3.1587 cm diameter) is present at the bottom of the sample volume along with the mixture and a transparent single phase solution is established in the Pyrex tube (3.1750 cm I.D.) at a pressure 500-1000 psi above the cloud point for a given temperature. The entire cell is then inverted rapidly and the terminal velocity of ball is measured at the mid-point of its fall by measuring the time required for the ball to fall 2 cm. The terminal velocity is also measured in the neat solvent mixture keeping the CO₂ concentration constant while the mass of the absent solute is replaced with additional hexane. Terminal velocity measurements are repeated 10 times and average terminal velocity is recorded.

Relative viscosities are reported and defined as the ratio of the viscosity of the solution with a dissolved thickener to the viscosity of the pure fluid, $\mu_{\text{solution}}/\mu_0$. Assuming that the density is not significantly affected by the dilute thickener concentration, the ratio of fall times between two points, $t_{f,\text{sol}}/t_{f,0}$, also represents the relative viscosity as shown below.

$$\text{Relative Viscosity} = \frac{\mu_{\text{sol}}}{\mu_0} = \frac{t_{f,\text{sol}}}{t_{f,0}}$$

Where, μ_{sol} is viscosity of solution containing a specified amount of thickener, μ_0 is viscosity of the pure fluid, $t_{\text{f,sol}}$ is fall time of ball in solution with thickener compound and $t_{\text{f,0}}$ is fall time of the ball in the fluid without the thickener. Our group has used this procedure previously with a falling cylinder to determine the effectiveness of a polyfluoroacrylate polymer to thicken CO_2 [33,34,58]. For experiments conducted with liquid CO_2 at 25°C , the surface-area average shear rate at the surface of the falling ball is roughly $70000/(\text{relative viscosity}) \text{ s}^{-1}$ [59].



Figure 3.1 Falling ball in Pyrex tube prior to assembly

3.3 SYNTHETIC METHODS AND CHARACTERIZATION

The functionalized silicone compounds studied in this work were designed via a collaboration of the University of Pittsburgh (Lee, Enick and Beckman) and GE Global Research (Perry, Doherty and O'Brien). Synthesis and characterization were performed by our collaborators at General Electric Global. General synthetic procedures provided by GE Global are reported throughout this document. Compound naming/numbering is consistent only within their respective chapters. Cross chapter referencing will include the relevant chapter information. For example, if compound 3a from chapter 5 is referenced in chapter 6, the compound will be referred to as compound 5-3a.

4.0 PHASE BEHAVIOR OF LINEAR PDMS WITH AROMATIC ENDGROUPS

Numerous investigators have tailored novel molecules with highly CO₂-philic moieties to enhance their solubility in liquid or supercritical CO₂. CO₂-philes composed of fluoroalkane [16,44,60–62], polyfluoroacrylate [34,63–66] and polyfluoroethers [67–69] have been particularly effective, however their expense and the environmental persistence of some of these fluorinated compounds and their degradation products have limited their widespread commercial use. Highly oxygenated amorphous hydrocarbon polymers, such as polypropylene glycol, polyvinyl acetate or amorphous polylactic acid, exploit Lewis acid-base interactions between the carbon atom of CO₂ and the ether and carbonyl oxygens, and between hydrogen atoms and the oxygen of CO₂ to impart CO₂-philicity [15,35,41,70–73]. However, the pressure required to attain solubility in CO₂ with these oxygenated hydrocarbon oligomers and polymers can be unacceptably high. Low molecular weight sugar acetates [74] and oligomers of cellulose triacetate exhibit a high degree of CO₂-philicity, although high molecular weight cellulose triacetate polymers are CO₂-insoluble due to their crystallinity and consequent high melting temperatures [14].

Polydimethyl siloxane (PDMS) has emerged as a compromise CO₂-philic segment between the previously mentioned fluorinated materials and oxygenated hydrocarbons. Although it is not as CO₂-philic as a polyfluoroacrylate, it is much more soluble in CO₂ than oxygenated hydrocarbon polymers of comparable molecular weight [70]. PDMS is an

inexpensive, environmentally benign polymer [75] that is commercially available in large amounts over an extremely wide molecular weight range. Although PDMS is most commonly found in a trimethylsilyl-terminated product, it is also available in a hydroxy-terminated form that is also CO₂ soluble [76]. Commercially available forms of PDMS are typically polydisperse, although a narrow molecular weight distribution can be obtained via supercritical CO₂ fractionation [77]. Extremely high molecular weight PDMS has even been suggested as a CO₂-thickener for improved mobility control during CO₂ enhanced oil recovery, although the large amount of toluene (e.g. 20 vol.% toluene + 80 vol.% CO₂) that is required as a co-solvent is problematic [30]. CO₂ swells PDMS extensively, therefore PDMS has been suggested as a pre-combustion CO₂-selective solvent for the extraction of CO₂ from a warm, gaseous post-water-gas shift reactor stream that also contains hydrogen and water [55,78].

Phase behavior of mixtures of CO₂ and high molecular weight hydroxy-terminated [76] and trimethylsilyl-terminated [79–81] PDMS (38000 < Mw < 170000) have been thoroughly examined at concentrations below ~10wt% PDMS in CO₂ over the 25-180 °C temperature range. For example, at 50°C, the cloud point pressure of a 5wt% solution of PDMS (Mw 38900) in CO₂ is approximately 27 MPa. However, phase behavior data for mixtures of CO₂ and lower molecular weight (<10000 g/mol) trimethylsilyl-terminated PDMS are not plentiful. Alessi *et al.* [82] have studied the solubility of low molecular weight PDMS (5970 and 2000) samples over a temperature range of 40-60°C at dilute concentrations (<0.1wt%) using a gravimetric method. Our group considered PDMS as a pre-combustion CO₂ solvent and studied the swelling of low molecular weight PDMS (Mn = 237) by CO₂ [55]. There remains a substantial gap in the literature for bubble and cloud point pressures for mixtures of CO₂ with low molecular weight PDMS in the 410 – 10000 g/mol range commensurate with the size of small molecule thickeners.

Therefore, the first objective of this study was to determine the phase behavior of a series of trimethylsilyl-terminated PDMS samples (Mw 410 - 10000 g/mol) at dilute concentrations of 1-4wt% in CO₂ at 23°C and 40°C. It is expected that mixtures of CO₂ and the lowest molecular weight PDMS will exhibit the greatest degree of miscibility, as evidenced by the lowest two-phase pressure boundaries.

PDMS is of particular interest in the generation of CO₂-soluble amphiphiles because this silicone polymer is relatively easy to end-functionalize. Therefore PDMS has been used as a CO₂-philic segment in conjunction with CO₂-phobic functional groups in the design of novel CO₂-soluble dispersants [83], surfactants [84–88], chelating agents [89], and post-combustion CO₂ capture solvents [90], as shown in Table 4.1. However, the effect of varying the molecular weight of the PDMS segment on the CO₂-solubility of an end-functionalized PDMS has not been systematically documented in these prior studies. Therefore, the second objective of this study was to determine whether there is an optimal PDMS molecular weight for enhancing the CO₂-solubility of a compound composed of a CO₂-philic PDMS segment that is decorated with a CO₂-phobic group (e.g. ionic, polar, hydrogen-bonding, chelating, associating or aromatic).

Table 4.1 Novel CO₂-soluble compounds composed of a CO₂-philic PDMS segment and CO₂-phobic functional groups.

Ref.	PDMS MW	No. of DMS Units	Head group; CO ₂ -phobe	Application
[83]	9900	131	pyrrolidone carboxylic acid, monomethylmethacrylate (required cosolvent)	dispersant
[84]	5000- 20000	70-270	poly(methyl acrylate), poly(acrylic acid)	surfactant
[85]	8280	110	pyrrolidone carboxylic acid, poly(ethylene glycol-co-propylene glycol)	surfactant
[86]	1900	26	allyl glycidyl ether, ammonium chloride	surfactant
[87]	9623	130	methacryloxy	surfactant
[88]	890- 13000	12-175	sulfonate, carboxysulfonate, poly(propylene glycol), poly(ethylene glycol)	surfactant
[89]	150-220	2-3	diphosphate	ligand
[90]	70-670	1-9	alkyl primary and secondary amines	post-combustion CO ₂ capture solvent

Based on our prior studies of fluoroether-functionalized surfactants [69], it is unlikely that the greatest CO₂ solubility will be attained for the lowest molecular weight PDMS segment. If the molecular weight of the PDMS is too low, the favorable enthalpic interactions between the PDMS and CO₂ can be overwhelmed by the highly unfavorable enthalpic interactions between CO₂ and the CO₂-phobic groups, rendering the compound CO₂-insoluble. However, if the molecular weight of the PDMS is too high, the compound may be CO₂-insoluble due to entropic effects associated with the disparity in the molecular weights of CO₂ and PDMS, coupled with the unfavorable enthalpic interactions associated with the CO₂-phobic functionalities and CO₂. It is therefore likely that an optimal PDMS molecular weight exists at which the end-functionalized PDMS exhibits the greatest solubility in CO₂.

The third objective of this study was to synthesize numerous other end-functionalized CO₂-soluble PDMS-based compounds based on these principles and rank the CO₂-phobicity of the functional groups based on acquired cloud point data.

4.1 MATERIALS

Six oligomers and polymers of dimethyl siloxane were received from Gelest and used as received. Table 2 provides a list of the average molecular weight and number of repeat units for these compounds. The average molecular weights and corresponding number of repeat units of five α,ω -bis(2-ethylnaphthyl)polydimethylsiloxane (PDMS-NAP) materials prepared according to the procedure which follows are also included in Table 4.2.

Table 4.2 Polydimethylsiloxane (PDMS) and α,ω -bis(2-ethylnaphthyl)polydimethylsiloxane (PDMS-NAP) samples.

Composition	Avg. MW Of compound	No. of Repeat DMS Units n of Fig 2.	Mw of PDMS segment
PDMS	410	3.3	410
PDMS	1250	14.7	1250
PDMS	2000	24.8	2000
PDMS	3780	48.8	3780
PDMS	5970	78.3	5970
PDMS	9430	125	9430
PDMS-NAP	454	0	132
PDMS-NAP	1181	9.8	859
PDMS-NAP	1530	14.5	1207
PDMS-NAP	2679	30.0	2357
PDMS-NAP	5986	74.6	5664

4.1.1 General hydrosilylation procedure for vinyl compounds

Hydride terminated siloxane was dissolved in toluene in a three neck flask containing a magnetic stir bar and fitted with a N₂ inlet, thermometer and addition funnel. Approximately 0.1 molar equivalents of olefin were added to the stirring solution followed by 3-5 drops of a 4 mol% xylene solution of Karstedt's Pt⁰ catalyst resulting in a light yellow solution. The remaining olefin (10% molar excess relative to number of silicon hydrides) was introduced to the addition funnel and added dropwise (neat or as a toluene solution) to the stirring siloxane solution over the course of 5 minutes so as to manage the reaction exotherm and maintain a reaction temperature at or below 80°C. When the reaction was complete as determined by ¹H NMR spectroscopy, the reaction mixture was concentrated by rotary evaporation. For siloxanes containing three or less silicon atoms, products were isolated by vacuum distillation while siloxanes containing more than three silicon atoms were stripped under high vacuum (35 – 45 mTorr) at 125°C for several hours. A general reaction scheme is shown in figure 4.1.

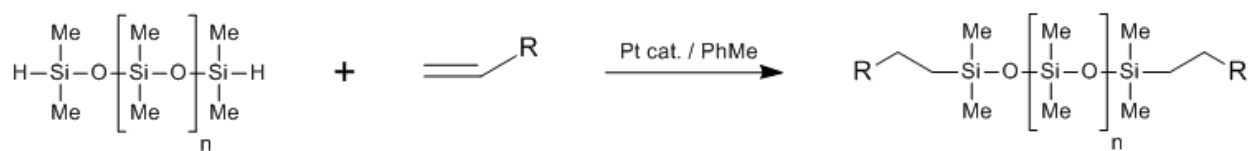


Figure 4.1 General hydrosilylation reaction scheme for vinyl compounds

4.2 RESULTS AND DISCUSSION

Naphthalene and anthracene groups have been used frequently in the design of simple organogelators due to their ability to promote self-assembly via π - π interactions [17,36]. Therefore, we selected the ethyl naphthalene functionality as the terminal associating groups on PDMS segments of varying molecular weight in hopes that the compound would not only dissolve in CO₂, but also associate and form a viscosity-enhancing supramolecular structure. Pressure-composition data at 35°C, Figure 4.2, confirms our hypothesis that naphthalene is indeed much less CO₂-philic [91] than PDMS (i.e. naphthalene is more CO₂-phobic), even though the molecular weight of the PDMS is 237. The limiting solubility of naphthalene in CO₂ at 35°C and extremely high pressures is ~6.5wt%, whereas the bubble point locus of the PDMS (Mw 237) – CO₂ mixtures remains flat at about 1000 psi. At higher concentrations of PDMS, the bubble point curve would extend to even lower pressures, reaching the vapor pressure of PDMS as its concentration approaches unity [55,92].

Once the choice of terminal CO₂-phobe was made, model end-terminal PDMS compounds were synthesized as described above and their phase behavior in CO₂ compared to that of un-functionalized PDMS materials. The molecular structures of the compounds used in this study are shown in Figure 4.3.

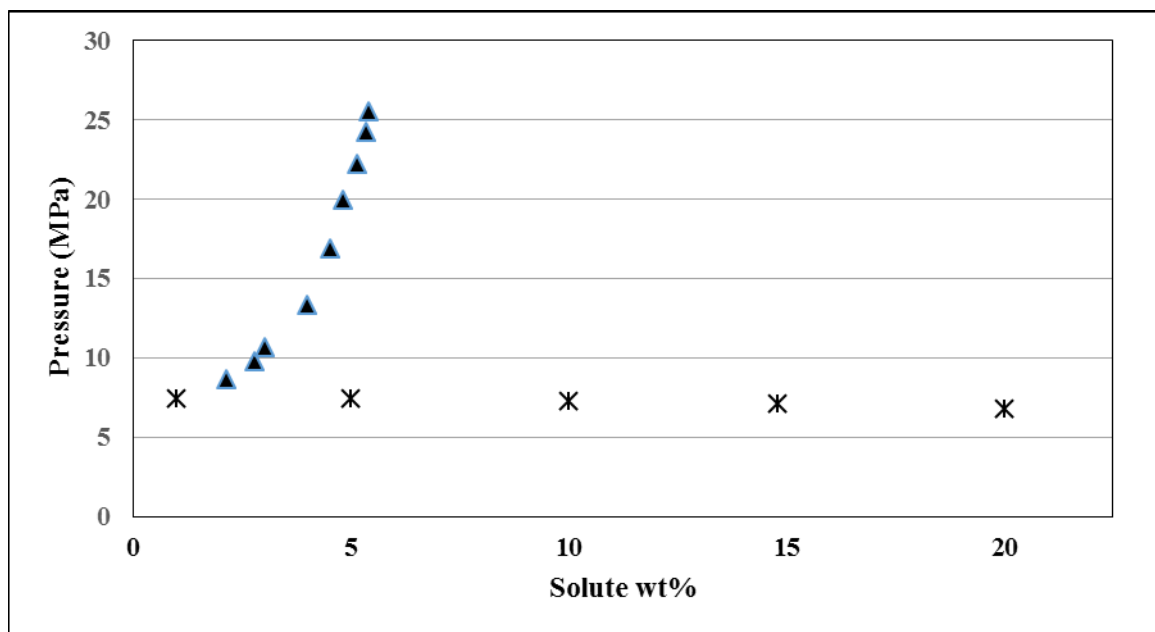


Figure 4.2 A comparison of the solubility of CO₂-phobic naphthalene (Mw 128.17) (triangles, reference [91]) and CO₂-philic PDMS (Mw 237) (stars, this work) in CO₂ at 35°C. Naphthalene cloud point pressures indicate a limiting solubility of 6.5wt% at extreme pressure. The PDMS-CO₂ mixture bubble point data are indicative of a high degree of miscibility between PDMS 237 and CO₂.

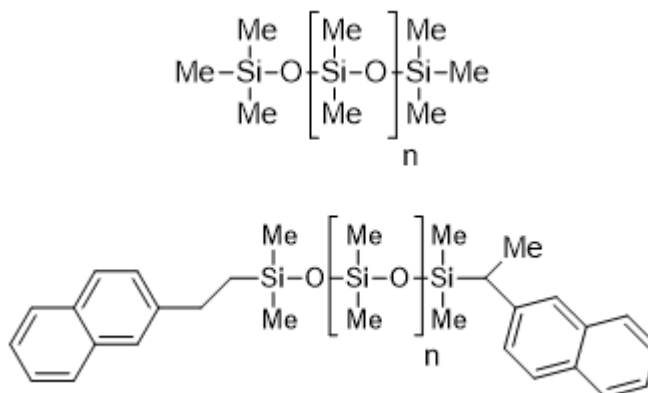


Figure 4.3 Structures of PDMS (top) and ethylnaphthalene-terminated PDMS (PDMS-NAP) (bottom). The two possible end groups shown on the ethylnaphthalene-terminated PDMS illustrate that this compound is a mixture of isomers.

4.2.1 Trimethylsilyl-terminated Linear Silicones

Pseudo-binary pressure-composition (P-x) diagrams for mixtures of dilute amounts of the PDMS in CO₂ have been determined at 23°C and 40°C, Figures 4.4 and 4.5, respectively, for the PDMS samples listed in Table 4.2. All of these trimethylsilyl-terminated linear silicones formed homogenous one phase solutions at elevated pressure at concentrations up to 4wt% PDMS. As expected, the cloud point pressure loci increase with increasing concentration and PDMS chain length. Upon slow isothermal expansion and depressurization at 23°C, the mixtures containing PDMS with an average molecular weight equal to or greater than 2000 exhibited cloud points, while CO₂ mixtures containing PDMS with average molecular weights of 1250 or less exhibited bubble points. At 40°C, all mixtures exhibited cloud points upon expansion.

For mixtures containing PDMS with an average molecular weight of 410 or 1250 at a sub-critical temperature of 23°C (the critical temperature of CO₂ is 31.1°C), Figure 4.4, the bubble point pressure data is fairly flat and can be extended to the vapor pressure of CO₂ (y-intercept in Figure 4.4). A CO₂-rich vapor phase and a PDMS-rich liquid phase co-exist (V-L₁ equilibrium) below these bubble point loci. At higher PDMS concentrations (not shown in Figure 3), the bubble point curves would decrease until the vapor pressure of the silicone oil was attained at a concentration of 100% PDMS, as shown in our prior studies for a mixture of CO₂ and low molecular weight PDMS at 25°C [55,92]. For mixtures containing PDMS with an average molecular weight of 2000 or more at 23°C, Figure 4.4, a CO₂-rich liquid and a PDMS-rich liquid are in equilibrium (L₂-L₁) at pressures below the cloud point loci. These cloud point curves are therefore not extended to the vapor pressure of CO₂ because a small V-L₂ region occurs at very low concentrations of PDMS; the location of this V-L₂ region on the P-x diagram was not experimentally determined in this study.

For mixtures containing 1-4wt% PDMS with an average molecular weight of 410 or more at a temperature of 40°C, Figure 4.5, a CO₂-rich fluid and a PDMS-rich fluid are in equilibrium (F-L₁) at pressures below the cloud point loci.

The loci found in Figures 4.4 and 4.5 represent the lowest possible cloud point pressures that a compound containing a PDMS oligomer or polymer of average molecular weight up to 9430 and one or more CO₂-phobic functional groups can be expected to exhibit at 23°C or 40°C, respectively. For example, if one desires to design a CO₂-soluble surfactant with a polar or ionic head group that is soluble at 1wt% in CO₂ at 40°C at a pressure less than 13 MPa, the average molecular weight of the PDMS would have to be less than 3780. Figure 4 shows that a pressure of 1875 psi is required to dissolve 1wt% un-functionalized PDMS Mw 3780, therefore pressures greater than 1875 psi would be required to dissolve the same PDMS after a CO₂-phobic group is incorporated into its structure.

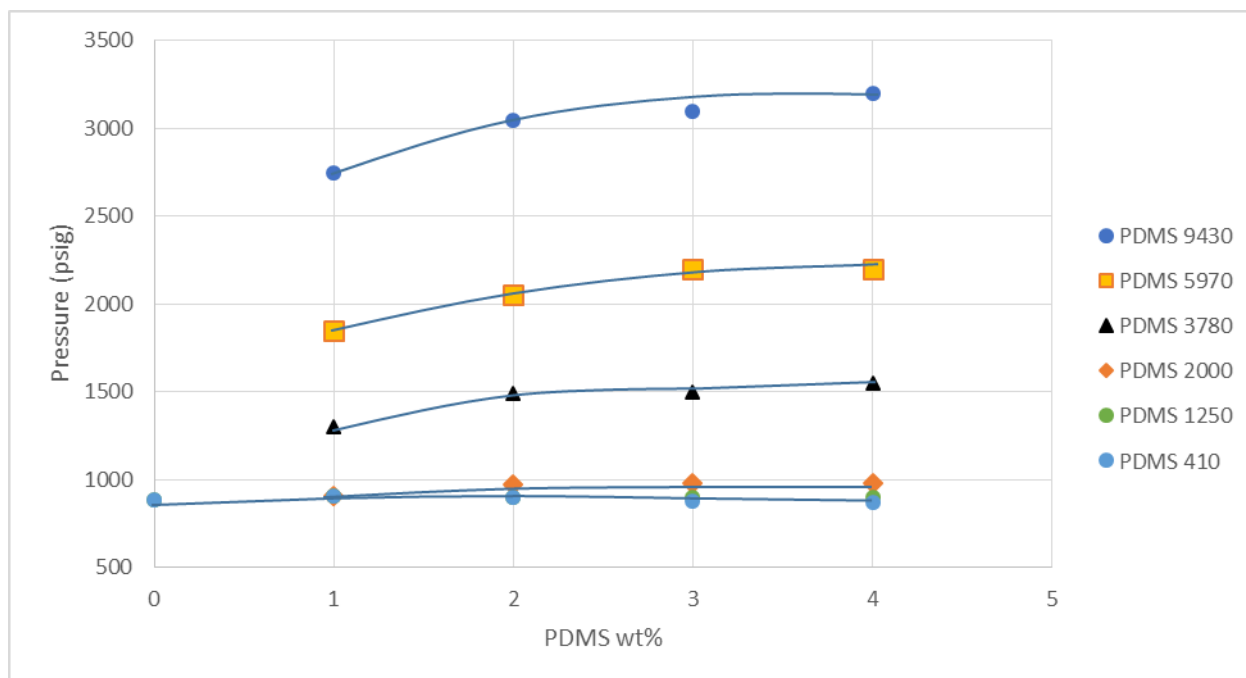


Figure 4.4 Two-phase boundaries of trimethylsilyl-terminated PDMS in CO₂ at 23° C. Mixtures containing PDMS 410 or 1250 exhibited bubble points; mixtures containing PDMS 2000, 3780, 5970 or 9430 exhibited cloud points. The curves are guides to the eye; they are not model results.

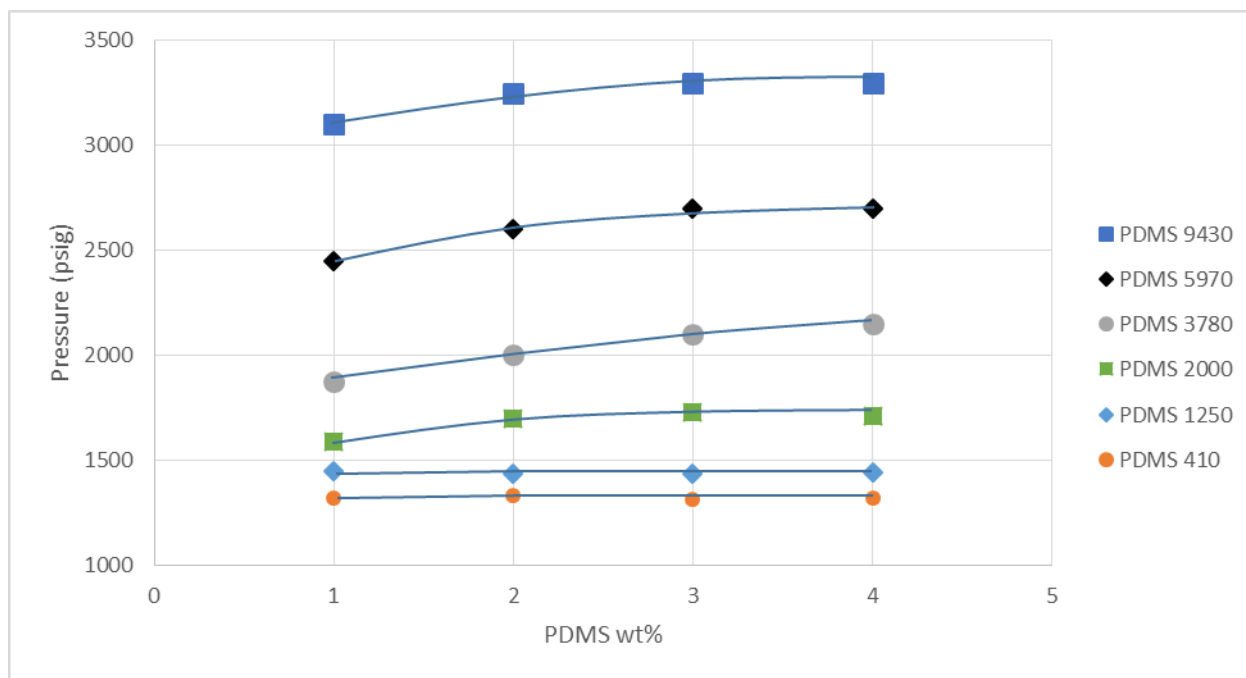


Figure 4.5 Solubility of trimethylsilyl-terminated PDMS in CO₂ at 40° C. All data represent cloud point data. The curves are guides to the eye; they are not model results.

4.2.2 PDMS-NAP Phase Behavior in CO₂

The two-phase liquid-liquid (CO₂-rich liquid – PDMS-NAP-rich liquid) boundaries for mixtures of PDMS-NAP and CO₂ at 23°C are found in Figure 4.6. Results for **PDMS-NAP 443** and **5974**, the lowest and highest molecular weight versions of PDMS-NAP, are not illustrated because each is CO₂-insoluble up to 10,000 psi. It is likely that the lowest molecular weight PDMS-NAP was insoluble because the CO₂-phobicity (i.e. unfavorable enthalpic interactions between CO₂ and ethyl naphthalene) of the two terminal ethyl-naphthalene groups could not be compensated for by the favorable CO₂-PDMS interactions of the very short PDMS chain. The highest molecular weight PDMS-NAP was probably insoluble because of the combined effects of the unfavorable enthalpic interactions between the terminal groups and CO₂ and the unfavorable entropic effects associated with the increased molecular weight of the PDMS. The optimal polymer molecular weight (of those listed in Table 4.2) for enhancing the CO₂ solubility of PDMS terminated at each end with ethyl naphthalene is 2357 for the PDMS-2679. The cloud point pressures of the CO₂ - **PDMS-NAP 2679** compound range from 2700-4200 psi over the 1-4wt% concentration range at 23°C. The cloud point pressure for an un-functionalized PDMS with a comparable PDMS molecular weight can be estimated from Figure 4.4 as roughly 1000 psi. The CO₂-phobicity of the terminal ethyl-naphthalene groups is responsible for the higher cloud point pressure values of the CO₂ - PDMS-NAP 2679 mixture.

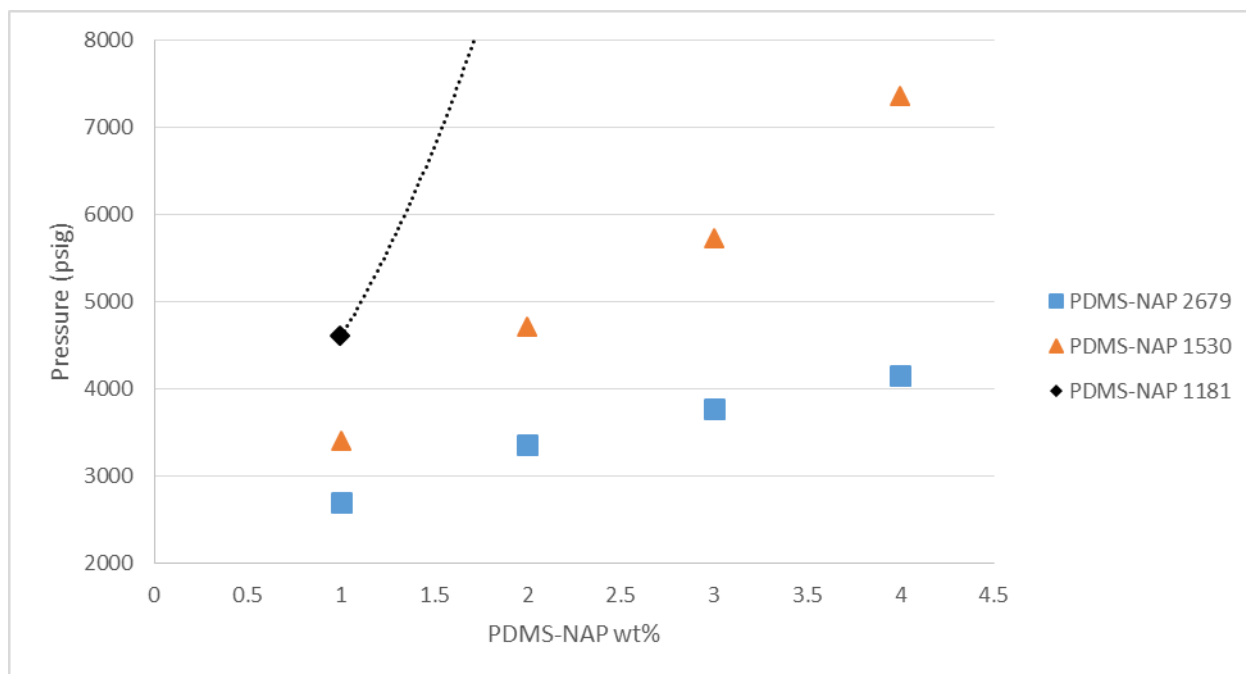


Figure 4.6 Solubility of the PDMS-NAP compounds in CO₂ at 40° C, as represented by cloud point data.

PDMS-NAP 1181 is soluble at 1wt%, but is insoluble at 2wt%. The curves are guides to the eye; they are not model results. PDMS-454 and PDMS-NAP 5986 are not shown because they are insoluble to 10,000 psi.

4.2.3 CO₂-solubility of Other End-functionalized PDMS Compounds

In the previous example, a PDMS-based compound with 9.8 repeat units functionalized on both ends with ethylnaphthalene (**PDMS-NAP 1181**) was determined to be soluble at 1 wt% in CO₂ at 23°C. Two examples of PDMS end-functionalized with ethyl naphthalene moieties that were 1-4wt% soluble in CO₂ were generated by incorporating either 14.5 or 30.0 DMS repeat units (**PDMS-NAP 1530** and **2679**, respectively). In order to demonstrate that a wide variety of CO₂-soluble end-functionalized PDMS compounds could be generated in a similar manner, many other end groups were selected. In most cases, these functionalities were selected because they had the potential to associate in solution, therefore the resultant molecule would have the potential to not only dissolve in CO₂, but to also associate in solution and thicken the CO₂. The ethylnaphthalene-terminated result is also provided in Table 4.3.

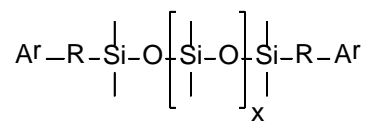
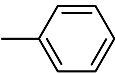
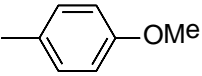
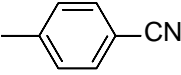
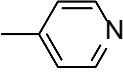
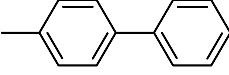
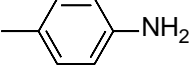
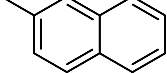
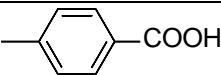


Table 4.3 End-functionalized Polydimethylsiloxane (PDMS) samples.

Compound	R	X	Ar	Type of two-phase boundary	Cloud Point (psig) at 1 wt%, 23 °C
A	-CH ₂ -CH ₂ -	14.5		Bubble Point	870
B	“	14.5		Bubble Point	870
C	“	14.5		Cloud Point	960
D	“	14.5		Cloud Point	1210
E	“	14.5		Cloud Point	1330
F	“	14.5		Cloud Point	2400
PDMS-NAP 1530	“	14.5		Cloud Point	3400
G	“	14.5			Insoluble

A simple phenyl group was also examined as a comparison to the naphthyl group to determine if the number of aromatic rings played an important role in CO₂ solubility. Several different chain lengths were tested for solubility that ranged from 0 to 14.5 repeat units (Table 4.4).

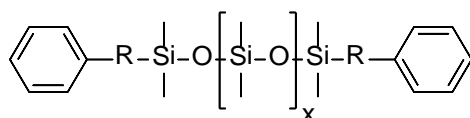


Table 4.4 Bubble Point Pressures of CO₂-(Phenyl-R-functionalized PDMS) mixtures.

Compound	R	X	Two-phase boundary pressure (1 wt%, 23 °C) psig
H	-CH ₂ -CH ₂ -	0	860
I	“	1	880
J	“	7.4	870
A	“	14.5	870

In general, PDMS containing 10-40 repeat units proved to be effective segment length for generating a CO₂-soluble compound. Table 4.3 lists the results in order of increasing cloud point pressure values for equivalent PDMS chain lengths therefore it provides an approximate ranking of the CO₂-phobicity of the R group, with the least CO₂-phobic group on top and the most CO₂-phobic group on the bottom. For example, if the R-PDMS_n-R compound has a low cloud point pressure as for compound A with ethylbenzene end groups, then the R group is only mildly CO₂-phobic. Similarly, 4-methoxyphenethyl, 4-cyanophenethyl, ethyl pyridine and ethyl biphenyl groups are also shown to be mildly CO₂-phobic functionalities. Conversely, a higher cloud point pressure classifies the R functionality as CO₂-phobic. For example, the benzoic acid, ethyl naphthalene and aniline R groups exhibit high cloud points or insolubility as a result of strong

intermolecular interactions such as hydrogen bonding (benzoic acid, aniline), rigid π - π stacking (naphthalene), and carbamate formation (aniline). One caveat related to anilines is that although primary and secondary amines may quickly form highly self-associative, CO₂-phobic ammonium carbamates upon exposure to CO₂ [90], the aniline groups in compound **F** have a much higher pK_b than their aliphatic analogs resulting in much slower reaction kinetics. This is due to the aniline nitrogen's lone pair electrons contributing to the adjacent aromatic resonance structures rendering the amine less reactive. Given enough time, the anilines may form completely insoluble ammonium carbamate salts but we did not observe this in our experimental timeframe of less than 4 hours. Conversely, unpublished results from our group assessing bis-aminopropylsilicones confirm that aliphatic primary amines immediately form CO₂-insoluble salts with PDMS portions ranging from 1 to 15 repeat units in length.

Table 4.4 shows the two-phase boundary pressures resulting from slow expansion of 1wt% single phase mixtures consisting of CO₂ and one of the four ethylbenzene functional compounds **H**, **I**, **J**, and **A**. Upon expansion, all mixtures exhibited bubble point pressures below which a CO₂-rich vapor phase and a PDMS-rich liquid phase co-exist (V-L₁ equilibrium). These relatively low two phase boundary pressures in relation to their ethylnaphthalene functional PDMS counterparts indicate that the ethylbenzene groups are more CO₂-philic than ethylnaphthalene. Interestingly, the length of the PDMS portion had very little bearing on bubble point pressure in the range of molecular weight included in this study indicating the feeble strength of benzene-benzene interactions. The comparable bubble point pressures of compounds **H**, **I**, **J**, **A**, **PDMS 410** and **PDMS 1250** provide further evidence that the ethylbenzenes contribute minimally to solute-solute interactions.

Although the number of aromatic rings plays a role in CO₂-solubility, rigidity of the functional group must also be considered. Clearly, two ringed aromatics as seen in molecule **E** and **PDMS-NAP 1530** raise the two-phase boundary pressure compared to the single ring as seen in molecule **A**. It appears that the biphenyl group used in molecule **E** is more CO₂-philic than the naphthyl group used in **PDMS-NAP 1530** based on the trend in cloud point pressures. This may be due to ability of the biphenyl rings to rotate around the central phenyl-phenyl linkage, potentially allowing the linked phenyl groups to adopt more favorable geometric conformations which can interact favorably with each other or with CO₂.

4.3 VISCOSITY ENHANCING POTENTIAL

All of the functionalized molecules in this study were low viscosity liquids in their neat form indicating that the functional groups did not significantly change PDMS structure-property relationships. If they were unable to form strong networks via physical intermolecular interactions in neat form, it was deemed that they would not be able to thicken CO₂, especially while dissolved at dilute concentrations. (There are no known examples of non-reactive oil-, water- or compressed gas-thickeners that are low viscosity liquids in pure form.) Therefore, these compounds were disqualified as potential thickener candidates. Future candidates relying on physical interactions will be screened with this pure physical state assessment method. This method would not be used for low viscosity reactive candidates such as amine-containing molecules.

4.4 CONCLUSIONS

Pressure-composition diagrams for mixtures of 1-4wt% trimethylsilyl-terminated PDMS of $M_w < 10000$ and CO_2 systems have been determined at 23°C and 40°C. The two-phase pressure loci of the PDMS in CO_2 are fairly flat and increase to higher pressure values with longer polymer chain lengths. These two-phase boundaries represent the lowest possible pressure at 23°C and 40°C required to dissolve a PDMS-based compound with $410 < PDMS\ M_w < 10000$ that is functionalized with one or more CO_2 -phobic functionalities.

To illustrate this concept, the solubility of five ethylnaphthalene-terminated PDMS compounds has been determined at 23°C. The solubility of the ethylnaphthalene-terminated PDMS in CO_2 reaches a maximum value at a molecular weight of 2679 as evidenced by its low cloud point pressure values (increasing from 2700-4200 psi over the 1-4wt% concentration range). The cloud point pressure for an un-functionalized (i.e. TMS-terminated) PDMS with a comparable PDMS molecular weight is approximately 1000 psi. Ethylnaphthalene-terminated PDMS compounds with lower molecular weights are less CO_2 soluble because increasingly weaker favorable interactions between CO_2 and the shorter CO_2 -philic PDMS polymer chain cannot compensate for the unfavorable enthalpic interactions between CO_2 and the CO_2 -phobic ethylnaphthalene groups. For higher molecular weight ethylnaphthalene-terminated PDMS, the unfavorable enthalpic interactions between the ethylnaphthalene groups and CO_2 , coupled with the unfavorable entropic effects associated with the increased molecular weight of the PDMS, render the compound much less CO_2 soluble.

Seven other end groups were assessed by incorporating them into molecules that contained 14.5 DMS repeat units and comparing their two phase boundary pressures. General ranking of terminal group CO_2 -phobicity was determined by comparing the molecules' two

phase boundary pressures to each other; a highly CO₂-phobic group would exhibit a higher boundary pressure than a less CO₂-phobic group. Generally, end groups with a high propensity to self-interact through mechanisms such as hydrogen bonding, π - π stacking and ammonium carbamate formation were most CO₂-phobic. It was also concluded that two ringed aromatic functionalities like naphthalene and biphenyl groups were more CO₂-phobic than benzene based groups but rigidity of the systems may also play a role as seen in the differing cloud point pressures of PDMS-NAP 1530 and molecule **A**.

Although they did raise CO₂-phobicity of an otherwise CO₂-philic PDMS, all studied end groups were deemed too weak to promote self-assembly as evidenced by their pure physical state of a low viscosity liquid. Future thickener candidates will be screened in their pure states and will ideally be extremely high viscosity liquids or low melting point solids.

5.0 AROMATIC AMIDE END-FUNCTIONAL SILICONES

Although there have been reports concerning the use of aromatic moieties in the design of low molecular weight organogelators [17,22,36], it became apparent that aromatic moieties alone could not drive self-assembly of silicone based molecules through the observation that none of the functional groups mentioned in chapter 4 were capable of significantly changing the physical state of the PDMS chains. There have been many instances of hydrogen bonding used in conjunction with aromatic π - π gelators [20,25,39]. Addition of hydrogen bonding sites to thickener candidates would impart more CO₂-phobicity increasing the likelihood of forming the supramolecular structures needed to increase viscosity. Therefore, silicone based thickener candidates containing aromatic amide based groups for the CO₂-phobic associating moieties were considered.

5.1 LINEAR AROMATIC AMIDE ENDFUNCTIONAL PDMS

Initial target materials, such as **2** below, were readily prepared via the reaction of aminopropyl terminated PDMS (**1**) with acid chlorides in the presence an HCl scavenger, typically trimethylamine (TEA). The general reaction scheme is shown in figure 5.1. Hexane, chloroform and THF were used at various times as solvent. Initially linear, low molecular weight compounds ($x = 1, 5, 10$) as shown in Table 5.1 were prepared.

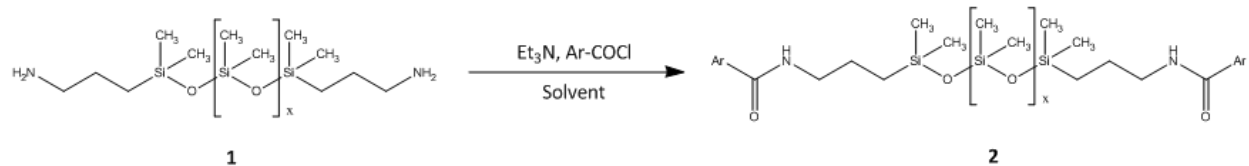


Figure 5.1 Preparation of Low MW Linear PDMS Bisamides

Table 5.1 Low MW, Linear PDMS Bisamides

Compound	Ar	x	Physical State
3a		10	Liquid
3b		5	Liquid
3c		1	Liquid
4a		10	Liquid
4b		5	Liquid
4c		1	Liquid
5a		10	Liquid
5b		5	Liquid
6a		10	Waxy Solid
6b		5	Waxy Solid

As mentioned in Chapter 4, the physical state of each compound was used as a gauge for potential associating power. As shown in Table 5.1, compounds with phenyl, 4-methoxyphenyl, and naphthyl substituted amide endgroups were moderately viscous liquids. The fact that these neat materials were neither very viscous, nor solids indicated that the amides were not interacting as strongly as desired. This was especially apparent in the shortest varieties with high end group molar concentrations relative to the internal siloxane portion. Stronger associations were seen in waxy compounds (**6a** and **6b**). The electron withdrawing nitro groups para to the amide may have increased the acidity of the amide NH bond making it more prone to hydrogen bonding.

Cloud points for the derivatives containing ten dimethylsiloxyl (DMS) groups in CO₂ at 1wt% and 60°C are summarized in Table 5.2. High pressures and temperatures were required to attain dissolution due to the strong intermolecular interactions. In addition, compound **5a** was insoluble at all pressures tested.

Table 5.2 Cloud Point Pressures at 60°C

Compound	Cloud Point (psi)
3a	6800
4a	7000
5a	Insoluble
6a	9000

As shown in Chapter 4, lengthening the PDMS portion of these endfunctional molecules can impart more CO₂-philicity and improve their solubility. Therefore, higher molecular weight derivatives, up to x = 50, with 4-nitrobenzamide endgroups were prepared. Even with longer PDMS chains, these compounds remained waxy solids because of favorable nitrobenzamide

interactions. The melting behavior of each was characterized using differential scanning calorimetry (DSC). As shown in Figure 5.2, the peak temperature of the melting endotherms were inversely related to the chain length. As the chain length increases, the molecules take on more of the flexible PDMS behavior lowering the melting temperatures.

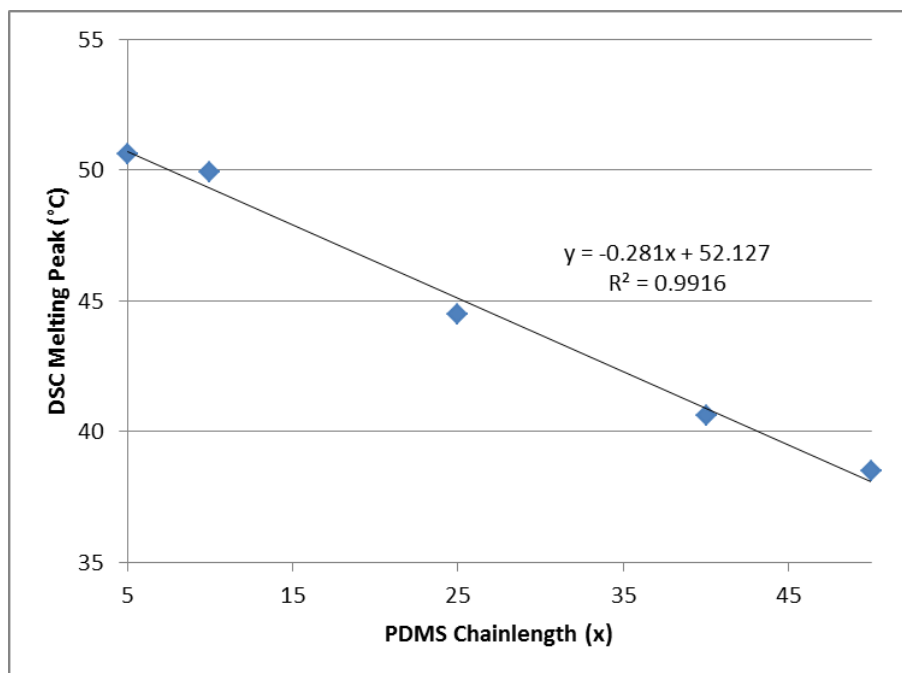


Figure 5.2 DSC Melting Peak Temperature vs PDMS chainlength for Bis 4-Nitrobenzamides

Increasing the PDMS chain length to 40-50 significantly improved the solubility of these compounds in CO₂ as shown by the cloud point data in Table 5.3. Although mixtures needed to be heated to establish a single phase solution, the solute did not precipitate out of solution upon cooling. However, falling ball viscometry experiments showed no change in viscosity even when the concentration of these materials in CO₂ was increased to 5 wt%. Therefore, linear 4-nitrobenzamide end functional candidates were deemed as inefficient CO₂ thickener candidates.

Table 5.3 Cloud Point Pressures (psi) at various temperatures for 1wt% linear PDMS 4-Nitrobenzamides in CO₂ solutions with x=40 and 50

Compound	X	25°C	40°C	60°C
6c	40	3050	2950	3400
6d	50	2800	2900	3500

Based on the results above, other aromatic groups with electron withdrawing groups para to the amides were explored. The first of these endgroups was biphenyl-4-carboxamide (or 4-phenylbenzamide) as shown in Figure 5.3.

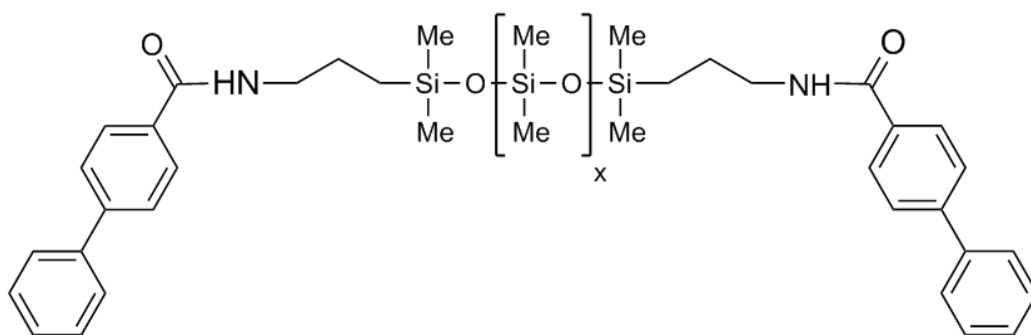


Figure 5.3 Compounds 7a (x= 25), 7b (x=40)

PDMS derivatives with x=25 (**7a**) and 40 (**7b**) were synthesized and evaluated. Both derivatives were waxy solids with melting transitions (DSC endotherm peaks of 102°C and 90°C respectively) that were substantially higher than similar 4-nitrobenzamides apparently due to stronger intermolecular interactions. Consequently, both derivatives were insoluble in CO₂ up to 60°C.

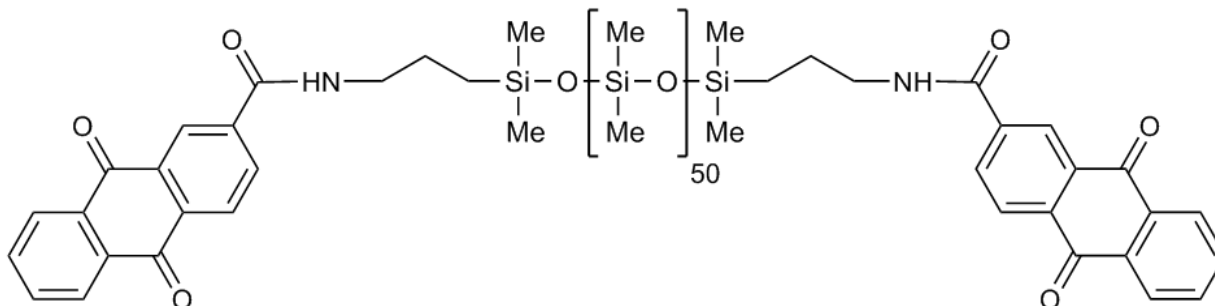


Figure 5.4 Compound 8

The next compound prepared, compound **8** shown in figure 5.4, contained anthraquinone-2-carboxamide (AQCA) endgroups attached to a 50 repeat unit long PDMS chain like compound **6d**. Compound **8** was a solid with a melting endotherm that peaked at approximately 48°C, about 10°C higher than compound **6d**. As shown in Figure 5.5, compound **8** was clear and somewhat rubbery as opposed to the hazy, soft wax forms of the other strongly associating compounds. Compound **8** melted and flowed upon heating and subsequently regenerated the clear solid upon cooling. All AQCA functional materials mentioned in this study exhibited the same general behavior.

Compound **8** was soluble at 1 wt% in CO₂ after heating to 60°C but precipitated out when the solution was isobarically cooled at 9000 psi to below 40°C. Cloud point pressures were 6700 psig at 60°C and 8300 psig 40°C. Unfortunately, falling ball viscometry did not indicate any increase in viscosity at 1wt% and 40°C.



Figure 5.5 Solid D40+ Bisamides: 4-Nitrobenzamide (left), Anthraquinone-2-carboxamide (center) and Biphenyl-4-carboxamide (right).

Out of the functional groups examined, AQCA groups were deemed to be the most efficiently associating groups based on compound **8**'s ability to thicken hexane while similar linear compounds **6c**, **6d**, **7a** and **7b** had no effect to the naked eye. At 5-10 wt% in hexane, there was an obvious increase in viscosity while at 15 wt%, the mixture formed a soft gel after a heating and cooling cycle.

5.2 MULTIFUNCTIONAL AQCA PDMS THICKENERS

Although the strongly interacting AQCA groups were identified, their implementation as endgroups on linear architectures was not successful in thickening CO₂. In an attempt to provide a higher likelihood of viscosity enhancing network formation, branch points were introduced to the silicone cores. Extension of PDMS at the branch with subsequent functionalization results in a molecule with more self-associating endgroups than the linear chains. The addition of

endgroups to promote association rendered molecules more CO₂-phobic and therefore required delicate tuning of PDMS to endgroup ratio in order to maintain CO₂-philicity. The starting branched aminosilicones were synthesized as shown in Figure 5.6.

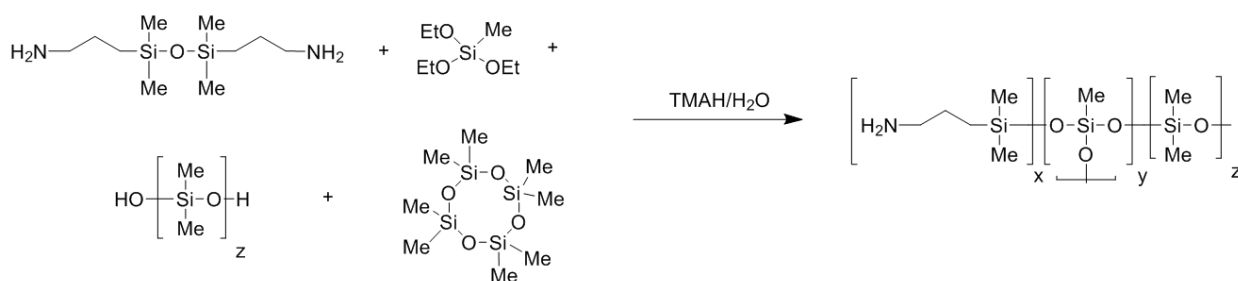


Figure 5.6 Synthesis of Branched Aminosilicones

Methyltriethoxysilane was hydrolyzed and reacted with bis(aminopropyl)tetramethyldisiloxane (GAP-0), octamethylcyclotetrasiloxane (D₄), and a low molecular weight silanol fluid in the presence of tetramethylammonium hydroxide (TMAH) catalyst. X values of 3-4 were targeted with y = 1-3.5. Furthermore, in order to maintain scCO₂ solubility z values were selected such that the D:M' ratio was close to 20:1. Once the reactions were complete, the catalyst was deactivated and volatiles were removed by heating up to ~165°C under vacuum (20-40 torr). After cooling and filtration through a small amount of Celite, the resulting polymers were clear, colorless, low viscosity oils.

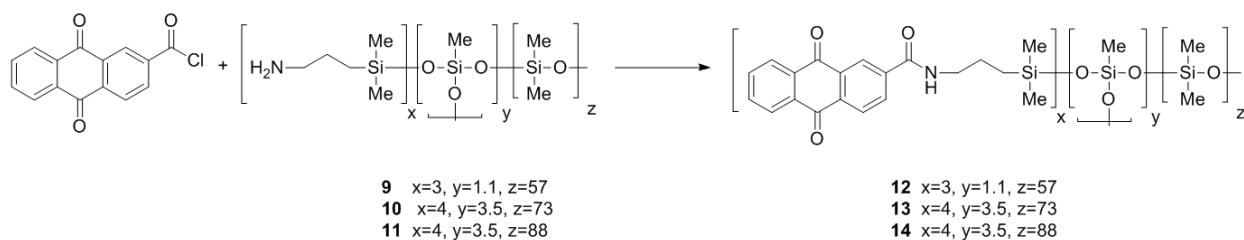


Figure 5.7 Preparation of Branched Anthraquinone Amides

The anthraquinone amides were then prepared as before by reacting the branched aminosilicones with anthraquinone-2-carbonyl chloride in the presence of TEA (Figure 5.7). Like the linear AQCA terminated compound **8**, these branched derivatives were clear yellow solids with DSC melting endotherms that peaked in the 46-52°C range. Furthermore, they were all found to gel hexanes at concentrations of approximately 10 weight percent. At 1wt%, compounds **12-14** were not soluble in CO₂ up to 60°C. However, dissolution of compounds **13** and **14** was possible with the use of hexanes after heating. As shown in Figure 5.8 below, compound **13** was also able to thicken the high pressure hexane/CO₂ mixture when evaluated with the falling sphere viscometer. The hexane to thickener mass ratio used for all tests was 2:1. All tests were performed at a pressure of 500 psi above the cloud point of the solution to ensure that a single transparent phase was being analyzed.

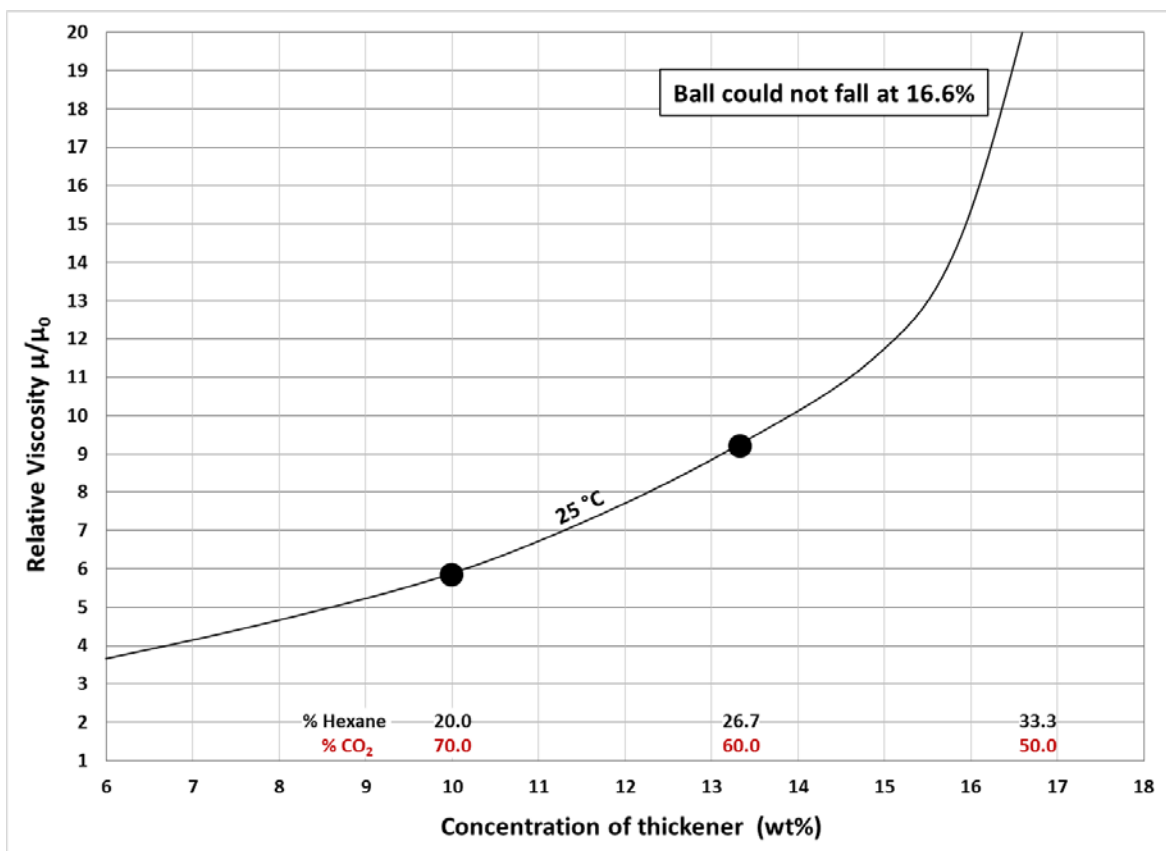


Figure 5.8 Viscosity increase at 25°C for a Hexane Solution of Compound 13 in a CO₂ rich solution; The curves are guides to the eye; they are not model results.

High temperature data is reported at initial dissolution conditions. For the 50°C experiment; at ~10% thickener (20% hexane, 70% CO₂), the transparent solution at 6000 psi was about 3 times as viscous as the CO₂:hexane mixture with no thickener. For the 60°C experiment; at ~13.3% thickener (26.7% hexane, 60% CO₂), the transparent solution at 5000 psi was about 3 times as viscous as the CO₂:hexane mixture with no thickener. Similar performance was also noted with compound **14** but the increase in DMS:AQCA molar ratio from that of **13** diminished the viscosity enhancing capabilities at the same mass concentrations.

Data for the 25°C experiments is reported after cooling the high temperature solutions except at 16.6% thickener where no initial heating was required for dissolution; at a concentration of ~16.6 wt% thickener (33.3wt% hexane, 50wt% CO₂), the transparent solution was so viscous that the Pyrex ball was unable to fall. At ~13.3 wt% thickener (26.7wt% hexane, 60wt% CO₂), the transparent solution at 3000 psi was about 9 times as viscous as the CO₂:hexane mixture with no thickener. At ~10 wt% thickener (20wt% hexane, 70wt% CO₂), the transparent solution at 8200 psi was about 6 times as viscous as the CO₂:hexane mixture with no thickener. We were unable to attain a single phase solution at 6.7% thickener (13.3% hexane, 80% CO₂).

Table 5.4 Viscosity Increase for Silicone Anthraquinone Amides

Compound	Wt %	T (°C)	Relative Viscosity
13	10	25	5.8
13	13.3	25	9.2
13	16.6	25	>20
13	10	50	2.7
13	13.3	60	2.8
14	10	25	2.8
14	13.3	25	3.5
14	16.6	25	8

Multifunctional linear PDMS architectures were also explored as an alternate method to increase the AQCA functionality. Both terminal and pendant AQCA groups were synthesized and evaluated to probe architectural effects on solubility and thickening capability.

In order to broaden the types of backbone structures that could be readily synthesized, the method of attaching the AQCA onto the siloxane was also modified. It was determined that the allyl amide of anthraquinone-2-carboxylic acid, compound **15**, would readily undergo hydrosilylation reactions with SiH functional silicones. Compound **15** was available from the reaction of anthraquinone-2-carbonyl chloride with allylamine (Figure 5.9).

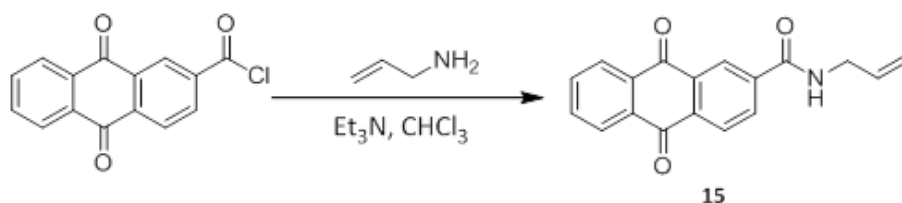


Figure 5.9 Allyl Anthraquinone-2-Carboxamide **15**

Hydrosilylation reactions with **15** were performed in toluene, a solvent in which **15** is sparingly soluble. However, **15** was miscible enough to allow reactions to proceed and eventually all of the material went into solution. Once this occurred, the reaction was generally at or near completion. In addition to acting as indicator of reaction progress, this limited solubility also appears to suppress side reactions such as olefin isomerization.

The first synthetic targets for compounds made via hydrosilylation of **15** were tetrafunctional compounds containing longer linear CO₂-philic PDMS sections than prior linear molecules to compensate for the additional AQCA groups. These polymers were prepared as illustrated in Figure 5.10. First, vinyl terminated polymers **16** and **17** were reacted with excess

methyltris(dimethylsiloxo)silane **18** in the presence of Karstedt's catalyst to give the intermediate hydride functional compounds **19** and **20**. After residual **18** was removed under vacuum, compound **15** was added to form the anthraquinone-2-carboxamide terminated compounds **21** and **22**.

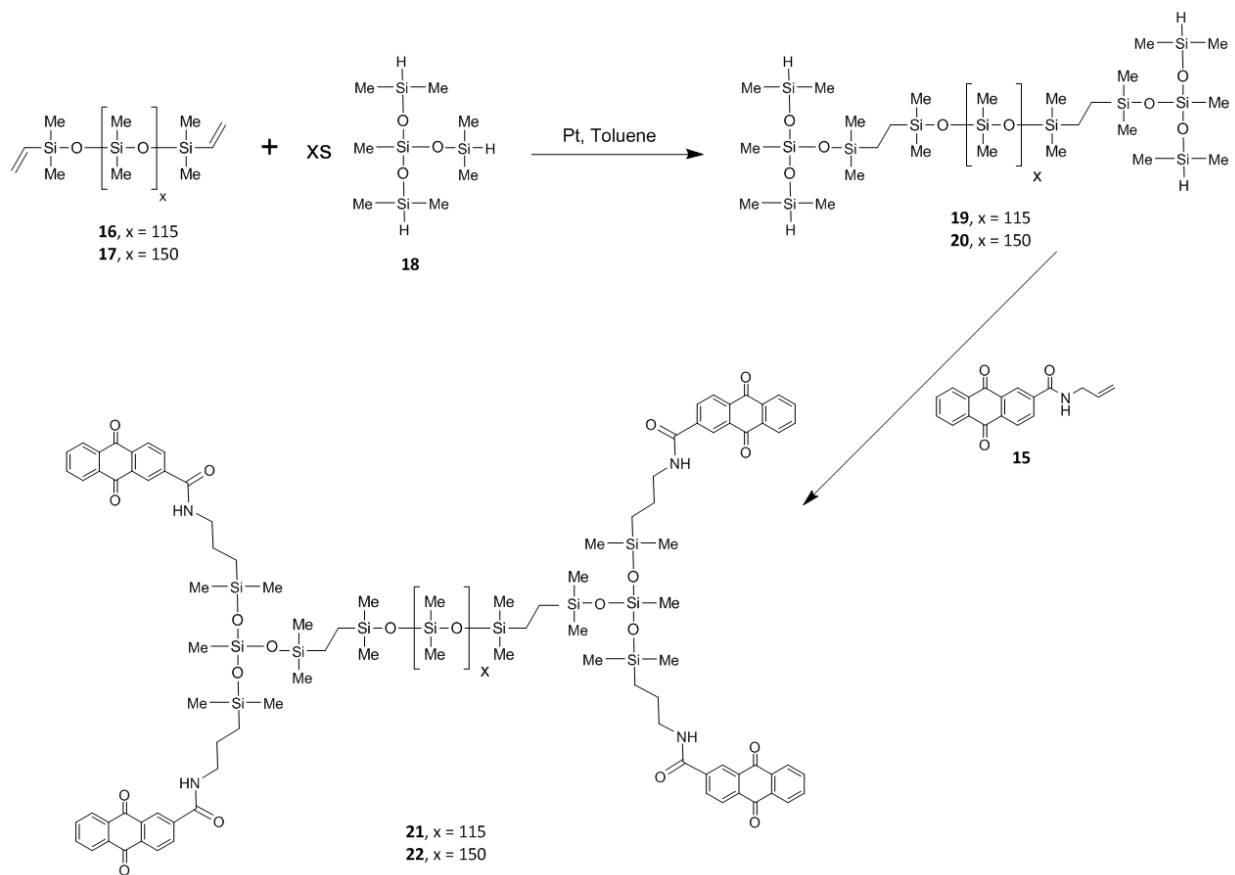
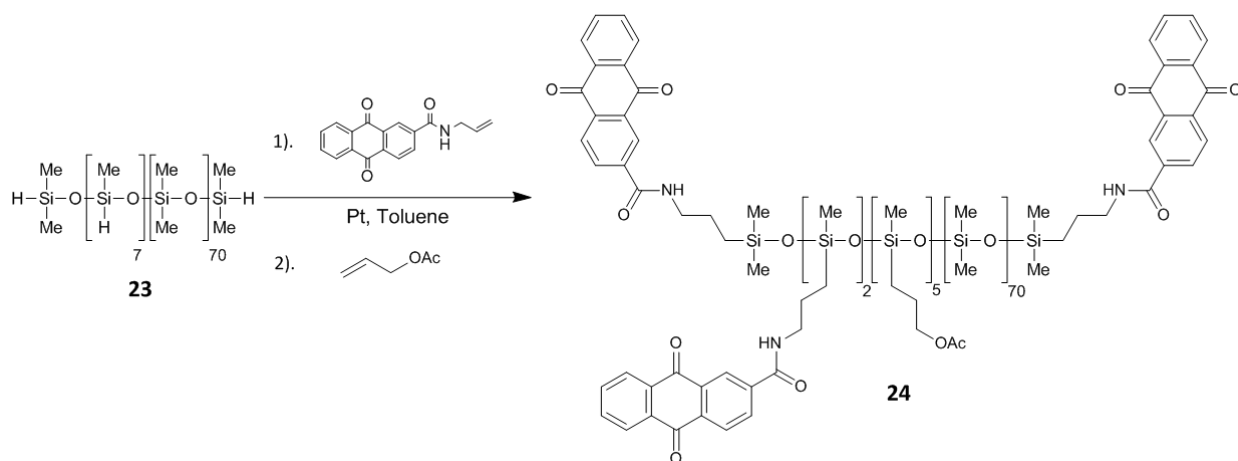


Figure 5.10 Synthesis of Compounds 21 and 22

Despite the use of an excess of **18**, some diaddition leading to chain extension was observed. Thus the structures shown in Figure 8 for compounds **19**, **20**, **21** and **22** are somewhat idealized and reflect the major reaction products. Both **21** and **22** were clear, brown, somewhat rubbery solids that readily dissolved in chloroform. DSC analysis of both materials indicated multi-

Unlike the previously mentioned AQCA functional compounds, compounds **21** and **22** exhibited very poor solubility in hexanes. When loaded at 10 wt % in refluxing solvent, only a small fraction of the material appeared to dissolve. However, the portion that did dissolve caused the mixture to gel upon cooling to room temperature. Based on their low miscibility with hexane and their high melting points relative to other compounds, it was concluded that neither **21** nor **22** would be likely to dissolve in a dense CO₂ rich environment. Therefore, another structural motif was examined as shown in Figure 5.11.



In this case, silicone **23**, containing hydrides on both the chain ends and some randomly distributed along the backbone, was first reacted with allyl anthraquinone-2-carboxamide **15**. Once all of **15** was consumed as determined by proton NMR, excess allyl acetate was added to

complete the synthesis. The basis of using acetate functional groups was to maximize CO₂-philicity through since acetates are known CO₂-philes [78]. Like the other AQCA based materials, compound **24** was a clear, rubbery solid that melted/flowed on heating and resolidified on subsequent cooling. DSC analysis showed a trimodal endotherm with peaks at ~49°C, 61°C, and 67°C. It was found to dissolve in hot hexane at 10 weight %, and solutions thus obtained would gel on cooling to room temperature.

Unfortunately, compound **24** was insoluble at 1wt% in neat CO₂ but was able to dissolve in a CO₂ rich solution when hexane was used as a cosolvent. Falling ball viscosity showed that this compound was also able to thicken a mixture of hexane and CO₂. At 16.67wt% **24**/33.33wt% hexane/50wt% CO₂ the mixture was so viscous that the ball would not fall. At 13.33% **24**/26.67% hexane/60% scCO₂, the relative viscosity was 3.1 times that of a mixture of hexane and scCO₂ at 25°C/8000 psi and 1.7 times the viscosity at 60°C/6500 psi. Thus, compound **24** was a somewhat less efficient thickener than branched polymer **13**.

5.3 CONCLUSIONS

As an extension to the weakly associating aromatic functional molecules studied in chapter 4, a series of aromatic amide functionalized, low molecular weight polydimethylsiloxanes were synthesized and their solubility and thickening ability in CO₂ rich atmospheres were evaluated. Aromatic amide terminated PDMS oligomers with simple or electron rich aromatic groups were moderate viscosity oils in their neat form. Therefore, they were deemed nonthickeners based on their insufficiently low self-interaction.

Attachment of electron deficient aromatic groups such as 4-nitrophenyl, biphenyl or anthraquinone onto these amides yielded solid. The 4-nitrobenzamides and biphenylcarboxamides derivatives were waxy solids that did not thicken CO₂ rich solutions. The former was soluble in neat CO₂ but the amide groups did not associate enough to provide a significant change in viscosity while the latter compounds were insoluble.

All anthraquinone-2-carboxamide (AQCA) functional compounds were clear, somewhat rubbery solids dissolved in hexanes with heating and formed gels with subsequent cooling back to room temperature. Some branched versions with higher levels of functionality were able to dissolve in and thicken CO₂ rich mixtures when hexane was used as a cosolvent. The compound responsible for the greatest increase in viscosity was AQCA terminated branched PDMS **13**.

6.0 CYCLIC AMIDES AND UREAS

Our initial attempts to thicken dense CO₂ in Chapter 4 using non-fluorous associating small molecules focused on end-functionalized polydimethylsiloxane (PDMS) oligomers. These materials contained a short linear PDMS core with various aromatic end groups (phenyl, naphthyl, anthracenyl, etc.) responsible for generating the necessary intermolecular interactions via π - π stacking. Despite exhibiting good solubility in dense CO₂ at 1 wt%, none of these additives increased the solution viscosity. As shown in Chapter 5, replacing the end groups with aromatic amides while making adjustments to the PDMS core molecular weight and geometry resulted in materials which were capable of gelling hexanes and which are still soluble in dense CO₂-rich solutions. For example, compound **5-13** was shown to increase the solution viscosity at 25°C and 8200 psi by a factor as high as 6 at 10 wt% with the addition of 20 wt% hexanes as a co-solvent.

In order to maximize the intermolecular interactions provided by the amide groups while increasing CO₂ solubility, we redesigned the structure of the thickener molecule according to Figure 6.1. A mildly CO₂-phobic central aliphatic or aromatic ring system was chosen to orient the remainder of the molecule. In particular, cyclohexane and benzene groups have proven useful in this regard, even at dilute concentration, when combined with appropriate associating groups [93–96]. Attached to these core ring systems are linking groups, X, which are responsible for forming the intermolecular interactions necessary to thicken or gel the solvent. A variety of

associating groups and types of intermolecular interactions are possible, however we have focused on hydrogen bonding groups including amide and urea linkages. In order to balance the CO₂-phobicity of the core group and linking groups, a CO₂-philic group must be appended to each of the linking groups described above to promote dissolution in CO₂. CO₂-philic groups selected from heavily acetylated [53,70] or siloxane [27,30] moieties were used since both of these structural types were shown to impart CO₂ solubility to polymeric and small molecule materials.

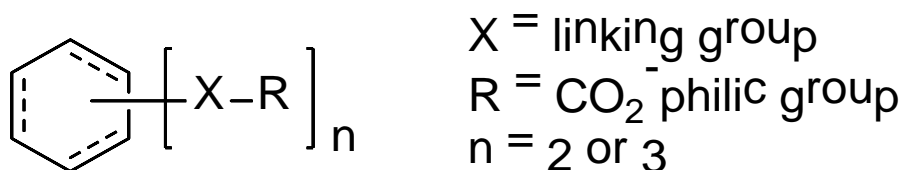


Figure 6.1 Structural components of small molecule CO₂ thickeners

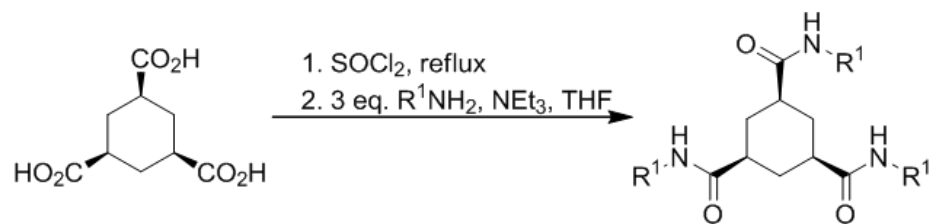
A series of cyclic amide and urea materials were prepared and screened as small molecule thickeners for organic solvents, dense CO₂ and mixtures thereof. In addition to a cyclohexane or benzene core, both of which are mildly CO₂-phobic, these molecules contained amide or urea groups responsible for self-assembly necessary for increasing solution viscosity. These groups also function to connect siloxane or heavily acetylated CO₂-philic segments to the cyclic core of the thickener molecule. Many of these compounds were shown to thicken conventional non-polar organic liquids (e.g. toluene, hexane), usually after heating and cooling the mixture. Attaining both solubility and self-assembly in CO₂ proved much more challenging. Several ester, amide and urea containing compounds were discovered that are soluble in dense CO₂ at low loadings (0.5–2 wt%). For linear siloxane segments, increasing the number of repeat

units provides greater solubility in dense CO₂. Branched siloxane segments were shown to have superior solubility characteristics in dense CO₂ to linear siloxanes of similar silicon content. However, only the propyl tris(trimethylsiloxy) silyl-functionalized benzene trisurea and trisureas functionalized with varying proportions of propyl tris(trimethylsiloxy)silyl and propyl-poly(dimethylsiloxane)-butyl groups exhibited remarkable viscosity increases (e.g. 3-300-fold at 0.5-2.0wt%) in CO₂, although high concentrations (18-48wt%) of an organic co-solvent such as hexane were required to attain dissolution in a CO₂ rich environment.

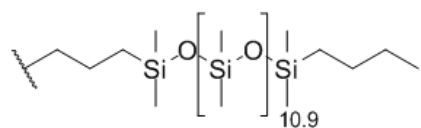
6.1 SYNTHESIS

Several di- and tri-substituted cyclohexane cores were chosen as starting points based on reports in which long chain aliphatic amide functionalized materials gelled a variety of polar and nonpolar organic solvents at loadings of 0.1 – 5 wt% [93–95]. Despite the lack of highly CO₂-philic siloxane or acetate functional groups in these materials, three aliphatic carboxamide materials reported by Hanabusa *et. al.* were prepared as benchmark materials. Trisamide **1** [94] and bisamide **8** [95] were prepared as described in the literature and shown in Figure 6.2 and 6.3(A). The related bisamide **10** was prepared by dehydrating octadecylamine and *trans*-1,2-cyclohexanedicarboxylic acid with dicyclohexyl carbodiimide (DCC) as shown in Figure 6.3(B). Using similar procedures, several commercially available linear and branched aminopropyl end-functionalized siloxanes of varying lengths were used to prepare the corresponding bis- and trisamide derivatives **2-4** and bisamide **11**. Pentaacetylated D-glucamine [53] was subjected to the conditions shown in Figure 6.2 to produce the pentadecaacetylated trisamide **5**. In order to explore siloxanes with longer aliphatic linking groups, a commercially available undecanoic acid

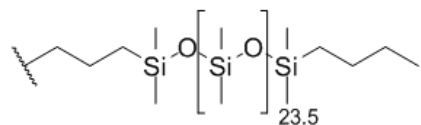
end-functionalized siloxane was dehydrated in the presence of DCC and (1*R*,2*R*)-(-)-1,2-diaminocyclohexane to give bisamide **9**. Branched siloxane trisamides **6** and **7** were also prepared using the conditions described in Figure 6.2 from the corresponding aminopropyl siloxanes **15** and **16**, these syntheses are shown in Figure 6.4.



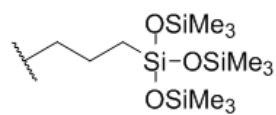
$R^1 = C_{18}H_{37}$



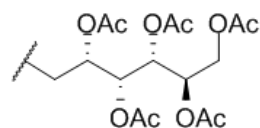
1



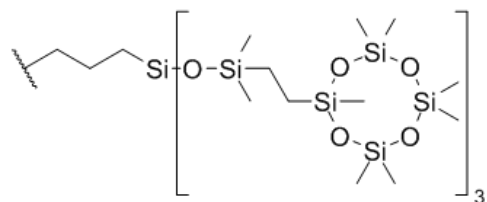
2



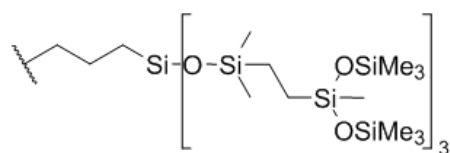
3



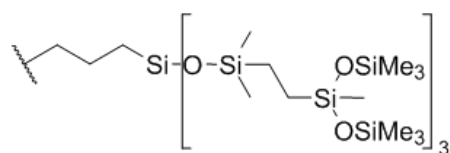
4



5



6



7

Figure 6.2 Synthesis of cis-1,3,5-cyclohexanetrissamides.

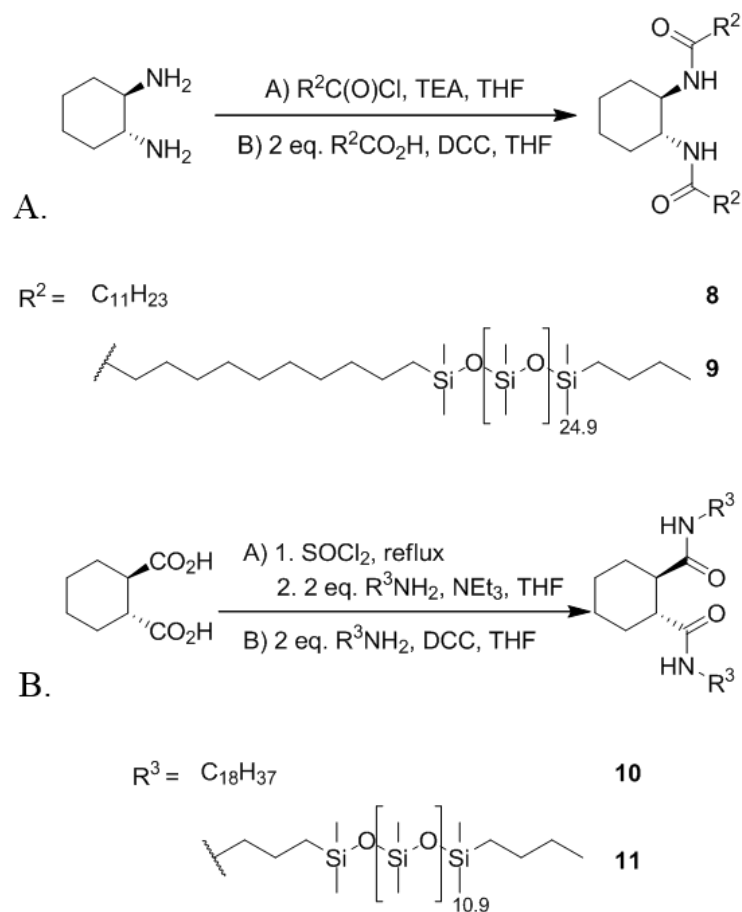


Figure 6.3 Synthesis of trans-1,2-cyclohexanebisamides.

Equilibration of 3-aminopropyltris(trimethylsiloxy)silane **12** with excess 1,3-divinyltetramethyldisiloxane **13** in the presence of catalytic Me_4NOH provides the vinyl functionalized intermediate **14** after distillation. Hydrosilylation of **14** using Karstedt's catalyst with heptamethylcyclotetrasiloxane, bis(trimethylsiloxy)methylsilane and 1,1,1,3,3,5,5-heptamethyltrisiloxane yields the branched aminopropyl siloxanes **15-17**, respectively. Both anti-Markovnikov (A) and Markovnikov (B) products are obtained for aminopropyl siloxanes **15** (A:B = >98:2), **16** (A:B = 83:17) and **17** (A:B = 91:9) and these mixtures were used without further purification in the synthesis of **6**, **7** and **31-33**.

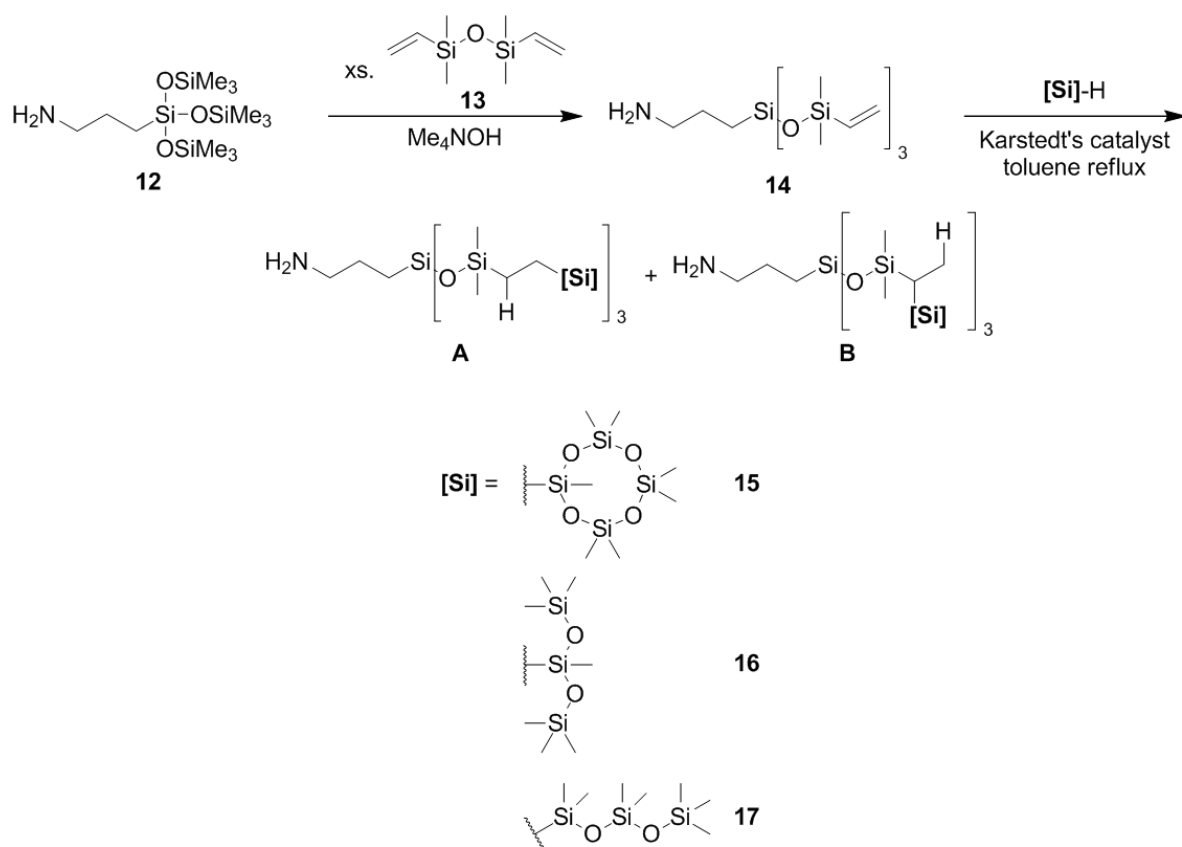


Figure 6.4 Synthesis of branched aminopropyl siloxanes 15 – 17.

Replacing the cyclohexane core with an aromatic moiety such as a benzene ring also yields materials which thicken and/or gel a variety of organic solvents, albeit at slightly higher concentrations than analogous thickeners with cyclohexane cores [93–97]. One benzene triester and several benzene bis- and trisamides were prepared by reaction of the appropriate acid chloride with the corresponding siloxane or acetate functionalized amines or alcohols as depicted in Figures 6.5, 6.6, and 6.7. As before, commercially available aminopropyl end-functionalized siloxanes were used to prepare amides **18** – **20**, **22** and **23** while pentaacetylated D-glucamine was used to prepare trisamide **21**. Bisamide **24** featuring a styrenic linking group was prepared from the aniline functionalized siloxane isolated following hydrosilylation of 4-vinylaniline with $\text{HSiMe}_2(\text{OSiMe}_2)_{24}\text{OSiMe}_2\text{Bu}$ using Karstedt's catalyst. Commercially available carbinol end-functionalized siloxane was used to prepared benzene triester **25**.

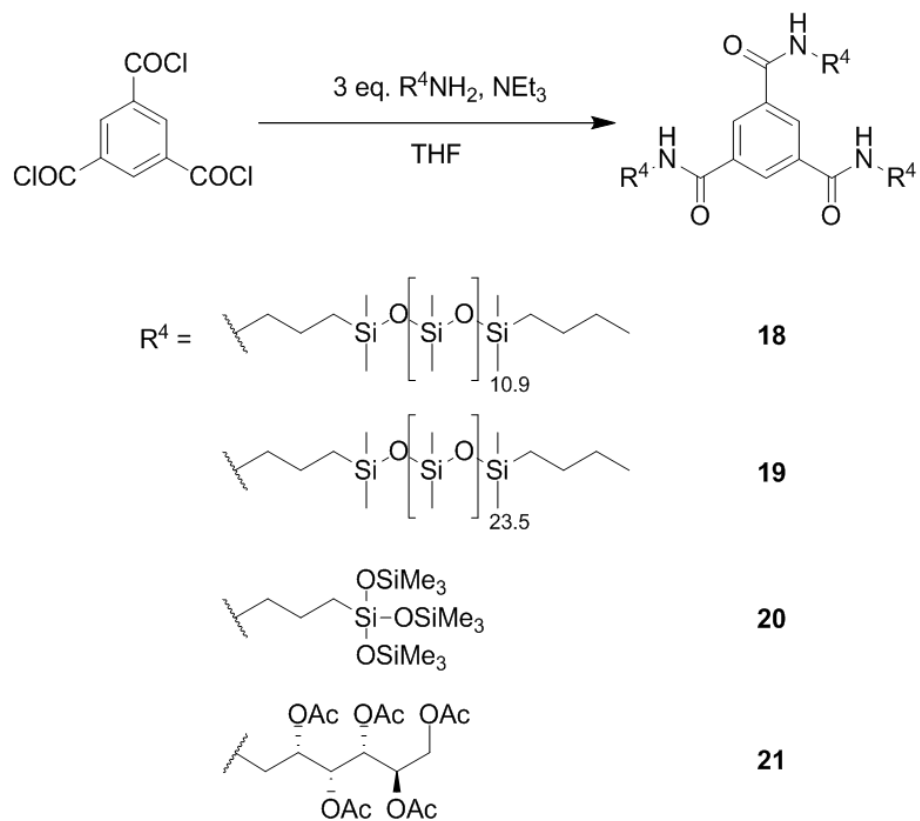


Figure 6.5 Synthesis of benzene trisamides 18-21.

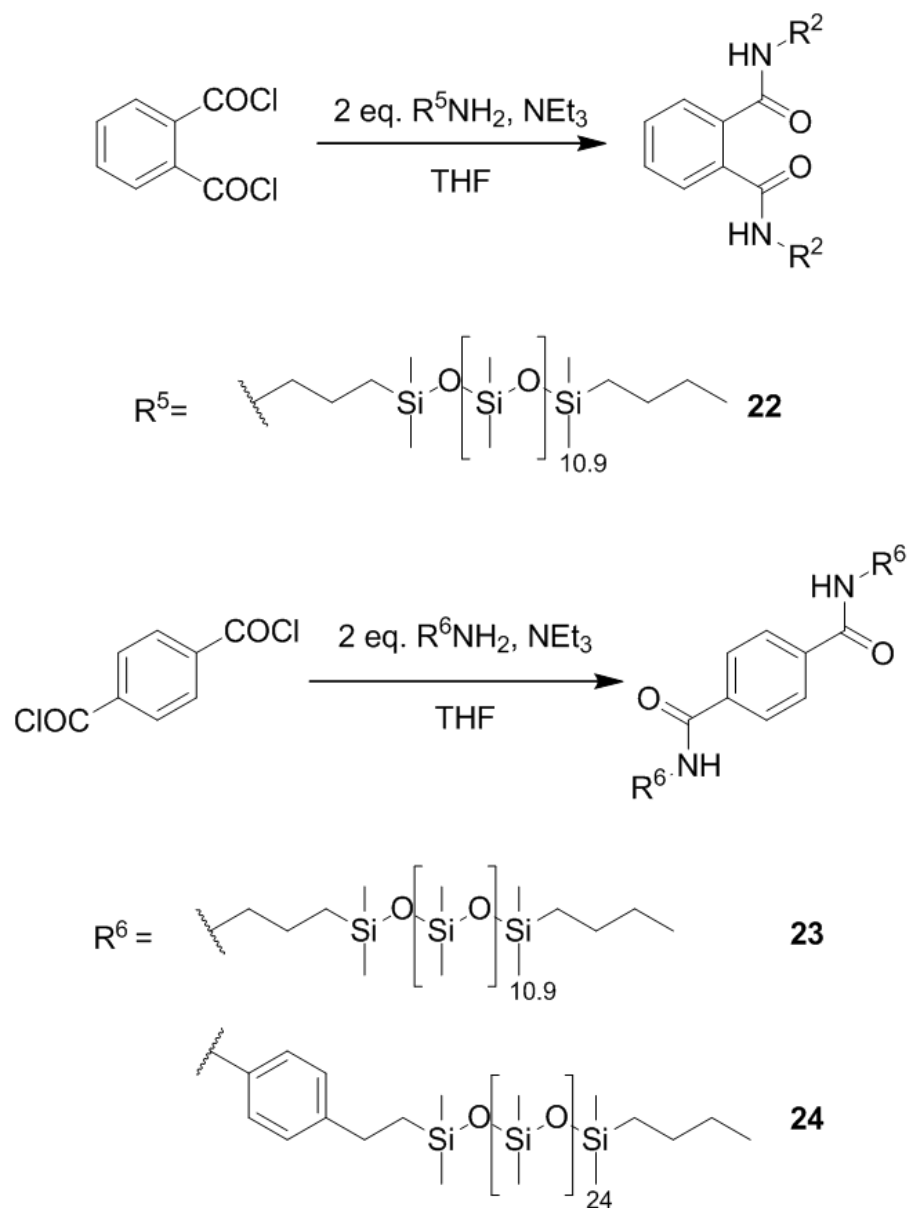


Figure 6.6 Synthesis of benzene bisamides 22-23.

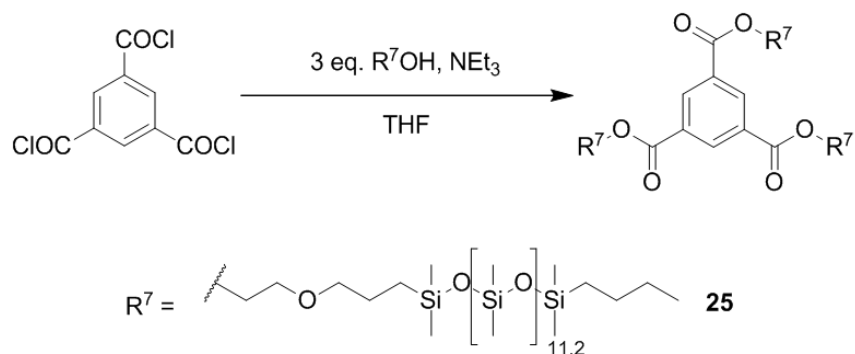


Figure 6.7 Synthesis of benzene triester 25.

In an effort to increase the number of hydrogen bonding groups relative to the amides described already, several benzene tris- and bisureas were prepared according previously published methods [97] and as depicted in Figures 6.8 and 6.9. The desired acid chloride is first converted to the corresponding di- or triacyl azide which after an aqueous workup is subjected to a Curtius rearrangement to yield the desired di- or triisocyanate. Ureas **26**, **27**, **31-33** and **37** were prepared by the addition of the corresponding aminopropylsiloxane while **28** and **34** are derived from pentaacetylated D-glucamine and 3,3-dimethylbutylamine. Compounds **29** and **30** were prepared from the corresponding aminodecyl functionalized siloxanes to study the impact of a longer hydrocarbon linker, while keeping a relatively short (10 – 15 OSiMe₂ repeat units) siloxane fragment compared to diamide **9**. The aminodecyl functionalized siloxanes were themselves prepared by hydrosilylation of 9-decenenitrile with HSiMe₂(OSiMe₂)_nSiMe₂Bu (n = 10 or 15) using Karstedt's catalyst followed by reduction [98] with lithium aluminum hydride. The synthesis for compounds **35** and **36** is identical to that used for the remaining urea containing materials until the point at which the aminosilicone is added to the *in-situ* generated benzene triisocyanate. For these materials, a mixture of the aminopropyl end-functionalized siloxanes depicted in Figure 6.8 is added with the stoichiometry indicated.

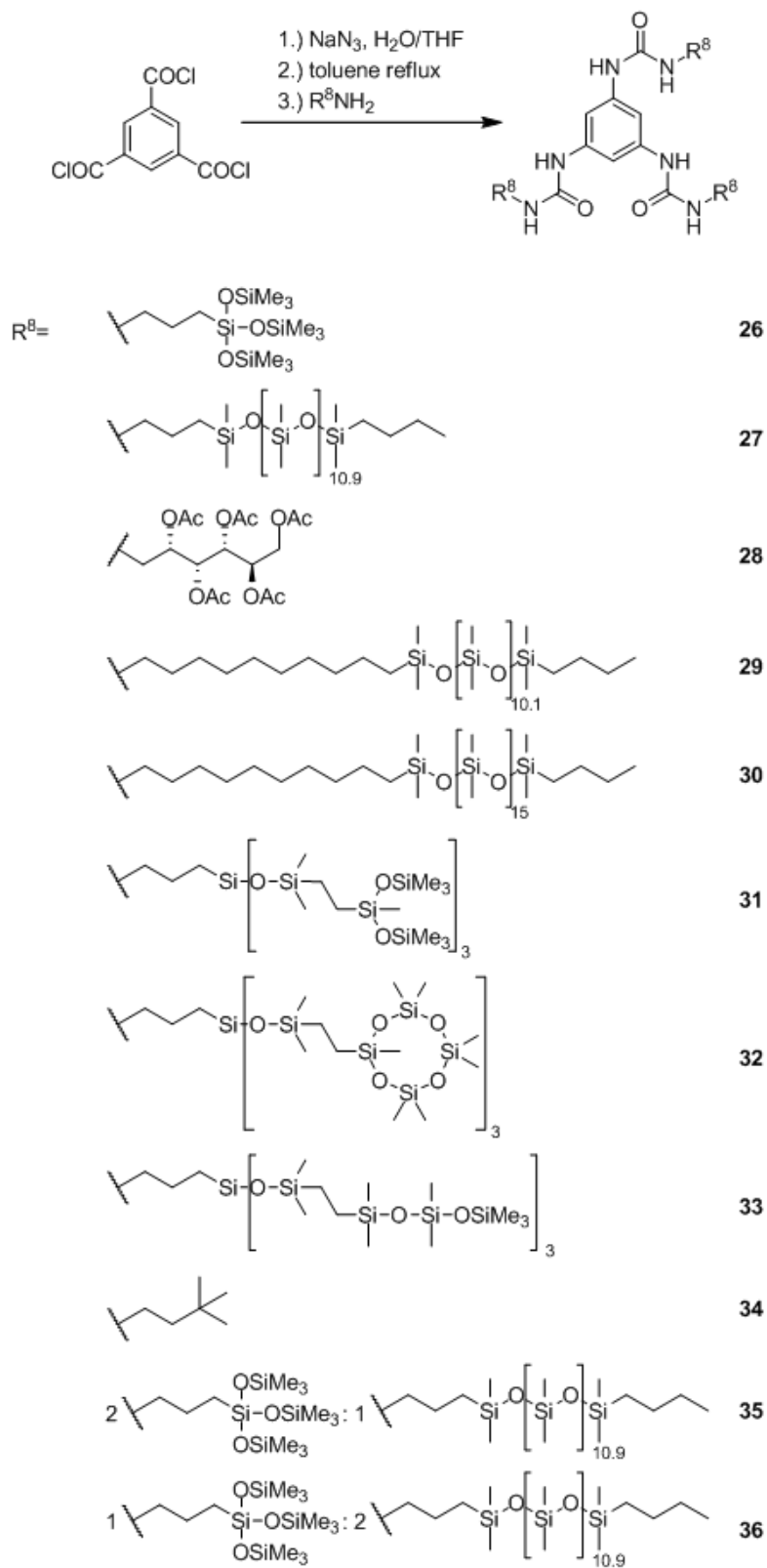


Figure 6.8 Synthesis of benzene trisureas 26-36.

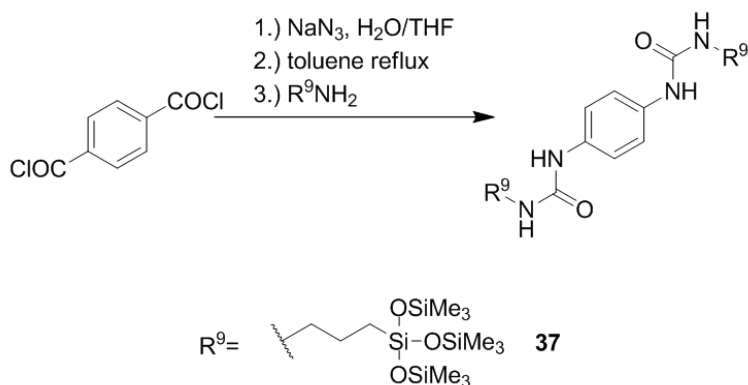


Figure 6.9 Synthesis of benzene bisurea 37.

6.1.1 Thickening ability in organic solvents

Screening experiments were performed in hexanes and toluene at room temperature and pressure to evaluate each compound's ability to thicken organic solvents and the results are presented in Table 6.1. For these experiments, 1 and 5 wt% solutions of each compound were prepared in sealed glass vials and heated to obtain homogeneous solutions. After cooling to room temperature, the vials were tilted and visually compared with vials containing neat hexanes or toluene to arrive at the results given in Table 6.1. While the capability of any particular compound to thicken hexanes and/or toluene was indeed encouraging, it was not a prerequisite for further testing in dense CO_2 .

Table 6.1 Organic liquid thickening and CO₂ solubility data for compounds 1-11 and 18-34.

Compound	physical state	thickens organic solvents				soluble in dense CO ₂ at 1 wt%
		hexanes		toluene		
		1 wt%	5 wt%	1 wt%	5 wt%	
1	powder	G[94]	G[94]	G[94]	G[94]	No
2	clear gel	N	N	N	N	No
3	soft gel	N	N	N	N	No
4	waxy solid	N	S	N	S	No
5	powder	N	N	N	N	No
6	tacky gum	N	N	N	N	Yes
7	viscous liquid	N	N	N	N	Yes
8	powder	hazy G	hazy G	G	G	No
9	liquid	N	N	N	N	Yes
10	waxy solid	N	N	N	N	No
11	viscous liquid	N	N	N	N	Yes
18	clear gel	N	N	N	N	No
19	soft gel	N	hazy S	N	N	Yes
20	powder	N	N	N	N	No
21	powder	I	I	N	N	Yes
22	clear gel	N	N	N	N	Yes
23	tacky solid	N	N	N	N	No
24	clear gel	N	N	N	N	No
25	liquid	N	N	N	N	Yes
26	powder	V	hazy G	S	S	No
27	waxy solid	S	I	N	N	No
28	powder	N	N	N	S	No
29	tacky solid	S	S	S	S	No
30	rubbery solid	N	N	N	N	No
31	liquid	N	N	N	N	Yes
32	viscous liquid	N	N	N	N	Yes
33	viscous liquid	N	N	N	S	Yes
34	powder	I	I	I	I	No
35	clear gel	S	M	S	V	No
36	clear gel	S	S	S	M	No
37	powder	S	S	S	S	No

N- soluble but no thickening, S- slightly thicker, M- moderately thicker, V- very thick, G- gelled, I- insoluble

6.2 HIGH PRESSURE PHASE BEHAVIOR

Results for solubility of compounds **1-11** and **18-37** in dense CO₂ at 1 wt% with temperatures ranging 25°C to 100°C are shown in Table 6.2. Temperature specific cloud point pressures and relative viscosities for materials soluble in neat CO₂ or a CO₂-rich solution are reported in Table 6.2. The physical appearance of the compounds in Table 6.1 varied significantly, from low viscosity liquids to waxy solids to solid powders suggesting a wide range of self-interaction strengths. As mentioned earlier in this work, the physical state of the pure materials can serve as an indicator of poor thickening ability but may not necessarily identify a good thickener. All compounds listed as a solid powder in Table 6.1 were insoluble at 1wt% in neat CO₂ except compound **21**.

The most commonly used CO₂-philic group used in this study was a linear siloxane containing an average of 13 silicon atoms as seen in compounds **2**, **11**, **18**, **22**, **23** and **27**. Compound **22**, a benzene 1,2-bisamide, was the only 1wt% CO₂ soluble material exhibiting a cloud point pressure of 4050 psig at 40°C. Changing the amides' locations with respect to each other as with compound **23** or adding a third amide as seen in compound **18** resulted in greatly reduced CO₂ solubility.

Replacement of the central aromatic ring with a cyclohexane ring like in compound **2** also yields a CO₂-insoluble material. However, compound **2** is soluble at 5 wt% in a 10 wt% toluene and 85 wt% CO₂ solvent mixture at 25°C containing with a moderate cloud point of 3900 psi. Triester analogue **25** is a low viscosity liquid material which is soluble in dense CO₂ at 1 wt% with cloud points of 3900 psig, 4130 psig and 4460 psig at 25°C, 40°C and 60°C respectively. The lack of proton donors crucial to the self-assembly mechanism in the ester are likely responsible for the increased CO₂ solubility compared to compound **18** which can be

viewed as the amide analog. Unsurprisingly, the addition of a proton donor via use of a urea over an amide further increases the likelihood of self-association yielding CO₂ insoluble compounds.

As seen in Chapter 4, lengthening a siloxane chain up to a certain point can increase the solubility of an otherwise CO₂-phobic molecule by varying the molar siloxane:CO₂-phobe ratio. This can be seen when comparing compounds **2** and **3** which differ in their silicone tail lengths but contain the same cyclohexane trisamide core. Much like compound **2**, compound **3** requires 10 wt% toluene as co-solvent to achieve a dissolution yet the cloud point was observed to be about 1100 psi lower than that of **2**. The benzene analogs **18** and **19** also display this trend where **19** exhibits a cloud point of 4500 psi at 1 wt% at 40°C in CO₂ whereas **18** was insoluble at all temperatures examined.

One must, however, take into consideration that the group connecting the associating core to the CO₂-philic tails also plays a role. Although the siloxane arms are much longer in bisamide **24** than in the case of bisamide **23**, no effect on CO₂-philicity was observed. The replacement of the propyl linkage with a more CO₂-phobic ethylphenyl group may have trivialized the effects of increased siloxane content. Another example can be observed when comparing **27** and **29**. Increasing the length of the aliphatic connecting group from C3 to C10 while holding the siloxane content relatively constant increases the temperature required for dissolution. Heating to 80°C was required to dissolve **27** at 0.5 wt% with a cloud point of 8300 psi while **29** exhibited a cloud point of 8610 psi at 0.5 wt% at 90°C.

Introducing branching into the structure of the siloxane moieties was also shown to have a significant impact on CO₂ solubility. The addition of linear or cyclic branches to the siloxane chains of cyclohexane trisamides **6** and **7** resulted in improved solubility at 1 wt% at 25°C with cloud points of 2600 psi and 2800 psi respectively. These are the lowest pressures observed for

the cyclohexane trisamides examined. A similar effect was observed with linear and cyclic branched siloxane functionalized benzene trisureas **31**, **32** and **33** which readily dissolved in dense CO₂ at 1 wt% at 25°C with cloud points of 1600 psi, 3000 psi and 1500 psi respectively. However, branched trisurea **26** which contains smaller branched siloxanes required a cosolvent content to achieve dissolution in a CO₂-rich solution. At 1.9wt% with 38.1 wt% hexanes, it exhibits a cloud point of 4870 psi at 25°C. Initial heating to 73°C was required to melt the solid powder. The difference in physical state alone between **26** and **31/32/33** indicates that a larger branched siloxane structure will yield a more amorphous compound. Hybrid tail compositions as seen in mixed trisurea **35**, containing both propyltris(trimethylsiloxy)silane and propylpoly(dimethylsiloxane) groups, required less co-solvent than **26** to attain a single phase solution with a cloud point of 4760 psi at 1.5 wt% with 18.5 wt % hexanes at 25°C. Similarly, a single phase solution of 2 wt% **36**, 18 wt% hexanes and 80 wt% CO₂ exhibits a cloud point of 2100 psi at 25°C. Both **35** and **36** did not require initial heating unlike **26**.

6.3 HIGH PRESSURE VISCOMETRY

Relative viscosity data shown in Table 6.2 was generated using close-clearance falling ball viscometry as described in Chapter 3.2. The relative viscosities were measured at the concentration and temperature indicated and at a pressure of at least 400 psi above the cloud point pressure to ensure a single phase solution was examined.

Of all of the compounds listed as being soluble in dense CO₂ at 1 wt% in Table 6.1 (**6**, **7**, **9**, **11**, **19**, **21**, **22**, **25** and **31 – 33**), only **21** and **32** were observed to moderately increase the viscosity of CO₂. Six other compounds which the laboratory screening experiments in hexanes and toluene identified as effective thickeners were also tested in dense CO₂ with hexanes or toluene as a co-solvent. Although cyclohexane trisamides **2** and **3** did not thicken hexanes or toluene at 5 wt%, both were shown to thicken toluene at 33 wt%. Despite the increased solubility of **2** and **3** at 5 wt% with 10 wt% toluene as co-solvent, neither compound thickened the CO₂ rich solution at 25°C or 40°C. From these results, it can be deduced that the use of linear or large branched siloxanes as CO₂-philes in these systems is not conducive to thickening at dilute conditions.

Table 6.2 Cloud point pressures and relative viscosities of compounds in dense CO₂.

Compound	Temperature (°C)	Conc. (wt%)	Co-solvent; conc. (wt%)	Cloud Point (psi)	Relative viscosity
2	25	5.0	toluene; 10.0	3900	1
3	25	5.0	toluene; 10.0	2820	1
6	25	1.0	-	2600	1
7	25	1.0	-	2800	1
9	25	1.0	-	950	1
9	40	1.0	-	1800	1
11	25	1.0	-	3900	1
19	40	1.0	-	4500	1
21	25	1.0	-	3180	1.3
22	40	1.0	-	4050	1
22	60	1.0	-	4125	1
25	25	1.0	-	3900	1
25	40	1.0	-	4130	1
25	60	1.0	-	4460	1
26	25	1.6	hexanes; 48.4	1280	300
26	25	1.3	hexanes; 38.7	5000	100
26	25	0.5	hexanes; 39.5	~800	14
29	90	0.5	-	8610	1
31	25	1.0	-	1600	1
32	25	1.0	-	3180	1.3
33	25	1.0	-	1500	1
35	25	1.5	hexanes; 18.5	4670	30
35	25	1.0	hexanes; 19.0	-	5
36	25	2.0	hexanes; 18.0	2100	3

Branched benzene trisurea **26** exhibited only slight thickening effects at both 1 and 5 wt% in toluene. However, the same concentrations in hexanes showed significant increases in viscosity to generate a high viscosity liquid at 1 wt% and a hazy gel at 5 wt% which does not move upon inversion of the vial. A single phase solution of 1.6 wt% **26** and 48.4 wt% hexanes mixture (3.2 wt% **26** in hexanes) in dense CO₂ at 25°C exhibited a remarkable increase in solution viscosity by a factor of 300. Dilution of this solution with more CO₂ to a composition of 1.3 wt% **26**, 38.7 wt% hexanes and 60 wt% CO₂ decreased the solubility of the thickener as the cloud point increases to 5500 psi at 25°C while decreasing the observed relative viscosity to a

factor of 100. As expected, reducing the concentration of **26** to 0.5 wt% with 39.5 wt% hexanes (1.25 wt% **26** in hexanes) yields a solution with a depressed cloud point of 800 psi at 25°C and depressed relative viscosity of 14.

The effects of disrupting crystallinity on CO₂-philicity and thickener behavior are shown by examination of compounds **35** and **36** which are hybrids of **26** and **27**. Benzene trisurea **35** contains on average two small branched siloxane substituents like those present in **26** and one linear siloxane substituent like those present in **27**. Similarly, on average **36** consists of one branched siloxane substituent and two linear siloxane substituents. Observation of their physical states as clear gels as opposed to a solid powder along with the lack of heating required for initial dissolution confirmed that the structural change successfully disrupted the crystallinity. Dissolution of trisurea **35** in both hexanes and toluene at 5 wt% produces high viscosity liquids while **36** gives a moderately viscous solution at 5 wt% in toluene and only slightly thicker solutions in hexanes and toluene at 1 wt%. In CO₂-rich environments, a mixture consisting of 1.5 wt% **35**, 18.5 wt% hexanes (7.5 wt% **35** in hexanes) and 80 wt% CO₂ yields a single phase solution at 25°C which exhibits an increase in solution viscosity by a factor of 30. A less pronounced, but expected, effect on solution viscosity was observed with a similar solution consisting of 2 wt% **36**, 18 wt% hexanes (10 wt% **36** in hexanes) and 80 wt% CO₂ that exhibited a relative viscosity of 3. The variation in tail composition and the resulting effects are shown graphically in Figure 6.10 which more clearly displays the necessary tradeoff between solubility and thickening when tailoring the tail compositions.

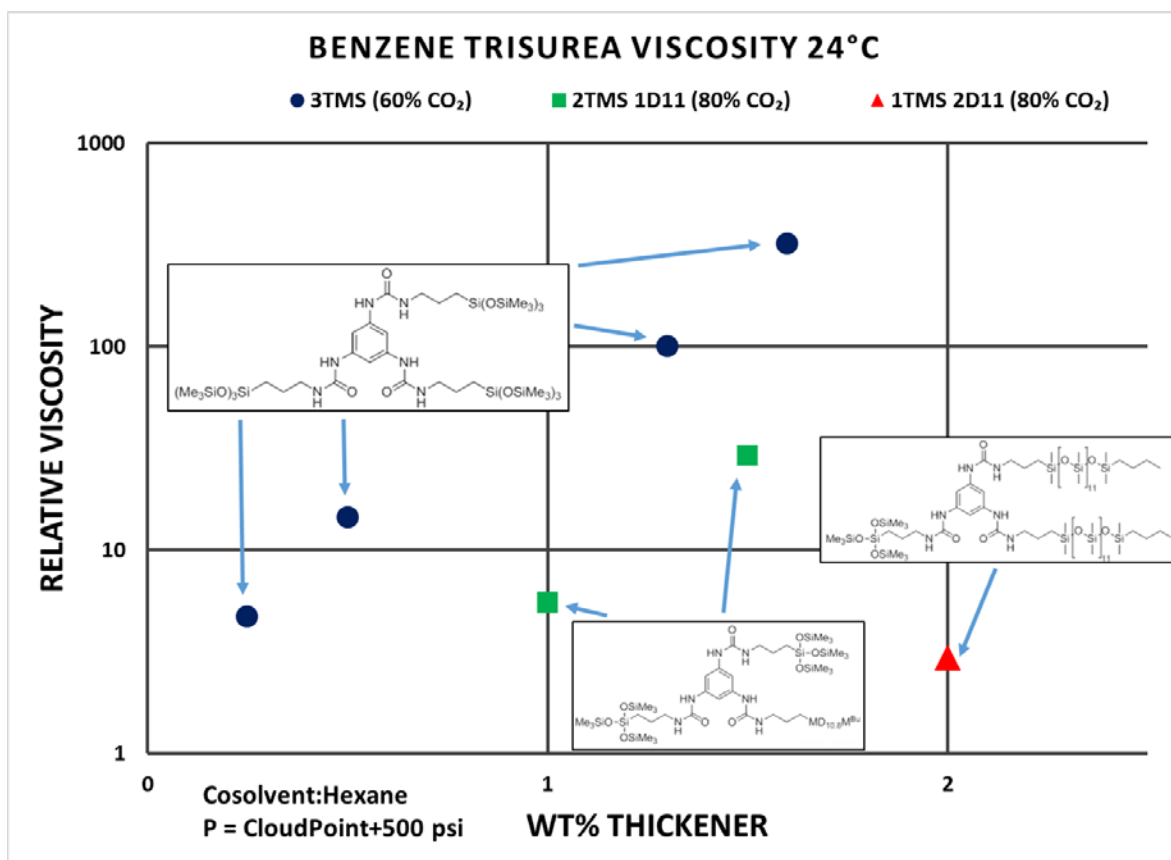


Figure 6.10 Comparison of benzene trisurea solution viscosities with varying tail composition; TMS represents the branched tail while D11 represents the linear tail

6.4 CONCLUSIONS

A wide variety of cyclic amide and urea materials were synthesized and tested for their ability to thicken hexanes, toluene and dense CO₂. Three structural classes in particular were explored. First, cyclohexane amide materials **1** - **11** were synthesized by reaction of the appropriate amine and carboxylic acid or acid chloride in the presence of base. These materials each contain two or three amide linking groups attached to siloxane or acetylated CO₂-philic groups and were modeled after the analogous alkyl amides which are known to thicken a wide variety of polar and non-polar organic solvents.

A second class of materials, **18** – **25**, featuring a benzene core was synthesized in a similar fashion. Many of these compounds also contain two or three amide linking groups attached to siloxane or acetylated CO₂-philic groups. Aromatic ureas, **26** – **36**, were prepared by reaction of the appropriate amine with the *in-situ* generated benzene di- or trisocyanate and make up the third and final class of materials examined. Here, the siloxane or acetylated CO₂-philic groups are connected to an aromatic core via two or three urea linkages which contain additional hydrogen bond donor and acceptor groups relative to the amides described above.

Several of these materials, **6**, **7**, **9**, **11**, **19**, **21**, **22**, **25** and **31** – **33**, were found to be sufficiently soluble in dense CO₂ at 1 wt% at 25°C to generate transparent single phase solutions. As seen when comparing **27** and **31/33**, CO₂-philic segments containing large branched siloxane groups were more soluble than linear siloxane groups with a similar number of silicon atoms. For linear siloxane based CO₂-philic segments, increasing the number of silicon atoms can significantly increase the solubility of the resultant material in dense CO₂ at the same mass concentrations.

Screening experiments in hexanes and toluene identified several materials which were capable of thickening or gelling these solvents at 1, 5 or in two instances 33 wt%. Based on these results, the addition of hexanes or toluene as a co-solvent enabled six additional compounds, **2**, **3**, **26**, **29**, **35** and **36**, to dissolve in dense CO₂. Out of the molecules studied in this work, urea linkages generally outperformed amide linking groups in terms of establishing the intermolecular interactions required to thicken dense CO₂-rich solutions as **26**, **32**, **35** and **36** are all benzene trisureas. This is not surprising considering the urea linkage contains twice as many hydrogen bond donor groups as the amides. The greatest increases in viscosity were observed with compound **26** but it also required the most cosolvent to achieve dissolution. Partial substitution of the tails in **26** yielded compounds **35** and **36** which were more amorphous clear gels. The reduced crystallinity of these compounds decreased the amount of cosolvent and eliminated the need for a heating cycle associated with **26** to obtain a one phase solution in CO₂ but also decreased the resultant solution viscosities. Compounds **21** and **32** were the only materials able to dissolve in dense CO₂ without a cosolvent while being able to very moderately increase the viscosity.

7.0 SUMMARY OF RESULTS

To date, an economically viable CO₂ thickener that does not use costly fluorinated functional groups has not been identified. In this work, three general classes of compounds were designed and synthesized as potential CO₂ thickener candidates. All molecules contain non-fluorinated, oxygen rich CO₂-philic portions to promote dissolution in CO₂ and CO₂-phobic groups to promote self-assembly of viscosity enhancing supramolecular structures via noncovalent interactions (π -stacking and hydrogen bonding).

Two-phase boundary pressures of various trimethylsilyl terminated silicones (410 < PDMS Mw < 10000) at 1-4 wt% in dense CO₂ were assessed. These two-phase boundaries represent the lowest possible pressure at 23°C and 40°C required to dissolve a PMDS-based compound that is functionalized with one or more CO₂-phobic functionalities. This concept is illustrated by the phase behavior studies on a series of ethylnaphthalene terminal silicones. Linear siloxanes (n=14.5) with CO₂-phobic aromatic endgroups that were CO₂ soluble at 1wt% showed no evidence of thickening CO₂ when solution viscosities were evaluated with falling sphere viscometry. Furthermore, the pure compounds were low viscosity liquids diminishing our confidence that they would be responsible for increasing viscosity at dilute conditions.

In an effort to increase solute-solute interactions to promote a change viscosity, a series of aromatic amide functionalized, low molecular weight polydimethylsiloxanes were synthesized and their solubility and thickening ability in CO₂ rich atmospheres were evaluated. Aromatic

amide terminated PDMS oligomers with simple or electron rich aromatic groups were found to be moderate viscosity oils indicating that the endgroups do not interact strongly enough to be thickeners. Attachment of electron deficient aromatic groups such as 4-nitrophenyl, biphenyl or anthraquinone onto these amides produced solid polydimethylsiloxanes, even at relatively higher degrees of polymerization on the PDMS core ($x=40-50$). The 4-nitrobenzamides and biphenylcarboxamides derivatives were waxy solids that did not thicken CO₂ rich solutions. The former was soluble but the amide groups did not associate enough to provide a significant change in viscosity and the latter compounds were insoluble. PDMS derivatives with anthraquinone-2-carboxamide (AQCA) endgroups were clear, somewhat rubbery solids. These compounds were found to act as thickeners and gelators for hexanes. In addition, they were able to thicken and/or gel mixtures of hexane and scCO₂ although a high mass concentration of at least 10wt% was necessary.

To gauge the effect of terminal associating endgroups vs core-associating groups, a second class of materials featuring cyclohexane/benzene bis- or tris-amide/urea cores with CO₂-philic silicone or sugar acetate tails was synthesized. Several of these materials were found to be sufficiently soluble in dense CO₂ at 1 wt% at 25°C to generate transparent single phase solutions. In general, CO₂-philic segments containing branched siloxane groups were more soluble than linear siloxane groups with a similar number of silicon atoms.

For linear siloxane based CO₂-philic segments, increasing the number of silicon atoms significantly increased the solubility of the resultant material in dense CO₂. Laboratory screening experiments in hexanes and toluene identified several materials which were capable of thickening or gelling these solvents at 1, 5 or in two instances 33 wt%. Based on these results,

the addition of hexanes or toluene as a co-solvent enabled six additional compounds to achieve single phase solutions in CO₂-rich atmospheres.

Benzene trisurea systems with siloxane tails exhibited the greatest change in solution viscosities. In general, highly crystalline benzene trisureas with propyl tris(trimethylsiloxyl)silane tails required a high amount of cosolvent, ~40wt%, and heating for initial dissolution but were able to increase viscosity by a factor of 14 at only 0.5wt%. Substitution of the crystalline tails with linear siloxanes produced less crystalline compounds that were more soluble in CO₂-rich atmospheres with less cosolvent, ~20wt%, with no initial heating for dissolution but also thickened to a lesser extent (3-30x). A benzene trisurea with cyclic siloxane tails was able to dissolve at 1wt% and 25°C in neat CO₂ without any heating but only increased the viscosity by about 20%. Similar results were observed with a pentadecaacetylated benzene trisamide.

Tables containing phase behavior and thickening ability of other compounds that fall within the molecular architectures documented in this work are attached in the appendix.

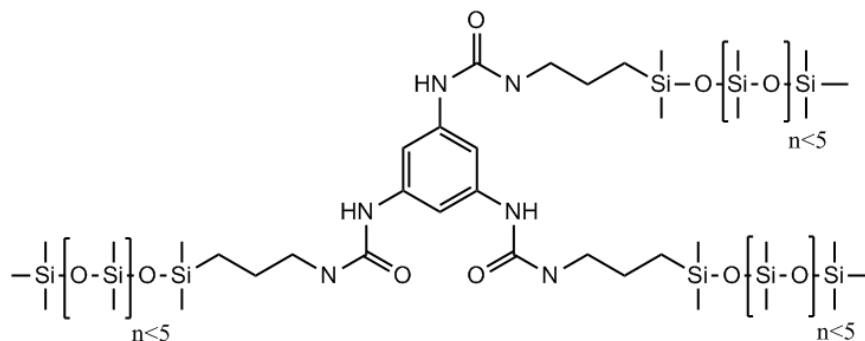
8.0 FUTURE WORK

In general, most of the molecular designs studied in this work were based on CO₂-philic siloxanes but the nature of specific CO₂-PDMS interactions has not been well studied. In the past, an ab-initio study on pairwise interaction between CO₂ and a dimethylsiloxane monomer would be useful for gaining insight on why PDMS is CO₂-philic; if the interaction potentials are weak, we can conclude that inclusion of PDMS in future molecular designs would mainly serve to increase entropy of mixing. However, ab initio calculations do not supply us with a realistic picture of the larger associating molecules of interest. A more promising route for modelling phase behavior between thickener candidates and CO₂ would be statistical associating fluid theory (SAFT) equations of state. These methods model molecules as chains of atom segments with their own parameters based on statistical mechanics and have been shown to accurately describe phase equilibria between two species with a large size disparity like hydrogen bonded associating polymer-solvent solutions even in the supercritical region [63,80,99–104]. Recent developments in second order group contribution methods may also allow us to build molecular models of cyclic amides/ureas that have very fine structural features like highly directional, geometry specific hydrogen bonding sites [99,105].

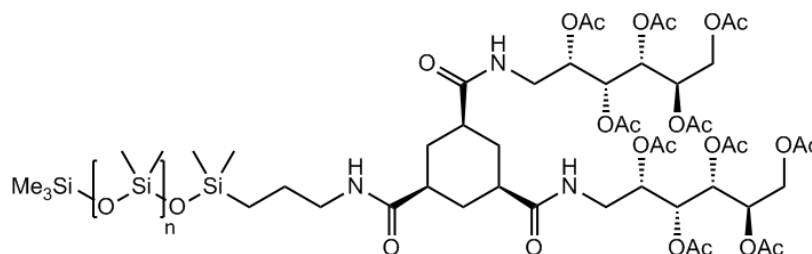
Quantitative spectroscopy studies in CO₂ would provide a much deeper understanding than simply inferring self-assembly based on viscosity data. In future studies, high pressure SANS experiments [38] should be employed to verify structural geometries regardless of

viscosity enhancement observations. For thickened solutions using 6-26, 6-35 and 6-36, SANS studies could put meaningful trends on fiber dimensions and their relation to CO₂-philicity. It would also be meaningful to reevaluate the candidates that dissolved in CO₂ but did not affect viscosity to confirm if the lack of thickening was due to relatively short (ie 10-mer) structures or lack of self-assembly altogether. This information would give much more confidence in directing future molecular designs.

The only compounds described in this work that dissolved in neat CO₂ while thickening, **6-21** and **6-32**, only exhibited modest increases in viscosity of 30%. While **6-32**, a highly viscous liquid, was made up of a highly associative benzene trisurea core with cyclic siloxane tails, **6-21** achieved comparable results through the use of more crystalline, CO₂-philic sugar acetate arms attached to relatively weaker interacting benzene trisamide cores. Comparing these two molecules enforces the notion that the use of a flexible siloxane may serve to increase the CO₂-solubility but at the expense of the highly ordered packing of molecules required for efficient thickening at dilute conditions. Therefore, molecules probing this balance should be synthesized and studied. Two families are shown below.



The benzene trisurea shown above would serve as a middle ground between **6-26** and **6-27**. Although we may expect to use a cosolvent, such a family of homotailed molecules would be useful in determining if a linear siloxane, if short enough, can be used to thicken at all. Previous iterations of this type have all contained tails comprised of at least 10 DMS units and did not thicken solvents.

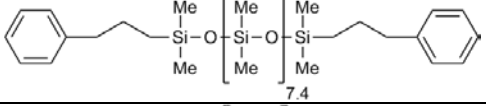
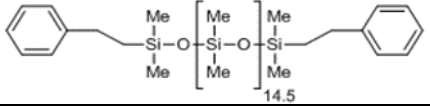
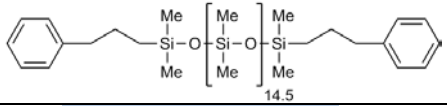
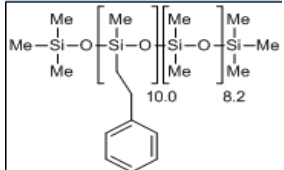
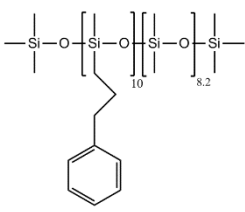
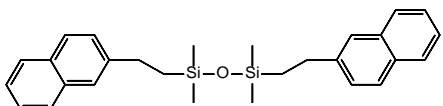
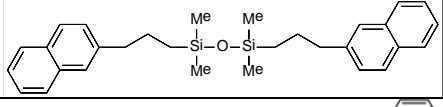
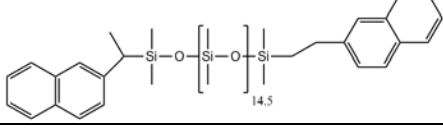
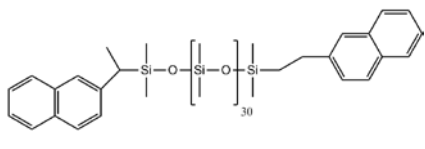
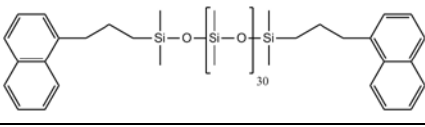
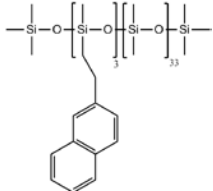


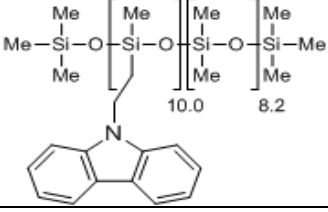
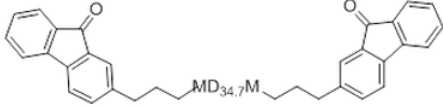
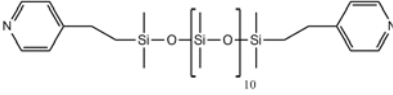
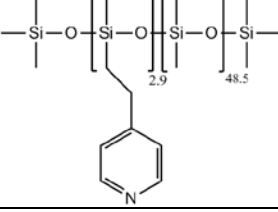
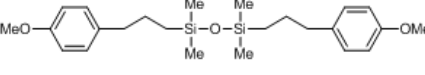
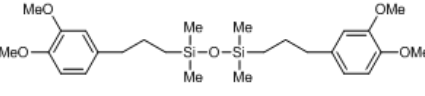
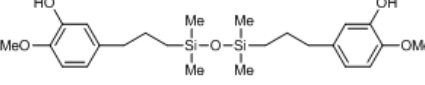
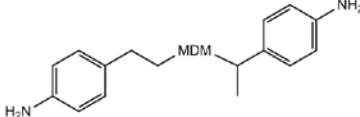
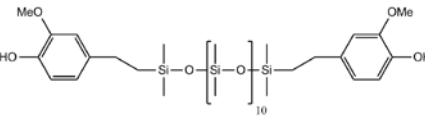
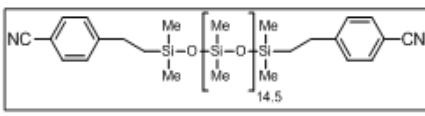
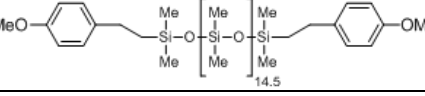
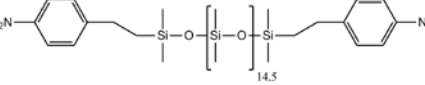
The second family of molecules could be based on the sugar acetate tailed cyclohexane trisamide, **6-5**. Although it was not found to be soluble in toluene, hexanes or CO₂, undocumented work shows that it can thicken acetones at 5wt%. This candidate could serve as a good candidate for a crystallinity variation study as seen in **6-26**, **6-35** and **6-36**. The highly CO₂-philic sugar acetates in the cyclohexane arrangement are rotated out of the hydrogen bonding plane due to stereochemistry of the amide-cyclohexane bonds allowing better stacking than **6-21**, the benzene core CO₂-soluble version. Adding a flexible siloxane tail to make a heterotailed molecule may decrease the melting point enough to attain solubility in CO₂ while maintaining stacking without the need for a cosolvent.

APPENDIX A

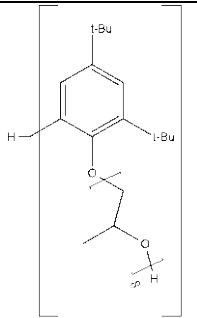
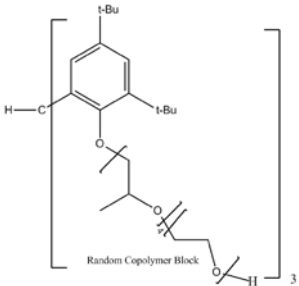
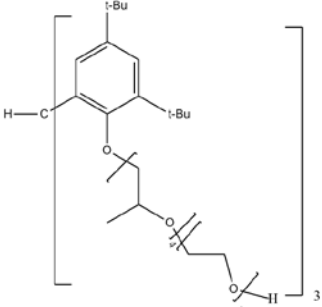
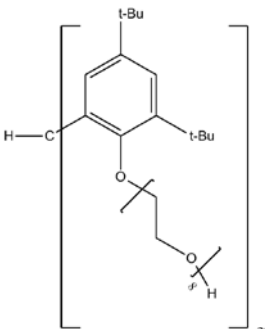
AROMATIC FUNCTIONAL COMPOUNDS

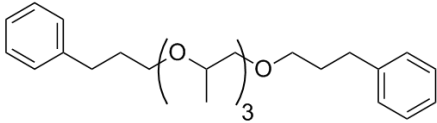
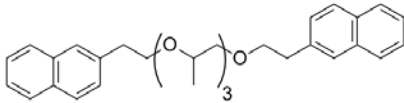
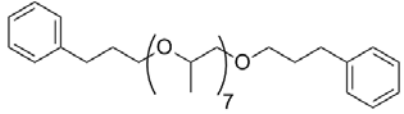
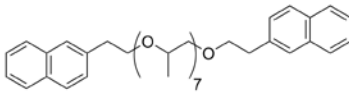
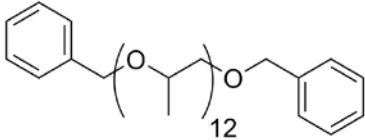
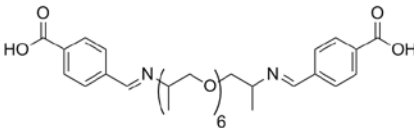
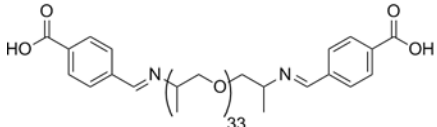
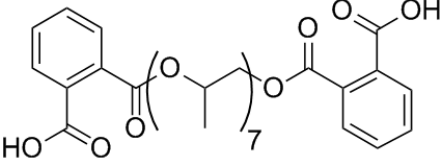
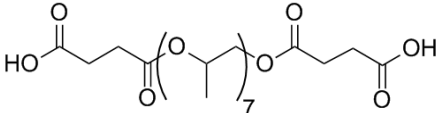
Code	Structure	Physical description	Soluble at 1wt in CO ₂ ? + Observations	CP 25C	CP 40C	CP 60C	Viscosity increase? At 1wt%
F1750-040		Type 1 low viscosity liquid	Yes	Bubble Point 860 psi			
F1717-019		Type 1 low viscosity liquid	Not yet tested				
F1750-042		Type 1 low viscosity liquid	Not yet tested				
F1717-023		Type 1 low viscosity liquid	Not yet tested				
F1750-038		Type 1 low viscosity liquid	Yes	Bubble Point 880 psi			
F1717-020		Type 1 low viscosity liquid	Not yet tested				
F1750-045		Type 1 low viscosity liquid	Yes	Bubble Point 870 psi			

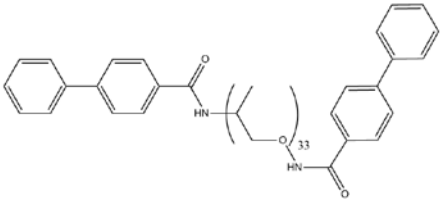
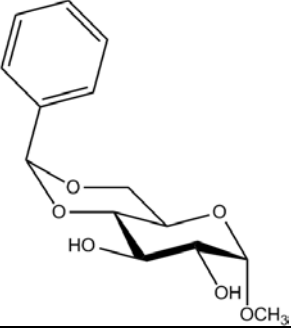
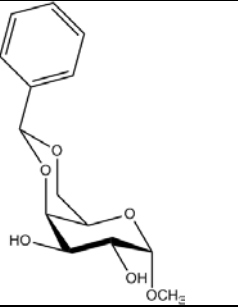
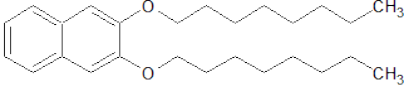
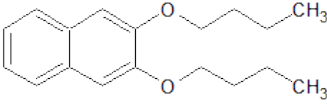
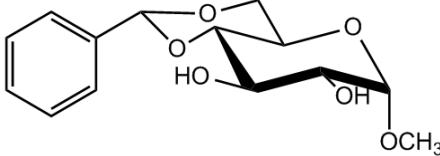
F1717-024		Type 1 low viscosity liquid	Not yet tested				
F1750-49		Type 1 low viscosity liquid	Yes	Bubble Point 870 psi	2000psi	2800psi	No
F1717-026		Type 1 low viscosity liquid	Not yet tested				
F1750-051		Type 1 med viscosity liquid	Not yet tested				
F1717-027		Type I low- medium viscosity liquid	No; too high of a ratio of a benzene: DMS; still low viscosity in pure form, may need naphthalenes instead	x	x	x	x
F1750-055		Type 1 med viscosity liquid;	No	<u>X</u>			
F1717-034		Type 1 med viscosity liquid	Not yet tested				
F1750-115		Type 1 Low med liquid	Yes	4060 psig			
F1750-117		Type 1 Low med viscosity liquid	Yes	2700 psig			
F1717-100		Type 1 Low med liquid	Not yet tested				
F1750-120		Type 1 Low med viscosity	Not yet tested				

F1750-063		Type I sticky tar makes sense it is sticky	Not yet tested	If F1750-051 didn't dissolve, this won't either			
F2095-103		Low Viscosity Liquid	Yes	4300 psi	3940 psi	4300 psi	
F1750-83		low viscosity liquid	Yes	1200 psi	1700 psi	2600 psi	Not yet tested
F1750-129		Low Viscosity Liquid	Not yet tested				
F1717-029		low viscosity liquid	Not yet tested				
F1717-032		low-med viscosity liquid	Not yet tested				
F1717-033		med viscosity liquid	Not yet tested				
F2095-77		Medium Viscosity	No	X	X		
D10 Eugenol		low viscosity liquid	Yes	4500 psi	4200 psi	4200 psi	Not yet tested
F1750-86		low viscosity liquid	Yes	950 psi	1650 psi	2600 psi	Not yet tested
F1750-067		Low viscosity liquid	Yes	Bubble Point 870 psi			
F1750-065		low viscosity liquid	Yes	2400 psi	2500 psi	3500 psi	

PITT/BASF COMPOUNDS

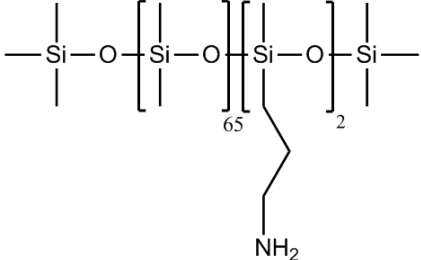
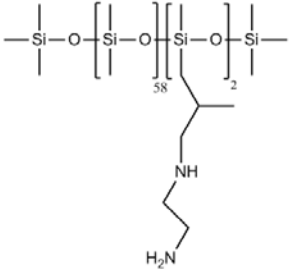
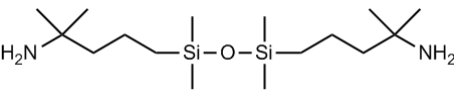
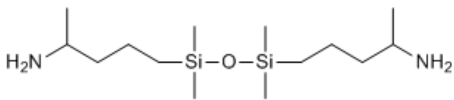
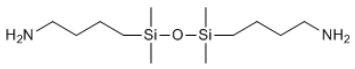
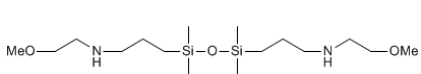
BASF 0817- 105		Type I medium viscosity liquid	Yes	2000 psi	2700 psi	3650 psi	X
BASF 0817- 106		Type I medium viscosity liquid	Yes	2300 psi	3500 psi	4350 psi	X
BASF MW156		Type I Medium viscosity liquid	No	X	X	X	X
BASF MW182		Type I Waxy solid Outstanding water and brine thickener at conc<1wt%	Yes	9000- 9200 psi <u>repeated</u>			X (tried at very dilute 0.1 wt% as well)

PIT-1		Type I low viscosity liquid	Yes	3500 psi				X
PIT-2		Type I medium viscosity liquid	Need to resynthesize					
PIT-3		Type I medium viscosity liquid	not yet tested					
PIT-4		Type I high viscosity liquid	not yet tested					
PIT-5		Type I medium viscosity liquid	not yet tested					
PIT-6		Type I or III waxy solid	No					
PIT-7		Type I or III high viscosity liquid	No	X	X	X		
PIT-8		Type I or III waxy solid	not yet tested					
PIT-9		Type I or III viscous liquid	not yet tested					

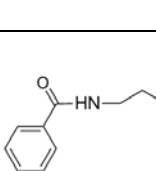
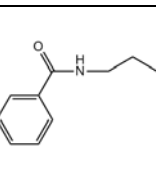
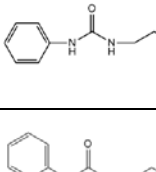
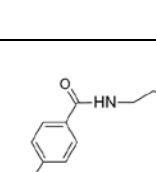
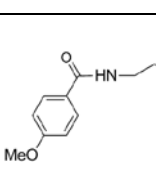
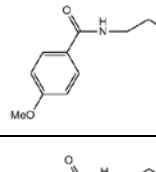
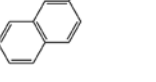
PIT-10		Type 1	No				
PIT-11		Type 1					
PIT-12		Type 1					
P-OG1		Type I white powder	Yes	4105 psi			X (2wt%) No viscosity change in solution but Formed crystals upon isochoric cooling
P-OG2		Type I yellow crystals	Yes		47.5 C	3857 psi	X (0.8wt% 50C) No viscosity change in solution but formed crystals upon cooling
9.0 igma		Type 1	No but formed fibers upon depressurization				

REACTIVE AMINES

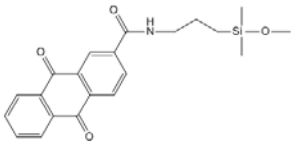
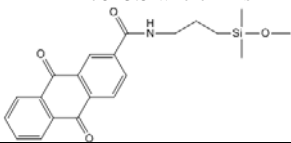
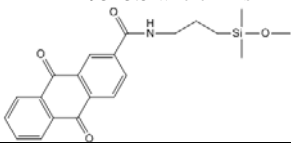
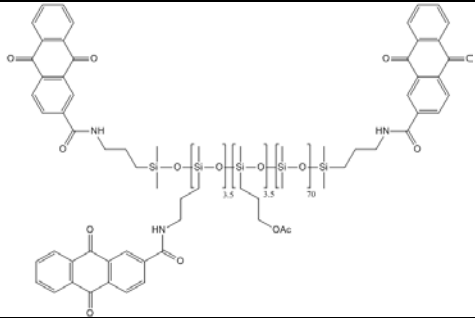
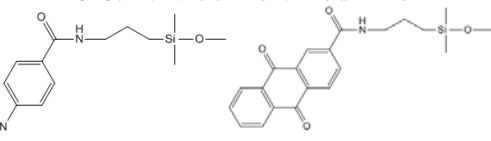

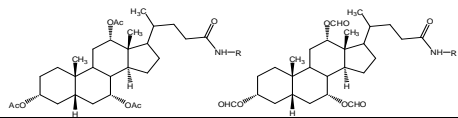
D-230		Type II low viscosity liquid	No				
SD-401		Type II low viscosity liquid	No				
GAP-0		Type II low viscosity liquid	No				Hexane thickener when CO ₂ bubbles through
GAP-1		low viscosity liquid	Not yet tested				
GAP-15		low viscosity liquid	No				
GAP-37		low viscosity liquid	Yes	X	X	Yes 7500 psi	
DMS-A11		low viscosity liquid					
DMS-A211		low viscosity liquid	No				
AMS-162		low viscosity liquid	No				

AMS-132		low viscosity liquid	YES	3100 psi	4000 psi	4250 psi	
AMS-242		low viscosity liquid	NO				
F1480-076 (DAB-Me2)		low viscosity liquid	NO				
F1091-152 (DAB-Me)		low viscosity liquid					
F1480-017 (DAB-0)		low viscosity liquid	NO				
F1850-56 (GAP-MEAP)		low viscosity liquid	NO				

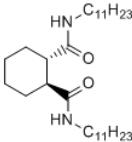
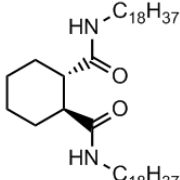
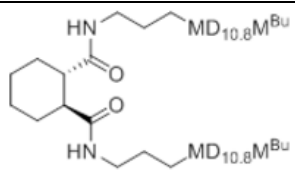
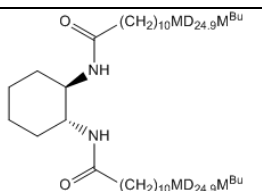
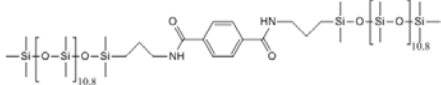
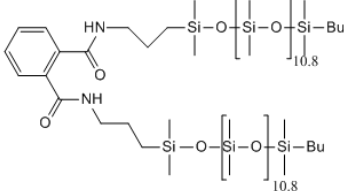
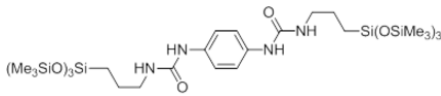
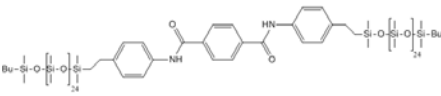
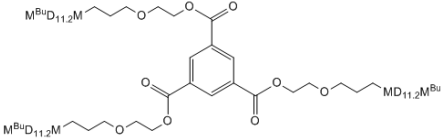
TERMINALLY FUNCTIONALIZED AROMATIC AMIDES

F2280-151		high viscosity liquid	Not yet tested					
F2280-150		med viscosity liquid	Not yet tested					
F2280-147		low-medium viscosity liquid	Yes	X	X	6800 psi	Not yet tested	
F1717-104		High Viscosity Liquid	No	X	X	X		
F1717-101		Medium viscosity Liquid	Not yet tested					
F2280-158		high viscosity liquid	Not yet tested					
F2280-157		med high viscosity liquid	Not yet tested					
F2280-153		medium viscosity liquid	Yes	X	X	7000 psi	Not yet tested	
F2280-162		medium viscosity liquid	No	X	X	X		

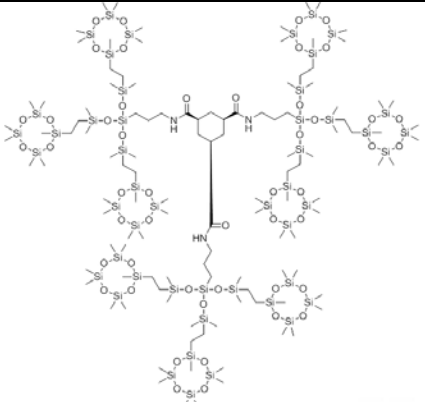
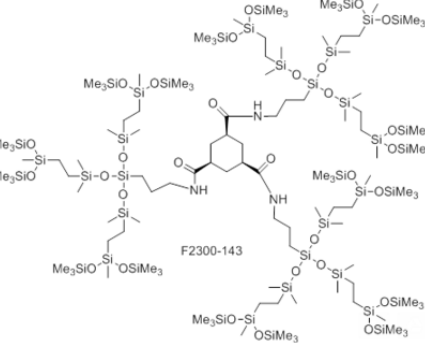
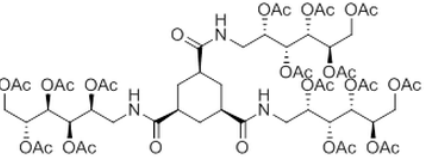
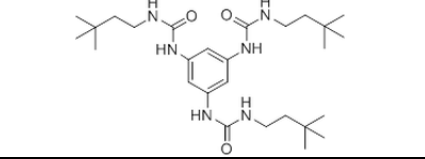
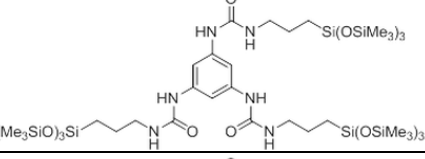
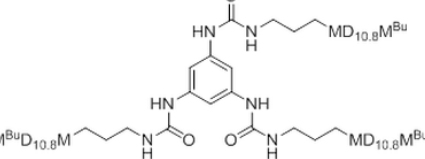
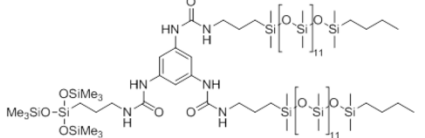
F2280-156		medium viscosity liquid	No	X	X	X	
F2280-161		waxy solid	No	X	X	X	
F2280-154-2		waxy solid	Yes	X	X	9000 psi	
F2008-75		Waxy paste	Yes	4700 psi	4450 psi	4200 psi	Not yet
F2008-61		Waxy paste	Yes	3050 psi	2950 psi	3400 psi	X (up to 4 wt%)
F2008-64		Waxy paste	Yes	2800 psi	2900 psi	3500 psi	X (even at 5wt%)
F2008-82		Waxy paste	Yes	7300 psi	5500 psi	5150 psi	X
F2008-85		Waxy Paste	Yes	X	X	8500 psi	Not yet
F2008-9		high viscosity liquid	No	X	X	X	

F2008-88	M3D57T1.1 where M is 	Jelly	No	X	X	X	
F2008-90	M4D78T3.5 where M is 	Chunks Gel	No but soluble with hexane cosolvent	X	X	X	
F2008-125	M4D93T3.5 where M is 	Chunks Gel	No	X	X	X	Yes when hexanes as cosolvent
F2142-4		Yellow Gel	No	X	X	X	
F2008-84	M3D57T1.1 where M is 1:1 molar mix of 	Jelly Like Paste	Yes	X	X	8350 psi	
F2008-117	M'D23D'2.1M' Equal parts Anthraquinone Amide and PPO (n=4.6) functionality	Gel	NO				
F2008-121	Same as 2008-117 but with longer PPO Chain	Gel	Not Yet Tested				
F2008-80		Medium Viscosity Liquid	Not yet tested				
F2142-55	M4D88T3.5 with 50:50 mix M of A:B 	Solid Gel	No but will dissolve with cosolvents				Yes with hexanes
F2142-50-2	"A" (acetylated cholate) from 2142-55		No				

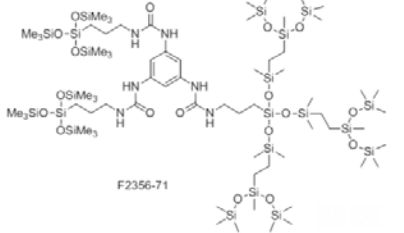
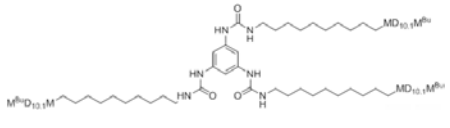
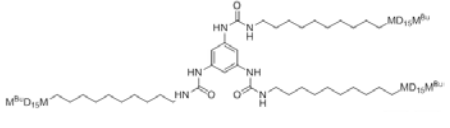
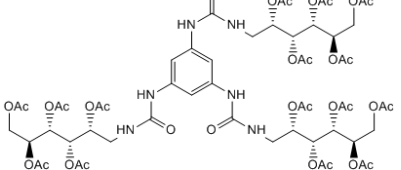
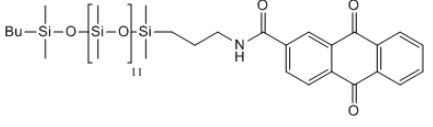
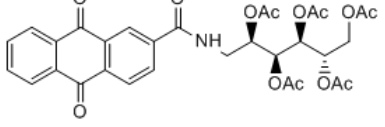
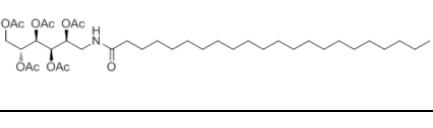
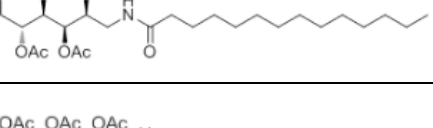
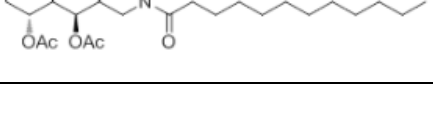
CORE ASSOCIATING CANDIDATES

F2095-46		white powder	No				
F2095-40		white powder	No				
F2095-53		Viscous Liquid	Yes	3900 psi			No
F2095-71		Low Viscosity Liquid	Yes	950 psig	1800 psig		
F1750-162		Clear Jelly	No				
F2095-13		Yellow Viscous Liquid	Yes	X	4100 psi	4150 psi	No
F2356-30		White Powder	No				not a hexane thickener
F1750-161		Waxy Paste	No				
F2095-110		Low Viscosity Liquid (CONTROL)	Yes	3900 psi	4140 psi	4460 psi	

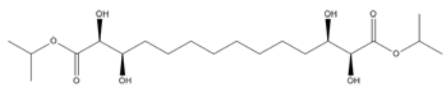

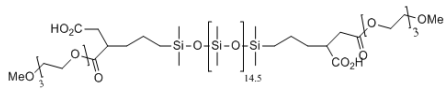

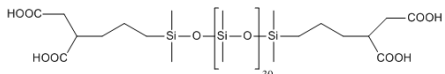
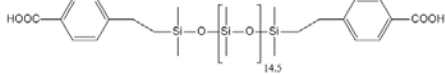
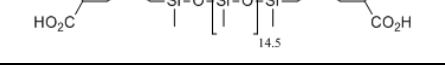
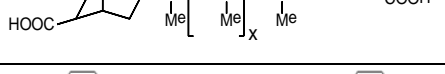
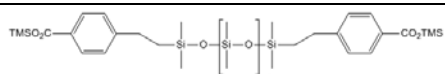

F2095-9		High Viscosity Liquid	No				
F2095-104		High Viscosity Liquid	Yes	X	4500 psig		NO
F2095-128		Crystalline Solid	No	X	X	X	
F2300-37		crystalline solid	Yes	3180 psig			Mild
F2095-42		white powder	No (tested at 0.25wt%) 7/28/2014 with hexanes	X	X	X	
F2095-133		Crystalline Solid	No (tried at 1wt% with 29%hexanes)				Thickens hexanes
F2095-57		High Viscosity liquid	No				
F2095-100		High Viscosity Liquid	No				

F2300-131		Very High Viscosity Liquid/Tacky Solid	Yes	2600 psi			No
F2300-143		Viscous Liquid	Yes	2800 psi			No
F2300-99		crystalline solid	No				Thickens acetone (>5wt%) and toluene
F2300-160		White Powder	No				
F2300-10		crystalline solid	No but will go in with 40% hexanes				Yes with hexanes
F2300-22		Gel like solid	No but will with hexanes				NO
F2356-57		gel-solid	No but goes in with hexanes-80%CO ₂				Yes with hexanes

F2356-36		gel-solid	No but goes in with hexanes-80% CO ₂				Yes with hexanes
F2356-113	<p>F2356-113</p>	Pale Gel	No but dissolves if hexanes added with 70% CO ₂				Yes (~300x with 2.25wt%)
F2300-102	<p>F2300-102</p>	Low-Medium Viscosity liquid	Yes	1600 psig			No
F2300-112		Medium Viscosity Liquid	Yes	3000 psi			Mild
F2300-116		Medium Viscosity Liquid	Yes	1500 psi			No
F2356-69	<p>F2356-69</p>	tacky yellow solid	No	x	x	x	

F2356-71		pale orange gel	No				
F2300-81		Rubbery Solid	No				
F2300-94		Rubbery Solid	No				
F2300-85		crystalline solid	No				
F2008-109		Clear Gel	No				
F2131-059		High Melt Solid	No but dissolves at 0.2wt% after heating to ~80°C	0.2% 7000 psi		83°C 0.2% 5000 psi	No (0.2wt%)
F2390-013 (labeled -012)		crystalline Solid	No but goes into CO ₂ with heating at 0.5wt%	X		2700 psi 0.5%	
F2390-24		Solid	Yes	1020 psi			No
F2390-18		Solid	Yes	900 psi			No

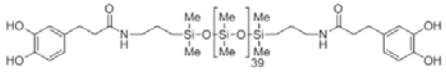
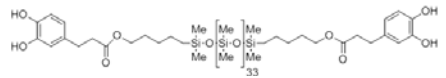
TERMINALLY HYDROGEN BONDING CANDIDATES

PIT-13		Solid	No (Not even in 24% hexanes, 75% CO ₂)				
Gelest DMS-B25		low-medium viscosity liquid	Yes	X	4280 psi	4460 psi	Not yet tested
F2008-48		low-medium viscosity liquid	No	X	X	X	
F1717-054		very waxy paste	No (Not in hexane either)	X	X	X	
F2008-36		medium viscosity liquid	No	X	X	X	
F1750-78		low-medium viscosity liquid	No	X	X	X	
F2008-47		medium viscosity liquid	No	X	X	X	
F1717-067/070		low-medium viscosity liquid	No	X	X	X	
F1750-130A		Medium Viscosity Liquid	Not yet tested				
F1750-130B		Low Viscosity Liquid	Not yet tested				

F1750-141A							
F1750-141B							
F1750-99		Type 1 Solid granules	Not yet tested				
F2131-114		Viscous Orange Liquid	No				

MISCELLANEOUS CANDIDATES

F1750-151		Low Viscosity	Yes	3000 psi	3250 psi	4160 psi	
F1750-152		Low Viscosity	Yes	2125 psi	2650 psi	3740 psi	NO
F2095-6		High Viscosity Liquid	NO				
F2131-82		Liquid					
F2131-80		Liquid					
F2131-83		Liquid					
F2008-100		High viscosity liquid	Yes	3wt% 5250 psi			
F2131-119		Low MP Solid (control)	Yes	X	X	6260 psig 50C	

F2131-125		Viscous Bluish Liquid	No				
F2131-129							

BIBLIOGRAPHY

- [1] F.I. Stalkup, Miscible Displacement, Henry L. Doherty Memorial Fund of AIME, Society of Petroleum Engineers of AIME, 1983. https://books.google.com/books/about/Miscible_Displacement.html?id=KvVLAAAACA-AJ&pgis=1 (accessed March 27, 2016).
- [2] F.I. Stalkup, Status of Miscible Displacement, J. Pet. Technol. 35 (1983) 815–826. doi:10.2118/9992-PA.
- [3] L. Koottungal, 2014 Worldwide EOR Survey, 2014. <http://www.ogj.com/articles/print/volume-112/issue-4/special-report-eor-heavy-oil-survey/2014-worldwide-eor-survey.html>.
- [4] B. Habermann, The Efficiency of Miscible Displacement As A Function of Mobility Ratio, Trans AIME. 219 (1960) 264–272.
- [5] R.M. Enick, D.K. Olsen, Mobility and Conformance Control for Carbon Dioxide Enhanced Oil Recovery (CO₂-EOR) via Thickeners, Foams, and Gels--A Detailed Literature Review of 40 Years of Research, in: SPE Improv. Oil Recover. Symp. (SPE 154122), 2012.
- [6] Carbon Dioxide Enhanced Oil Recovery, (2010) 32. https://www.netl.doe.gov/file-library/research/oil-gas/CO2_EOR_Primer.pdf.
- [7] R.M. Enick, J. Ammer, A Literature Review of Attempts to Increase the Viscosity of Dense Carbon Dioxide, Website Natl. Energy Technol. Lab. (1998).
- [8] M. McHugh, V. Krukonis, Supercritical Fluid Extraction: Principles and Practice, Elsevier, 2013. <https://books.google.com/books?hl=en&lr=&id=VTIvBQAAQBAJ&pgis=1> (accessed May 19, 2016).
- [9] D.K. Dandge, J.P. Heller, others, Polymers for Mobility Control in CO₂ Floods, in: SPE Int. Symp. Oilf. Chem., 1987.
- [10] C.F. Kirby, M.A. McHugh, Phase Behavior of Polymers in Supercritical Fluid Solvents, Chem. Rev. 99 (1999) 565–602. doi:10.1021/cr970046j.

- [11] E.J. Beckman, Supercritical and near-critical CO₂ in green chemical synthesis and processing, *J. Supercrit. Fluids*. 28 (2004) 121–191. doi:10.1016/S0896-8446(03)00029-9.
- [12] E.J. Beckman, A challenge for green chemistry: designing molecules that readily dissolve in carbon dioxide., *Chem. Commun. (Camb)*. (2004) 1885–8. doi:10.1039/b404406c.
- [13] P. Raveendran, Y. Ikushima, S.L. Wallen, Polar attributes of supercritical carbon dioxide., *Acc. Chem. Res.* 38 (2005) 478–85. doi:10.1021/ar040082m.
- [14] V.K. Potluri, J. Xu, R. Enick, E. Beckman, A.D. Hamilton, Peracetylated sugar derivatives show high solubility in liquid and supercritical carbon dioxide., *Org. Lett.* 4 (2002) 2333–5. <http://www.ncbi.nlm.nih.gov/pubmed/12098240> (accessed April 25, 2014).
- [15] D. Tapriyal, Y. Wang, R.M. Enick, J.K. Johnson, J. Crosthwaite, M.C. Thies, et al., Poly(vinyl acetate), poly((1-O-(vinyl-2,3,4,6-tetra-O-acetyl- β -D-glucopyranoside)) and amorphous poly(lactic acid) are the most CO₂-soluble oxygenated hydrocarbon-based polymers, *J. Supercrit. Fluids*. 46 (2008) 252–257. doi:10.1016/j.supflu.2008.05.001.
- [16] F. Rindfleisch, T.P. DiNoia, M.A. McHugh, Solubility of Polymers and Copolymers in Supercritical CO₂, *J. Phys. Chem.* 100 (1996) 15581–15587. doi:10.1021/jp9615823.
- [17] G. Clavier, M. Mistry, F. Fages, J.-L. Pozzo, Remarkably simple small organogelators: di-n-alkoxy-benzene derivatives, *Tetrahedron Lett.* 40 (1999) 9021–9024. doi:10.1016/S0040-4039(99)01918-8.
- [18] D.W. Knight, I.R. Morgan, A new organogelator effective at both extremes of solvent polarity, *Tetrahedron Lett.* 50 (2009) 6610–6612. doi:10.1016/j.tetlet.2009.09.070.
- [19] A.E. Alexander, V.R. Gray, Aluminium Soaps, their Nature and Gelling Properties, *Proc. R. Soc. A Math. Phys. Eng. Sci.* 200 (1950) 162–168. doi:10.1098/rspa.1950.0005.
- [20] S.S. Babu, V.K. Praveen, A. Ajayaghosh, Functional π -gelators and their applications., *Chem. Rev.* 114 (2014) 1973–2129. doi:10.1021/cr400195e.
- [21] P. Terech, R.G. Weiss, Low Molecular Mass Gelators of Organic Liquids and the Properties of Their Gels, *Chem. Rev.* 97 (1997) 3133–3160. doi:10.1021/cr9700282.
- [22] O. Gronwald, S. Shinkai, Sugar-integrated gelators of organic solvents., *Chemistry*. 7 (2001) 4328–34. <http://www.ncbi.nlm.nih.gov/pubmed/11695665>.
- [23] B. Escuder, J.F. Miravet, Silk-inspired low-molecular-weight organogelator., *Langmuir*. 22 (2006) 7793–7. doi:10.1021/la060499w.
- [24] M.B. Miller, W. Bing, D.R. Luebke, R.M. Enick, Solid CO₂-phases as potential phase-change physical solvents for CO₂, *J. Supercrit. Fluids*. 61 (2012) 212–220. doi:10.1016/j.supflu.2011.09.003.

- [25] M. George, R.G. Weiss, Molecular organogels. Soft matter comprised of low-molecular-mass organic gelators and organic liquids., *Acc. Chem. Res.* 39 (2006) 489–97. doi:10.1021/ar0500923.
- [26] P.J. Flory, Constitution of Three-dimensional Polymers and the Theory of Gelation., *J. Phys. Chem.* 46 (1942) 132–140. doi:10.1021/j150415a016.
- [27] J.P. Heller, D.K. Dandge, R.J. Card, L.G. Donaruma, Direct thickeners for mobility control of CO₂ floods, *Soc. Pet. Eng. J.* 25 (1985) 679–686. doi:10.2118/11789-PA.
- [28] S. Zhang, Y. She, Y. Gu, Evaluation of Polymers as Direct Thickeners for CO₂ Enhanced Oil Recovery, *J. Chem. Eng. Data.* 56 (2011) 1069–1079. doi:10.1021/je1010449.
- [29] R.S. Bullen, J. Mzik, J.P. Richard, Novel compositions suitable for treating deep wells, 4,701,270, 1987, 1987.
- [30] J.H. Bae, C.A. Irani, A laboratory investigation of viscosified CO₂ process, *SPE Adv. Technol. Ser.* 1 (1993) 166–171. <https://www.onepetro.org/journal-paper/SPE-20467-PA>.
- [31] L.L. Williams, J.B. Rubin, H.W. Edwards, Calculation of Hansen Solubility Parameter Values for a Range of Pressure and Temperature Conditions, Including the Supercritical Fluid Region, *Ind. Eng. Chem. Res.* 43 (2004) 4967–4972. doi:10.1021/ie0497543.
- [32] J.B. McClain, J.D. Londono, D.E. Betts, D.A. Canelas, E.T. Samulski, G.D. Wignall, et al., Characterization of polymers and amphiphiles in supercritical CO₂ using small angle neutron scattering and viscometry., in: *Abstr. Pap. Am. Chem. Soc.*, 1996: p. 145–PMSE.
- [33] J. Xu, A. Wlaschin, R.M. Enick, Thickening carbon dioxide with the fluoroacrylate-styrene copolymer, *Spe J.* 8 (2003) 85–91.
- [34] Z. Huang, C. Shi, J. Xu, S. Kilic, R.M. Enick, E.J. Beckman, Enhancement of the Viscosity of Carbon Dioxide Using Styrene/Fluoroacrylate Copolymers, *Macromolecules.* 33 (2000) 5437–5442. doi:10.1021/ma992043+.
- [35] D. Tapriyal, DESIGN OF NON-FLUOROUS CO₂ SOLUBLE COMPOUNDS, University of Pittsburgh, 2009. <http://d-scholarship.pitt.edu/6565/>.
- [36] P. Terech, G. Clavier, H. Bouas-Laurent, J.-P. Desvergne, B. Demé, J.-L. Pozzo, Structural variations in a family of orthodialkoxyarenes organogelators., *J. Colloid Interface Sci.* 302 (2006) 633–42. doi:10.1016/j.jcis.2006.06.056.
- [37] K. Trickett, D. Xing, R. Enick, J. Eastoe, M.J. Hollamby, K.J. Mutch, et al., Rod-like micelles thicken CO(2)., *Langmuir.* 26 (2010) 83–8. doi:10.1021/la902128g.
- [38] J. Eastoe, D.C. Steytler, B.H. Robinson, R.K. Heenan, A.N. North, J.C. Dore, Structure of cobalt Aerosol-OT reversed micelles studied by small-angle scattering methods, *J. Chem. Soc. Faraday Trans.* 90 (1994) 2497. doi:10.1039/ft9949002497.

- [39] A.R. Hirst, I.A. Coates, T.R. Boucheteau, J.F. Miravet, B. Escuder, V. Castelletto, et al., Low-molecular-weight gelators: elucidating the principles of gelation based on gelator solubility and a cooperative self-assembly model., *J. Am. Chem. Soc.* 130 (2008) 9113–21. doi:10.1021/ja801804c.
- [40] K. Hanabusa, T. Miki, Y. Taguchi, T. Koyama, H. Shirai, Two-component, small molecule gelling agents, *J. Chem. Soc. Chem. Commun.* (1993) 1382. doi:10.1039/c39930001382.
- [41] P.J.M. Stals, J.F. Haveman, R. Martín-Rapún, C.F.C. Fitié, A.R.A. Palmans, E.W. Meijer, The influence of oligo(ethylene glycol) side chains on the self-assembly of benzene-1,3,5-tricarboxamides in the solid state and in solution, *J. Mater. Chem.* 19 (2009) 124–130. doi:10.1039/B816418E.
- [42] J. Eastoe, G. Fragneto, B.H. Robinson, T.F. Towey, R.K. Heenan, F.J. Leng, Variation of surfactant counterion and its effect on the structure and properties of Aerosol-OT-based water-in-oil microemulsions, *J. Chem. Soc. Faraday Trans.* 88 (1992) 461. doi:10.1039/ft9928800461.
- [43] J. Roovers, Concentration Dependence of the Relative Viscosity of Star Polymers, *Macromolecules.* 27 (1994) 5359–5364. doi:10.1021/ma00097a015.
- [44] J.B. McClain, D. Londono, J.R. Combes, T.J. Romack, D.A. Canelas, D.E. Betts, et al., Solution Properties of a CO₂-Soluble Fluoropolymer via Small Angle Neutron Scattering, *J. Am. Chem. Soc.* 118 (1996) 917–918. doi:10.1021/ja952750s.
- [45] D.K. Dandge, C. Taylor, J.P. Heller, Associative organotin polymers. I. Symmetric trialkyltin fluorides: Synthesis and properties, *J. Polym. Sci. Part A Polym. Chem.* 27 (1989) 1053–1063. doi:10.1002/pola.1989.080270327.
- [46] J.P. Heller, F.S. Kovarik, J.J. Taber, Improvement of CO₂ flood performance: Third annual report, October 1, 1986--September 30, 1987, 1989.
- [47] C. Shi, Z. Huang, E.J. Beckman, R.M. Enick, S.-Y. Kim, D.P. Curran, Semi-Fluorinated Trialkyltin Fluorides and Fluorinated Telechelic Ionomers as Viscosity-Enhancing Agents for Carbon Dioxide, *Ind. Eng. Chem. Res.* 40 (2001) 908–913. doi:10.1021/ie0001321.
- [48] K.J. Mysels, Napalm. Mixture of Aluminum Disoaps., *Ind. Eng. Chem.* 41 (1949) 1435–1438. doi:10.1021/ie50475a033.
- [49] R.M. Enick, The Effect of Hydroxy Aluminum Disoaps on the Viscosity of Light Alkanes and Carbon Dioxide, in: *Proc. SPE Int. Symp. Oilf. Chem., Society of Petroleum Engineers*, 1991. doi:10.2118/21016-MS.
- [50] J. Eastoe, A. Dupont, D.C. Steytler, M. Thorpe, A. Gurgel, R.K. Heenan, Micellization of economically viable surfactants in CO₂, *J. Colloid Interface Sci.* 258 (2003) 367–373. doi:10.1016/S0021-9797(02)00104-2.

- [51] P. Lewis, An Attempt to Increase the Viscosity of CO₂ with Metallic Stearates, University of Pittsburgh, 1990.
- [52] C. Shi, The Gelation of CO₂: A Sustainable Route to the Creation of Microcellular Materials, *Science* (80-.). 286 (1999) 1540–1543. doi:10.1126/science.286.5444.1540.
- [53] I.-H. Paik, D. Tapriyal, R.M. Enick, A.D. Hamilton, Fiber formation by highly CO₂-soluble bisureas containing peracetylated carbohydrate groups., *Angew. Chem. Int. Ed. Engl.* 46 (2007) 3284–7. doi:10.1002/anie.200604844.
- [54] J. Eastoe, T.F. Towey, B.H. Robinson, J. Williams, R.K. Heenan, Structures of metal bis(2-ethylhexylsulfosuccinate) aggregates in cyclohexane, *J. Phys. Chem.* 97 (1993) 1459–1463. doi:10.1021/j100109a035.
- [55] M.B. Miller, D.-L. Chen, H.-B. Xie, D.R. Luebke, J. Karl Johnson, R.M. Enick, Solubility of CO₂ in CO₂-philic oligomers; COSMOtherm predictions and experimental results, *Fluid Phase Equilib.* 287 (2009) 26–32. doi:10.1016/j.fluid.2009.08.022.
- [56] D.G. Lemmon, E.W. , McLinden, M.O., Friend, Thermophysical Properties of Fluid Systems, NIST Chem. WebBook, NIST Stand. Ref. Database Number 69. (n.d.). <http://webbook.nist.gov/chemistry/fluid/> (accessed December 14, 2015).
- [57] A. Dhuwe, Thickeners for Natural Gas Liquids to Improve the Performance in Enhanced Oil Recovery and Dry Hydraulic Fracking, (2016). http://d-scholarship.pitt.edu/26533/1/12%2D2%2D15_latest_file.pdf (accessed March 28, 2016).
- [58] A. Dhuwe, J. Lee, S. Cummings, E. Beckman, R. Enick, Small associative molecule thickeners for ethane, propane and butane, *J. Supercrit. Fluids.* 114 (2016) 9–17. doi:10.1016/j.supflu.2016.03.019.
- [59] A. Dhuwe, J. Sullivan, J. Lee, S. Klara, S. Cummings, R. Enick, et al., Close-clearance high pressure falling ball viscometer assessment of ultra-high molecular weight polymeric thickeners for ethane, propane and butane, *J. Pet. Sci. Eng.* In Press (2016).
- [60] A. Galia, P. Pierro, G. Filardo, Dispersion polymerization of methyl methacrylate in supercritical carbon dioxide stabilized with poly(ethylene glycol)-b-perfluoroalkyl compounds, *J. Supercrit. Fluids.* 32 (2004) 255–263. doi:10.1016/j.supflu.2003.12.017.
- [61] A. Mohamed, M. Sagisaka, F. Guittard, S. Cummings, A. Paul, S.E. Rogers, et al., Low fluorine content CO₂-philic surfactants., *Langmuir.* 27 (2011) 10562–9. doi:10.1021/la2021885.
- [62] J. Eastoe, S. Gold, D.C. Steytler, Surfactants for CO₂., *Langmuir.* 22 (2006) 9832–42. doi:10.1021/la060764d.

- [63] G. Luna-Bárcenas, S. Mawson, S. Takishima, J.M. DeSimone, I.C. Sanchez, K.P. Johnston, Phase behavior of poly(1,1-dihydroperfluorooctylacrylate) in supercritical carbon dioxide, *Fluid Phase Equilib.* 146 (1998) 325–337. doi:10.1016/S0378-3812(98)00215-5.
- [64] P. André, P. Lacroix-Desmazes, D.K. Taylor, B. Boutevin, Solubility of fluorinated homopolymer and block copolymer in compressed CO₂, *J. Supercrit. Fluids.* 37 (2006) 263–270. doi:10.1016/j.supflu.2005.08.007.
- [65] M. Chirat, T. Ribaut, S. Clerc, F. Charton, B. Fournel, P. Lacroix-Desmazes, Extraction of Cobalt Ion from Textile Using a Complexing Macromolecular Surfactant in Supercritical Carbon Dioxide, *Ind. Eng. Chem. Res.* 52 (2012) 12129151443008. doi:10.1021/ie301754v.
- [66] L. Du, J.Y. Kelly, G.W. Roberts, J.M. DeSimone, Fluoropolymer synthesis in supercritical carbon dioxide, *J. Supercrit. Fluids.* 47 (2009) 447–457. doi:10.1016/j.supflu.2008.11.011.
- [67] R. Enick, E. Beckman, A. Yazdi, V. Krukonis, H. Schonemann, J. Howell, Phase behavior of CO₂–perfluoropolyether oil mixtures and CO₂–perfluoropolyether chelating agent mixtures, *J. Supercrit. Fluids.* 13 (1998) 121–126. doi:10.1016/S0896-8446(98)00043-6.
- [68] R.P. Nielsen, R. Valsecchi, M. Strandgaard, M. Maschietti, Experimental study on fluid phase equilibria of hydroxyl-terminated perfluoropolyether oligomers and supercritical carbon dioxide, *J. Supercrit. Fluids.* 101 (2015) 124–130. doi:10.1016/j.supflu.2015.03.011.
- [69] D.A. Newman, T.A. Hoefling, R.R. Beitle, E.J. Beckman, R.M. Enick, Phase behavior of fluoroether-functional amphiphiles in supercritical carbon dioxide, *J. Supercrit. Fluids.* 6 (1993) 205–210. doi:10.1016/0896-8446(93)90028-V.
- [70] Y. Wang, L. Hong, D. Tapriyal, I.C. Kim, I.-H. Paik, J.M. Crosthwaite, et al., Design and evaluation of nonfluorous CO₂-soluble oligomers and polymers., *J. Phys. Chem. B.* 113 (2009) 14971–80. doi:10.1021/jp9073812.
- [71] L. Hong, D. Tapriyal, R.M. Enick, Phase Behavior of Poly(propylene glycol) Monobutyl Ethers in Dense CO₂, *J. Chem. Eng. Data.* 53 (2008) 1342–1345. doi:10.1021/je800068v.
- [72] T. Sarbu, T. Styranec, E. Beckman, Non-fluorous polymers with very high solubility in supercritical CO₂ down to low pressures, *Nature.* 405 (2000) 165–8. doi:10.1038/35012040.
- [73] C. Drohmann, E.J. Beckman, Phase behavior of polymers containing ether groups in carbon dioxide, *J. Supercrit. Fluids.* 22 (2002) 103–110. doi:10.1016/S0896-8446(01)00111-5.
- [74] P. Raveendran, S.L. Wallen, Sugar Acetates as Novel, Renewable CO₂ -philes, *J. Am. Chem. Soc.* 124 (2002) 7274–7275. doi:10.1021/ja025508b.

- [75] D. Graiver, K.W. Farminer, R. Narayan, A Review of the Fate and Effects of Silicones in the Environment, *J. Polym. Environ.* 11 (n.d.) 129–136. doi:10.1023/A:1026056129717.
- [76] D. Sanli, C. Erkey, Demixing pressures of hydroxy-terminated poly(dimethylsiloxane)–carbon dioxide binary mixtures at 313.2K, 323.2K and 333.2K, *J. Supercrit. Fluids.* 92 (2014) 264–271. doi:10.1016/j.supflu.2014.05.014.
- [77] S. Kim, Y.-S. Kim, S.-B. Lee, Phase behaviors and fractionation of polymer solutions in supercritical carbon dioxide, *J. Supercrit. Fluids.* 13 (1998) 99–106. doi:10.1016/S0896-8446(98)00040-0.
- [78] M.B. Miller, D.R. Luebke, R.M. Enick, CO₂-philic Oligomers as Novel Solvents for CO₂ Absorption, *Energy & Fuels.* 24 (2010) 6214–6219. doi:10.1021/ef101123e.
- [79] Z. Bayraktar, E. Kiran, Miscibility, phase separation, and volumetric properties in solutions of poly(dimethylsiloxane) in supercritical carbon dioxide, *J. Appl. Polym. Sci.* 75 (2000) 1397–1403. doi:10.1002/(SICI)1097-4628(20000314)75:11<1397::AID-APP12>3.0.CO;2-F.
- [80] Y. Xiong, E. Kiran, Miscibility, density and viscosity of poly(dimethylsiloxane) in supercritical carbon dioxide, *Polymer (Guildf).* 36 (1995) 4817–4826. doi:10.1016/0032-3861(95)99298-9.
- [81] M.L. O'Neill, Q. Cao, M. Fang, K.P. Johnston, Solubility of Homopolymers and Copolymers in Carbon Dioxide, 5885 (1998) 3067–3079.
- [82] P. Alessi, K. Ireneo, C. Angelo, F. Alessia, M. Mariarosa, Polydimethylsiloxanes in supercritical solvent impregnation (SSI) of polymers, *J. Supercrit. Fluids.* 27 (2003) 309–315. doi:10.1016/S0896-8446(02)00267-X.
- [83] M. Yates, P. Shah, K. Johnston, K. Lim, S. Webber, Steric Stabilization of Colloids by Poly(dimethylsiloxane) in Carbon Dioxide: Effect of Cosolvents., *J. Colloid Interface Sci.* 227 (2000) 176–184. doi:10.1006/jcis.2000.6850.
- [84] P.A. Psathas, S.R.P. da Rocha, C.T. Lee, K.P. Johnston, K.T. Lim, S. Webber, Water-in-Carbon Dioxide Emulsions with Poly(dimethylsiloxane)-Based Block Copolymer Ionomers, *Ind. Eng. Chem. Res.* 39 (2000) 2655–2664. doi:10.1021/ie990779p.
- [85] S. Kwon, K. Lee, W. Bae, H. Kim, Synthesis of a biocompatible polymer using siloxane-based surfactants in supercritical carbon dioxide, *J. Supercrit. Fluids.* 45 (2008) 391–399. doi:10.1016/j.supflu.2008.01.021.
- [86] T.A. Hoefling, D.A. Newman, R.M. Enick, E.J. Beckman, Effect of structure on the cloud-point curves of silicone-based amphiphiles in supercritical carbon dioxide, *J. Supercrit. Fluids.* 6 (1993) 165–171. doi:10.1016/0896-8446(93)90015-P.

- [87] K.A. Shaffer, T.A. Jones, D.A. Canelas, J.M. DeSimone, S.P. Wilkinson, Dispersion Polymerizations in Carbon Dioxide Using Siloxane-Based Stabilizers, *Macromolecules*. 29 (1996) 2704–2706. doi:10.1021/ma9516798.
- [88] R. Fink, E.J. Beckman, Phase behavior of siloxane-based amphiphiles in supercritical carbon dioxide, *J. Supercrit. Fluids*. 18 (2000) 101–110. doi:10.1016/S0896-8446(00)00052-8.
- [89] J.A. Dzielawa, A. V. Rubas, C. Lubbers, D.C. Stepinski, A.M. Scurto, R.E. Barrans, et al., Carbon Dioxide Solubility Enhancement through Silicone Functionalization: “CO₂-philic” Oligo(dimethylsiloxane)-substituted Diphosphonates*, *Sep. Sci. Technol.* 43 (2008) 2520–2536. doi:10.1080/01496390802122063.
- [90] R.J. Perry, T.A. Grocela-Rocha, M.J. O’Brien, S. Genovese, B.R. Wood, L.N. Lewis, et al., Aminosilicone solvents for CO₂ capture., *ChemSusChem*. 3 (2010) 919–30. doi:10.1002/cssc.201000077.
- [91] M. McHugh, M.E. Paulaitis, Solid solubilities of naphthalene and biphenyl in supercritical carbon dioxide, *J. Chem. Eng. Data*. 25 (1980) 326–329. doi:10.1021/je60087a018.
- [92] R.M. Enick, P. Koronaios, C. Stevenson, S. Warman, B. Morsi, H. Nulwala, et al., Hydrophobic Polymeric Solvents for the Selective Absorption of CO₂ from Warm Gas Streams that also Contain H₂ and H₂O, *Energy & Fuels*. 27 (2013) 6913–6920. doi:10.1021/ef401740w.
- [93] K. Hanabusa, Development of organogelators based on supramolecular chemistry, in: N. Ueyama, A. Harada (Eds.), *Macromol. Nanostructured Mater.*, Springer Series in Materials Science, Dordrecht, The Netherlands, 2004: pp. 118–137.
- [94] K. Hanabusa, A. Kawakami, M. Kimura, H. Shirai, Small Molecular Gelling Agents to Harden Organic Liquids: Trialkyl cis-1,3,5-Cyclohexanetricarboxamides., *Chem. Lett.* (1997) 191–192. doi:10.1246/cl.1997.191.
- [95] K. Hanabusa, M. Yamada, M. Kimura, H. Shirai, Prominent Gelation and Chiral Aggregation of Alkylamides Derived from trans-1,2-Diaminocyclohexane, *Angew. Chemie Int. Ed. English*. 35 (1996) 1949–1951. doi:10.1002/anie.199619491.
- [96] Y. Yasuda, E. Iishi, H. Inada, Y. Shiota, Novel Low-molecular-weight Organic Gels: N,N',N''-Tristearyltrimesamide/Organic Solvent System., *Chem. Lett.* (1996) 575–576. doi:10.1246/cl.1996.575.
- [97] M. de Loos, J.H. van Esch, R.M. Kellogg, B.L. Feringa, C₃-Symmetric, amino acid based organogelators and thickeners: a systematic study of structure–property relations, *Tetrahedron*. 63 (2007) 7285–7301. doi:10.1016/j.tet.2007.02.066.
- [98] R.J. Perry, M.J. O’Brien, Amino Disiloxanes for CO₂ Capture, *Energy & Fuels*. 25 (2011) 1906–1918. doi:10.1021/ef101564h.

- [99] C. McCabe, A. Galindo, *Applied Thermodynamics of Fluids*, Royal Society of Chemistry, Cambridge, 2010. doi:10.1039/9781849730983.
- [100] F.M. Vargas, D.L. Gonzalez, G.J. Hirasaki, W.G. Chapman, Modeling Asphaltene Phase Behavior in Crude Oil Systems Using the Perturbed Chain Form of the Statistical Associating Fluid Theory (PC-SAFT) Equation of State[†], (n.d.). doi:10.1021/ef8006678@proofing.
- [101] I. Stoychev, J. Galy, B. Fournel, P. Lacroix-Desmazes, M. Kleiner, G. Sadowski, Modeling the Phase Behavior of PEO–PPO–PEO Surfactants in Carbon Dioxide Using the PC-SAFT Equation of State: Application to Dry Decontamination of Solid Substrates[†], *J. Chem. Eng. Data*. 54 (2009) 1551–1559. doi:10.1021/je800875k.
- [102] N. von Solms, M.L. Michelsen, G.M. Kontogeorgis, Computational and Physical Performance of a Modified PC-SAFT Equation of State for Highly Asymmetric and Associating Mixtures, *Ind. Eng. Chem. Res.* 42 (2003) 1098–1105. doi:10.1021/ie020753p.
- [103] V. Wiesmet, E. Weidner, S. Behme, G. Sadowski, W. Arlt, Measurement and modelling of high-pressure phase equilibria in the systems polyethyleneglycol (PEG)–propane, PEG–nitrogen and PEG–carbon dioxide, *J. Supercrit. Fluids*. 17 (2000) 1–12. doi:10.1016/S0896-8446(99)00043-1.
- [104] I. Stoychev, F. Peters, M. Kleiner, S. Clerc, F. Ganachaud, M. Chirat, et al., Phase behavior of poly(dimethylsiloxane)–poly(ethylene oxide) amphiphilic block and graft copolymers in compressed carbon dioxide, *J. Supercrit. Fluids*. 62 (2012) 211–218. doi:10.1016/j.supflu.2011.11.008.
- [105] A. Tihic, G.M. Kontogeorgis, N. von Solms, M.L. Michelsen, L. Constantinou, A Predictive Group-Contribution Simplified PC-SAFT Equation of State: Application to Polymer Systems, *Ind. Eng. Chem. Res.* 47 (2008) 5092–5101. doi:10.1021/ie0710768.